NAVIGATION for the GUIDANCE of a MOBILE ROBOT

by

Barry Steer

A Thesis submitted to the University of Warwick

for the degree of Doctor of Philosophy

Department of Computer Science. April, 1985

NAVIGATION for the GUIDANCE of a MOBILE ROBOT - A SYNOPSIS

This thesis is about how a vehicle can, without human intervention, be navigated and guided in its movements through its environment.

To move a real mobile robot so that it traces out a desired path, 'commands' need to be dispensed to the control systems of the actuators that drive the wheels that move the vehicle. Algorithms which issue such commands are called guidance algorithms. These can cause the vehicle to move about at the desired speed, in the desired direction, and can change the direction of motion, or can achieve some other 'complex' manoeuvre.

As commands from guidance algorithms are physically realised, and become the sensible motion of the mobile robot, the desired 'intentions' embodied in them become corrupted. To combat this corruption the mobile robot needs to keep track of where it is in relation to some reference system. This is navigation. The mobile robot needs to navigate so that 'commands' to the actuation systems can then be reformulated in terms of its navigated 'location', given the task it is doing, and where it has been commanded to go to.

In this thesis three navigational phases are distinguished for a wheeled 'robotic' vehicle. Their utility was tested and confirmed by experiment, using a 0.5 tonne mobile robot equipped with the relevant sensors, and actuation systems. The three phases of navigation are:-

1) Deduced reckoning based on the intrinsic motion of the vehicle to produce an initial estimate of the vehicle's position and heading.

2) The use of an absolute measurement of the vehicle's bearing to correct errors in the estimated heading.

3) The use of sonar range measurements to objects in the surroundings to correct errors in the estimated position. The positional coordinates, orientation, and extent of these objects being held in a 'world map'.

Two guidance algorithms to control a mobile robot's movement are needed, correctly sequenced and coordinated, to enable it to perform a range of useful activities. This thesis has examined:-

1) Guidance to achieve motion with zero curvature, for a specified distance, and orientated relative to some specified direction in the environment.

2) Guidance to achieve the reorientation of a vehicle, that has to move in order to turn, so that it can move forward again with zero curvature in a different direction.

Finally, a new technique that modulates the steering wheel angle with a time dependent Gaussian envelope is given. This technique is able to produce desirable changes in the position and heading of a path curvature limited vehicle, as it moves. Examples of manoeuvres possible with this technique are illustrated.

Barry Steer, April 1985

TABLE OF CONTENTS

List of Figures, Tables[T] and Photographs[P]

ACKNOWLEDGEMENTS

This thesis is the result of research carried out at the Robot Laboratory, in the Department of Computer Science, University of Warwick, in the United Kingdom.

My first thank you is to Dr. Madeline Larcombe, for the research experience, afforded by the environment, and the robot created by her, at the Robot Laboratory.

The second thank you is to my colleague and friend, Tim Atherton, for the many hours of discussion.

To my parents, a unique thank you.

Finally, I want to thank a long standing friend, Bill Wilkinson, who showed me there was more to know.

The financial support came from the Science and Engineering Research Council, and Lansing Bagnall, Basingstoke, U.K.

British Leyland, Canley, Coventry, U.K., made available the large test area that was needed to perform the experiments, and provided the joy.

0.0 INTRODUCTION

0.1 The nature and the scope of the problem

This thesis is about how a vehicle can, without human intervention, be navigated and guided in its movements through its environment. The collection of components and processes that are coordinated to achieve such an aim, on their own, being called an autonomous mobile robot.

To endow a 'mechanism' with all the abilities associated with a human driver, planning, navigating, guiding and regulating the passage of a vehicle on its way from one place to another, and through arbitrary, unfamiliar, surroundings, would be a major achievement. This has not been attempted in this work. Rather, one vehicle, moving within an industrial interior has been used to develop and demonstrate the algorithms that enable an onboard digital computer to keep track of where the vehicle is, that is to navigate, and to use this information to regulate the motion of the structure, that is to guide it, to achieve the types of tasks needed within that environment. This has been done using both the vehicle's intrinsic motion as feedback and by sensing the environment around the robot and using the information gained to assist the rules governing its actions.

0.2 A summary of the investigation

The problem initially identified was that of understanding the theoretical basis, and implementing in practice, the motion tasks that a mobile robot could use within its surroundings. The results of these efforts resulted in the experimental verification of two motion primitives or tasks that can be concatenated to move the vehicle along a route through its surroundings. The tasks identified were: firstly to move forward along a path for a specified distance with a specified bearing; and, secondly, to reorientate the mobile robot at the end of one path, enabling it to move along another path. A study was made of the techniques which can be used to locate the mobile robot to references other than its local surroundings. The properties of the space path moved along by the mobile robot were sensed and used to compute an estimate of its 'location'. As the robot continued to move this estimate became uncertain. To reduce the errors in its location estimate measurements were made, on the environment, from where it was actually located.

This work has tested, by experiment, the necessity of the two rules, proposed as part of the reportoire of a mobile robot. It has also tested, again by experiment, the application of the rules, proposed as being able to enable the mobile robot to navigate. A real vehicle, performing real acts, in real circumstances, being sensible proof that the theories thought to be needed to contribute toward an autonomous mobile robot, actually do work. Theories help us to look at our world and deal with our experience. The desire to develop a theory for a mobile robot, is to endow it with a practical means of dealing with its 'experience', limited though it is. Simulations were used to assess appropriate manoeuvres with the robot. However, experience shows that implicit assumptions in a simulation might work in that context, but may fail when put into real world practise.

0.3 Rationale

So why is this type of research necessary? The relevant answer depends on who you are and what your aims are. To move within an hostile environment requires either your protection or your replacement. The exploration of other planets by an autonomous robot has been proposed to overcome the time delays in communicating with, and controlling at a distance, a computer controlled vehicle carrying scientific instruments [Hooke 1973]. Although this application can wait indefinitely, there are hostile environments on this planet where a mobile robot would be desirable, and in, for example, certain radioactive environments, almost certainly essential, [Larcombe & Halsall 1984]. [Moravec 1981], sees an evolutionary parallel between the survival needs of non-sessile organisms in nature, and their associated and consequent rise in intelligence to meet these survival demands, and the 'survival' needs of a mobile artifact, monitored by our intelligence, and then endowed through our efforts with a 'synthetic intelligence'.

Whatever the motive, within its environment the mobile robot is envisaged as being able to locomote autonomously from one place to another. When it reaches the remote place its other 'abilities' are employed to perform some useful activity. This might be to manipulate the environment in some way, for example, to pick up, or put down some load. To cope with limits to a mobile robot's internal autonomy, an external agent may, from time to time and from place to place, be required to supervise and manage it. The external agent that does this could possibly be man, or another machine. A vehicle and its locomotion are required if the distances to be moved are beyond those convenient for manipulation from a fixed base. The understanding of the required components and processes necessary to extend the autonomy of a mobile robot in a 'simple' environment being a first move forward, toward a more effective mobile robot, working in a more 'complex' environment, [Bullock 1983].

This work originally formed part of the research aimed at developing techniques to guide and navigate an industrial truck automatically through an industrial interior.

0.4 The experimental vehicle

The experiments were performed using a pneumatic tyred battery powered, electrically actuated, tricycle vehicle. It weighed 500 kg. The vehicle was originally an industrial burden carrier. Its movement from place to place was directed by a human driver operating the electric drive motor or braking mechanism, through foot pedals, and by turning the steering wheel, while receiving sensory feedback about the results of these actions in the fashion used to control the speed and direction of a motor car.

To perform a similar function automatically the vehicle was modified to enable a digital computer to receive information about the surrounding environment, the vehicle's internal state and actions, and to process that information and direct its motion to complete the assigned tasks. Appendix A.1 contains further details of the modifications made to the experimental mobile robot. The environment used in the experiments was the interior of a factory. This was built from brick, wood, and steel, variously painted. The surface moved over was concrete, and was smooth and flat enough to be treated as a plane for the purposes of the experiments conducted.

0.5 The contribution of this thesis

The first contribution has been to invent a means of modulating the heading control variable of a path curvature limited vehicle, one which has to move in order to turn, in such a way that complex manoeuvres, can be automated. This technique can achieve such manoeuvres as parking in reverse between two cars, and overtaking a stationary or moving object and then returning to the original course. An initial investigation using an envelope of Gaussian form has been found to yield desirable results. Further work would be required to quantify the benefits of using this envelope. It is believed that this technique is original and useful.

The second contribution has been to the theory of navigation by deduced reckoning for a tricycle vehicle whose front steered wheel angle, and along track distance are measured. This theory has been extended to enable the effect of errors in these measurements on the accuracy and precision of the deduced position and heading to be computed. The experimental results agree with the theoretical predictions. It is shown that there is one turning circle for which the error in the deduced heading estimate is a minimum, and it is shown that the longitudinal errors accumulate less rapidly than the lateral errors. It is believed that this extended theory and its experimental confirmation is original.

Thirdly, a theoretical comparison between the dual rear wheel odometry system and the front steered wheel odometer steer angle system has been made. This comparison and the explicit conclusion that the rear wheel system, for equal changes in the radius due to loading effects is inherently more accurate is believed to be original.

Fourthly, it has been demonstrated experimentally that an optically read magnetic compass attached to the vehicle's structure can be used to reduce the accumulated uncertainty in the heading estimate obtained by deduced reckoning. It is shown why this recomputation of the estimated orientation of the robot should be carried out prior to reducing

the positional uncertainty using range measurements.

Fifthly, it has been demonstrated experimentally that sonar range measurements to objects in the robot's surroundings can be used to reduce the effect of accumulated errors in the estimated position of the robot.

The final contribution has been to explicitly distinguish between the navigation, and guidance for a mobile robot. These distinctions, their relations, and the relation of these aspects in an overall context as outlined in the systems structure of Figure 1.2, are believed to be original.

1.0 NAVIGATION for GUIDANCE

1.1 Introduction

For something to be autonomous means literally that it is self-ruling. This suggests that to give autonomy to a mobile robot is to transfer relevant rules or laws to it to enable it to cope with, and be effective in performing, its tasks. There is also the implication that the more rules which can be transferred, the more autonomous the robot will become. Since a rule is some form of statement of fact, and the fact is made, sustained and confirmed, through the repeated application of the underlying theory behind this fact, we may regard the imparted rules as the robot's theories into the way the world is. Any theory has a domain of validity inside which its application is relevant, and therefore true. Outside this domain the application of this theory can be said to be irrelevant because the errors between the observations and the predictions made based on that theory, become large, and through lack of agreement between theory and observation the results can be said to become false.

The previous paragraph expresses in an abstract way the purpose behind the navigation experiments. Their aim was to determine how far the mobile robot could move, using its 'rules of navigation', before the difference between the internal representation of the 'state' of the robot and reality became too large, and therefore the representation became false. The establishment of a domain of spatial validity within which these navigational rules remain valid is needed to provide direction and insight as to the need for further means to determine the location of the robot.

Since meta-rules to enable the robot to generate its own guidance and navigation rules do not exist, at this stage of the unfoldment of our ideas, the problem is viewed as one of providing the robot with appropriate and relevant rules that enable it to cope with its given surroundings and tasks. If the tasks and environmental circumstances of

the world are few in number and static then the rules may be few in number and static. As the environment increases in variety, and the tasks become more complex to describe, these extended circumstances will give rise to the need for the robot's capabilities to be extended in some way. Limits to its autonomy will become apparent as it fails to cope with an environment contrary to our aspirations for it. The eventual and certain failure of its rules in some circumstance, and its occasional inability to perform its tasks, should be regarded as normal. The activity of extending its autonomy is therefore a consequence, since at this phase of the research no robot has the equivalent of the human ability to 'learn directly from experience' and able to extend their own rules.

The autonomy of this robotic vehicle then resides partly in the a-priori information embedded in the algorithms. The content and form of these algorithms is designed in advance of the time and place they are applied with the intent of enabling the robotic vehicle to achieve its task. Autonomy also resides in the structure of the mobile robot that is: its vehicular structure; the form of locomotion; the actuators; the sensing devices; and the on board processor. The realistion of these in hardware is itself an expression of an explicit understanding of what was required to extend the autonomy of a mobile robot.

From the above remarks about autonomy it should be clear that the task of defining, in some closed form, a 'global' task for a mobile robot is indefinite, since extensions to the robot's autonomy, that the future will almost certainly bring, will permit a deeper and wider meaning to be attached to the word 'global'. A recursive definition is useful, but in terms of its prescriptive utility it is limited. For completeness the global task for the mobile robot is defined as: from an actual location performing a task. The term location is taken to mean a position and heading, in some frame of reference which will for the moment remain unspecified. Now the task it performs could be to stay where it is,

until some external event occurs. Or, the task it performs could be to move through its environment to another location and there perform some task. The spatial boundary conditions, when it moves, are that it should not, unless specifically programmed to do so, touch the objects in its surroundings. The temporal boundary conditions are that the time taken to complete the task should not exceed some predicted bound.

To observe the spatial boundary conditions when there are other objects in the environment blocking the direct route some other less direct way needs to be formed. The approach and methods used to produce and plan its routes would be contained in the robot's strategy. To be able to work out which is an optimum route without moving the mobile robot requires some form of preprogrammed representation of its surroundings. This representation has become known as its "world model", or "map". Although in this thesis a digital computer has been used to store this information, other 'analog' media may well be more appropriate. Interiors of buildings, and roadways lead to methods based on selecting which sequence of paths or roadways are to be followed in order to reach the required location.

Navigation is about the robot being able to obtain some initial estimate of its position and heading, and then as the vehicle moves through its environment doing its tasks, maintaining an accurate estimate of its position and possibly, the heading. The rules of navigation which are employed to maintain an estimate of its position and heading will produce estimates which differ from the 'true' values. To reduce this divergence, extra information about the position and heading of the vehicle may be obtained from measurements, made on certain qualities of the environment by sensors attached to the vehicle on its way. This can be done with the vehicle halted or while it moves. Viewed in this manner any sensibly observable quality in the surroundings which can be measured may provide this extra information. The source of this ambient information

could be man made or 'natural'.

The regulation of a navigationally determined parameter or its servoing in some way, whilst moving, gives rise to very specific observable behaviour. In an 'ordered' environment within an industrial interior that consists of highways and their intersections the two modes of guidance 'following' and 'reorientating' arise naturally from that environment. More specifically the vehicle is required to translate and to rotate by specifiable amounts. The term guidance is used to describe the algorithms which receive commands, from another process, about which task to perform, provide the commands to the vehicle's control systems which drive the mobile robot, and utilise the navigationally determined information to compute when the parameters of the task have been achieved.

The term guidance can also be applied to the algorithms which use direct feedback from objects within the 'sensor boundary' to alter the vehicle controls to move away from them or towards them. When the robot is to move away from an unmapped observable the term 'obstacle avoidance' is used, and when it is to move towards the observable the terms 'homing' and 'tracking' are appropriate.

The components and context of the research problem include the identification and provision of a structure, the mobile robot; a means of moving that structure around; defining and representing its surroundings; identifying and implementing the guidance algorithms to permit the robot's structure to achieve its tasks in that environment; the maintenance of a model of the robot's whereabouts in terms of its map; the identification and provision of the sensing means to acquire information that is hard to encapsulate in a fixed and determinate form, caused either through the uncertainties in the measurements, inexact models of the processes, or because of the changeable nature of the surroundings; and to identify and provide the means to communicate all of these things in a form appropriate to the artifact. A simplified schematic of the early ideas is illustrated

(see figure 1.1)

A more useful model (see figure 1.2) distinguishes between the forms of navigation and illustrates the relation between navigation, guidance, the vehicle, the mapped connectivity and observables, the task scheduling and planning. The rest of this chapter discusses the three phases of navigation and outlines the guidance experiments performed with the robot, and makes a few observations about the vehicle, the environment, and the need to produce a plan. The detailed theory and experimental support follow this chapter.

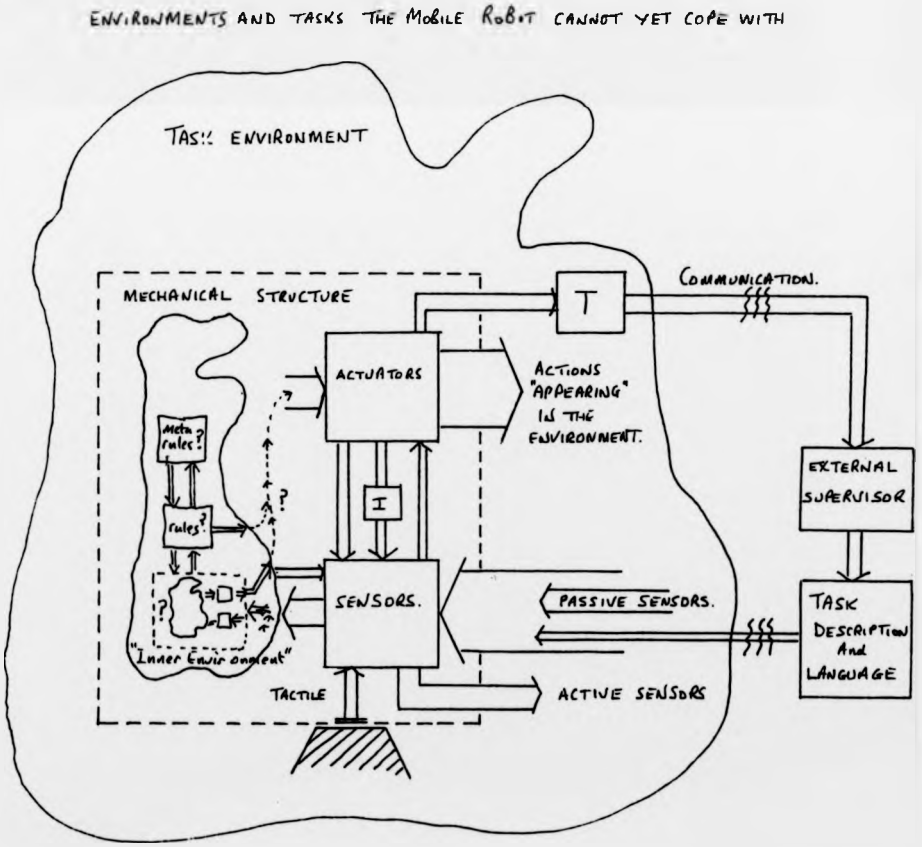

Figure 1.1 A generalised schema for the components of a mobile robot.

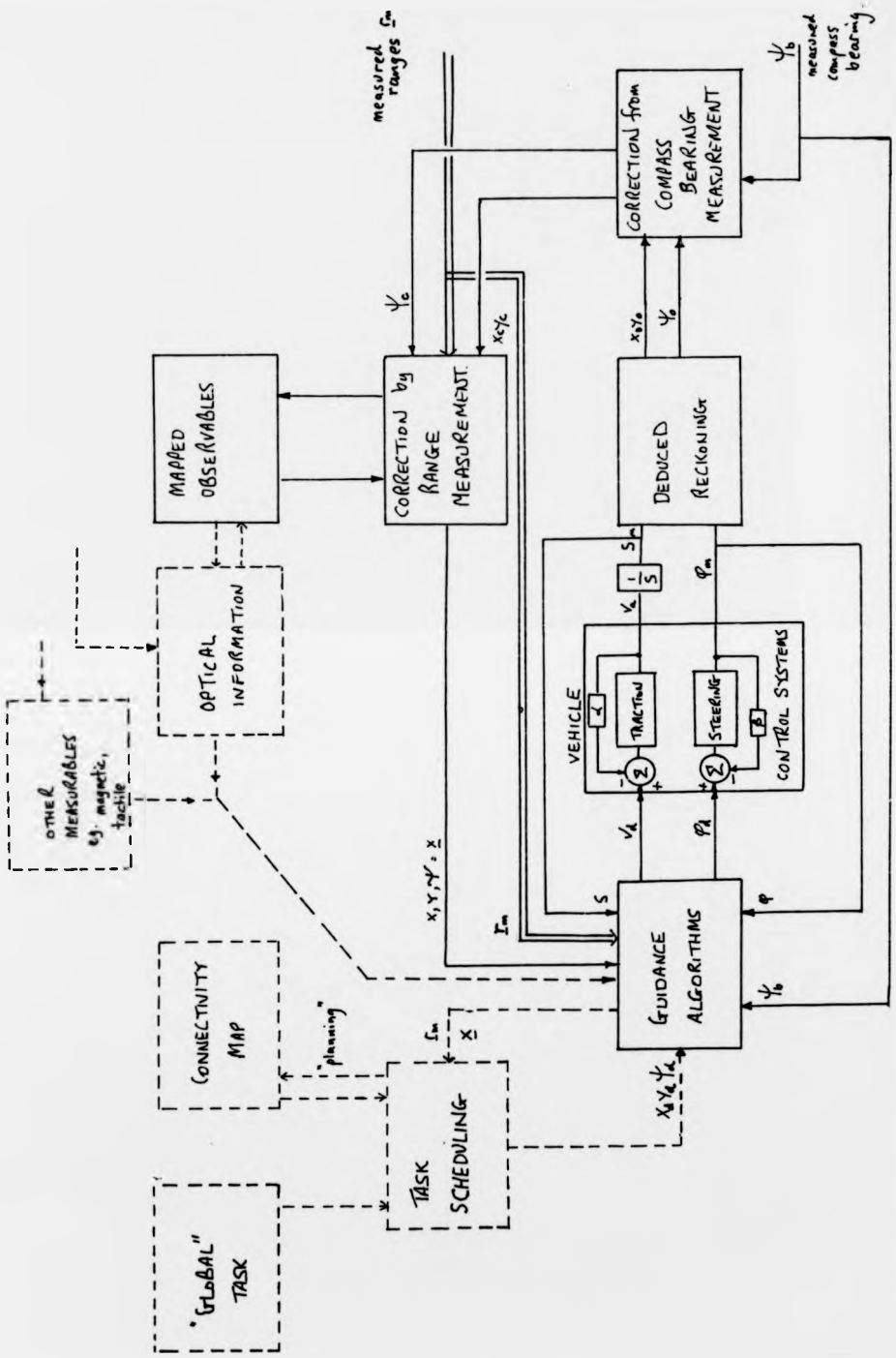

Figure 1.2 The relation between navigation, guidance and the mobile robot. Also shown is the research context within which they may be placed.

1.2 Navigation for Guidance

1.2.1 Deduced reckoning and the accumulation of errors

The programmed movement of parts of the vehicle's structure can result in the overall structure linked to these parts moving along a space path. Turning the drive wheels causes the chassis to move. The transformation of the intrinsic coordinates of this space path to another frame of reference, called a global coordinate system, enable its location to be known to all other objects whose coordinates are expressed in that global frame of reference. If the starting location is given to the robot in these global coordinates, and the robot could, without error, measure the properties of the space path, then it could accurately locate itself globally.

The mobile structure has embedded in it a local frame of reference. The axes of coordinates of this local frame of reference intersect at the differential point (see figure 2.1). The longitudinal axis of the vehicle is the x axis and is also the zero of the heading, or orientation of the robot. The global frame of reference consists of two intersecting orthogonal axes X , and Y . Where these two axes of coordinates intersect is the origin. The absolute bearing is taken as being relative to the direction of the north magnetic pole, and is taken to be the third axis. The global position of the structure is determined from the zero position of its local frame of reference to the zero of the global frame.

By measurement of the rolling rotation of the steered wheel by an odometer, and the steer angle of a tricycle vehicle, or the measurement of the differential rotation of the rear wheels with two odometers, the intrinsic properties of the space path may be estimated. The technique is called deduced reckoning, or dead reckoning. Other methods of determing the space path of vehicles exist. Some rely on measuring the inertial movement of the vehicle and integrating over time to obtain the space

path. These methods suffer from drift and accumulated errors that need to be corrected.

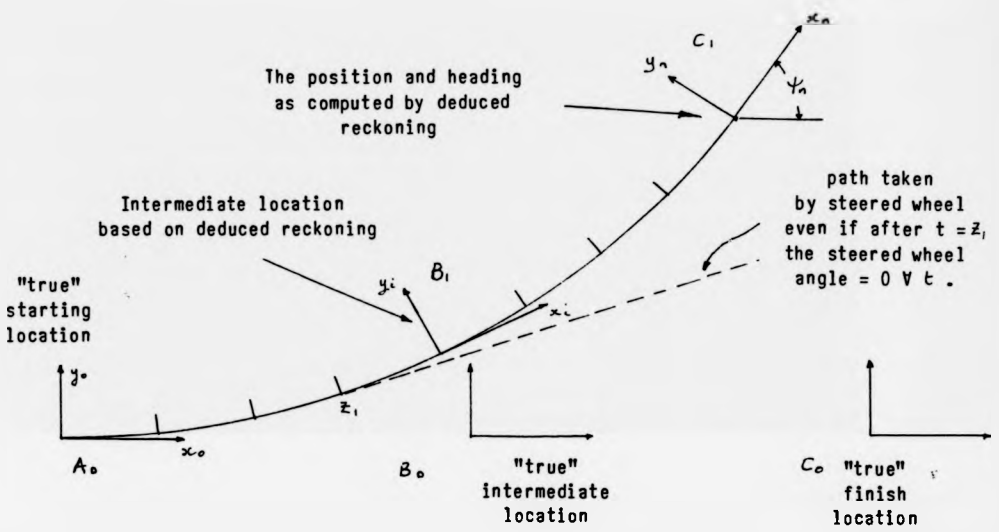

Figure 1.3 Navigation by deduced reckoning. This provides an estimate of the position and heading of the robot. This is based on measuring the distance moved by the steered wheel in rolling , and the angle the steered wheel is pointing, as it rolls. The robot's location is symbolised by the coordinate frame whose zero is positioned at the differential point, and whose orientation is parallel with the x axis. Three frames are illustrated at A_o, B_o, and C_o, to indicate the vehicle having actually moved forward with zero curvature. This being its 'true' track. The eventual divergence of any dead reckoned estimate from the actual track is symbolised by the frame at B_1 , and C_1 . The short normal lines along the deduced track illustrate the discrete nature of the technique. The divergence is illustrated here for a constant steer angle error. Although an error may exist for 'short' duration once present its effect remain. The tangential line is the track which would result even if after location, $\hat{t}_1$,

there was no further error in the steer angle.

The specification of the measurement system used to obtain the information put into the equations that correctly describe the space path enable quantitative statements to be made about how far and how long these measurements can be effectively used. Additionally if the noise statistics of these measurements are known or estimatable, then quantitative statements about the probable location of the robot may be made.

1.2.2 The need to correctly orientate the local frame

As the vehicle moves the computed position and heading can be in error. If a measurement is made that depends on the correct orientation of this frame then the projection of that measurement onto one or both of the other axes will cause an additional error to be introduced into the estimate of the position along those axes. This is the case for range measurements. These are made at some angle with respect to the vehicle's structure and this angle needs to be known A direct measurement of the magnetic bearing can be made and used to provide a correction to the computed heading. This is an 'absolute' measurement.

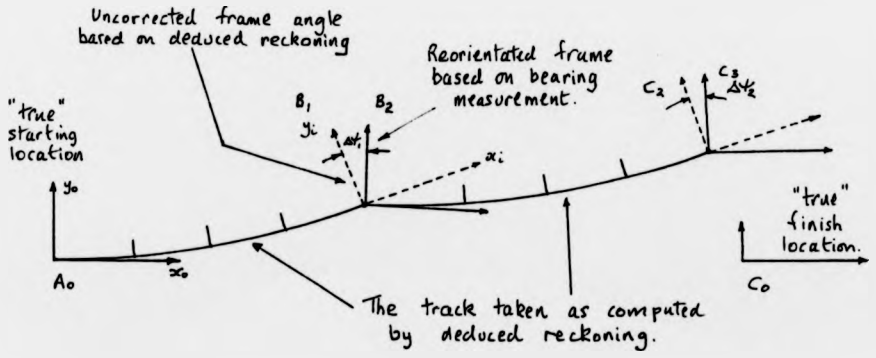

Figure 1.4 The corrected orientation of the robot's computed heading based

on the direct measurement of the compass bearing. The robot is again shown as having started from location A_o, and actually having moved to location C_o. By dead reckoning the computed position and heading is B_1. At this location a compass bearing measurement becomes available. This information is shown as having been used to modify the computed heading estimate, and this is reflected in the frame shown reorientated by $\Delta\psi_1$. The odometer and steer angle measurements continue then to be used to deduce the track from B_2, to C_2. At C_2, another compass bearing measurement becomes available. The information thus gained is illustrated as having been used once more to reorientate the frame this time by $\Delta\psi_2$.

1.2.3 Environmental sensing to reduce the remaining error

Although the orientation of the local frame has been corrected its position can still be in error. This error can be reduced. The embedding of objects of known geometric disposition into the global coordinate system will be briefly discussed as a means to represent physical objects other than the robot in the surroundings. These symbols and their relations are the map. If the vehicle carries further sensing instruments to acquire information from its ambient about the geometric relation of the structure of the robot to these original objects, then the information acquired can be used by the mobile robot to reduce its positional uncertainty. This is illustrated in figure 1.5

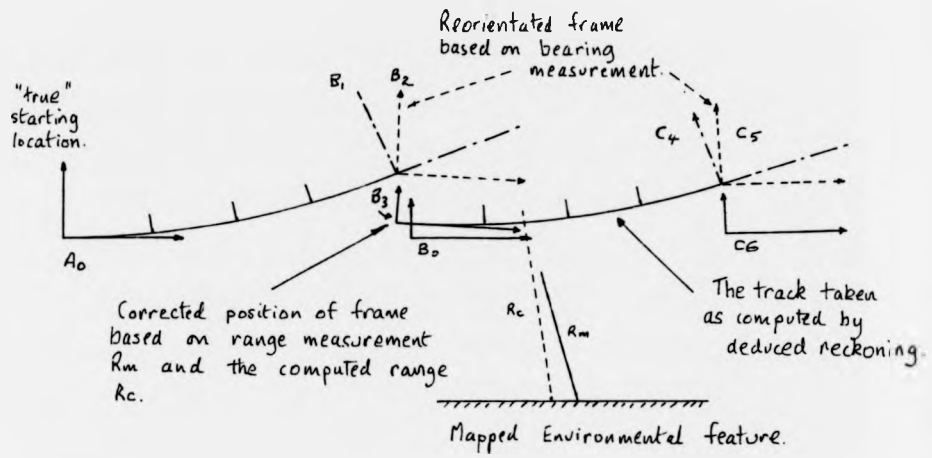

Figure 1.5 The repositioning of the zero of the local frame of reference based on range measurements. The vehicle is again symbolised as having moved forward with zero curvature from A_o, to B_o. The deduced position and corrected heading of the robot is illustrated at B_2. This computed location being based on odometer, steer angle, and compass bearing measurements, as previously described. At B_2, the first sonar range measurement becomes validly available. This is R_m, and is made from the robot's physical location. Based on the robot's computed location, and the known position and orientation of the range sensors a computed range R_c, can be calculated. The difference between these ranges can be used to notionally reposition the zero of the coordinate frame, the differential point from B_2, to B_3. As the vehicle continues to move the odometer, steer angle, and compass bearing measurements are once more used to locate the robot. At C_5, the next range measurement becomes available and this can be used to reposition the frame from C_5, to C_6. This location C_6, being near to where the robot was physically.

1.2.4 Uncertainty in the navigated location

The instruments used to make these environmental measurement may be expected to introduce additional errors. The specification of the statistics of the unwanted noise in the signal then places a further limit to the reduction of the uncertainty that is possible along each of the coordinate axis. The numeric accuracy of the algorithms may also influence the navigational accuracy

The rate at which these environmental measurements can be made may be also expected to limit the rate at which the uncertainty along each of the coordinate axes can be reduced, even if there were no measurement error. The rate of convergence of the algorithms used to process the measurements will also limit the rate at which the uncertainty can be reduced

Both the lower resolution limit and the rate at which the uncertainty is reduced may all be different along each of the three coordinate axes. The characteristic of the growth and decay of this uncertainty may vary from place to place. It may also vary at different times at the same place.

When the vehicle moves over ground that cannot be regarded as a plane, then in general three other coordinates are required to reference the mobile robot to an origin. Measurements to establish the position and orientation along the other three coordinates can be expected to contain errors, and these will also need to be reduced. The qualities selected for sensing for a mobile robot operating on a plane must in the first instance provide the information about the robot's position along the three coordinate axes. When available other measurements can be introduced to refine and augment this navigated position, and heading.

The use of an instrument to detect and process reflected light from objects in the environment to provide relevant and timely navigational data is not discussed in this thesis.

1.3 The vehicle

1.3.1 The vehicle and the environment

The physical structure to which the actuators processors and sensors are attached is the chassis of the mobile robot. The geometrical arrangement of the drive wheels, the steering mechanism and any supporting wheels being called the vehicle's architecture. A mechanism can be described kinematically. The spatial movement possible from a particular vehicle's architecture can be described kinematically. It is the properties of this space path which are measured to produce the deduced reckoned estimate of position and heading. Some mechanisms' kinematics permit unlimited changes to the curvature of their path. The curvature can be changed from zero to infinity, the 'turtle' architecture, for example. However, the inability of the castor, its static support mechanism, to retain its full castoring action above certain loads, coupled with the lateral torques generated when reversing direction, can reduce its usefulness in practical circumstances.

The environmental surface to be moved over affects which type of mechanism can and should be used to move the vehicle structure. Experience with vehicles on each surface has evolved mechanisms which provide the required tractive force and mobility. There are many such mechanisms. This research has not evaluated or compared these mechanisms. They include legged [McGhee 1979], wheeled [Nilsson 1969; Miller 1977; Moravec 1980; Marce 1981], and tracked [Larcombe 1978]. Each will have its own characteristics, and the selection of the mechanism is influenced by the environmental surface to be moved over. There are broadly two types of terrain for a ground based vehicle. Synthetic surfaces with a variety of coatings or 'natural' surfaces whose composition can vary from granite to clay. For a plane man-made surface that is hard and composed, for example, of concrete or tarmac and with atmospheric pressures and temperatures suitable for humans a pneumatic tyred vehicle is appropriate.

1.4 Guidance

The structure of the mobile robot was to be moved about in a controlled manner, by regulating the demands into the motor control systems that in turn caused the wheels to rotate and turn. Although these demands were initially modulated by direct measurement from the sensors, it is assumed that in a 'complete' system that the navigation processes would provide this information. The control algorithms were tested experimentally. The guidance system was assumed to receive its task commands from some other process called a task scheduler.

1.4.1 Longitudinal and lateral guidance

The vehicle was to be started and stopped in a controlled manner. From a stationary position the vehicle was moved forward for a fixed distance and then brought to rest. The longitudinal guidance from the odometer experiments demonstrate how this was done, and the fidelity of positional control that was possible. Briefly, the traction control system was calibrated, and the relevant speed demand to positional movement obtained. These 'open loop' relations were then used in a saturating proportional controller. The results were encouraging. Essentially, the vehicle could be moved forward over short distances, and positioned to within the resolution of the odometer. Beyond these distances the effects of non zero curvature motion were noticeable. To counteract this tendency, direct guidance from the measured lateral range was used to control the steered wheel angle as it move forward. The lateral motion of the vehicle was controlled by this guidance provided by the measured lateral range. Again a saturating proportional controller relating the difference between measured and demanded side range to steer angle was programmmed. To be able to do this the steering control system was calibrated. To test the sensitivity of this controller, a physical protrusion was used as an environmental pulse disturbance. The combined guidance of the lateral and longitudinal motion of the vehicle being subsumed under the one task

description of 'following'.

1.4.2 Guidance to reorientate

To move from one path segment to another requires that the direction of motion be changed. The kinematic description which follows from the form of the vehicle determines whether the rotation can be made without translation. The tricycle vehicle has to translate in order to rotate. The robot was placed in a 'T-junction' and using the 'following' task to initially move and stabilise the forward motion, the sonar range measurements to the environmental constraints were used to intiate a turn to take the robot from one path to another. The distance travelled along a constant curvature arc to steer angle relation was used to calculate when the robot heading had changed by a specified angle. The experiments to support this hybrid guidance are described.

1.4.3 Direct guidance

Direct guidance refers to the avoidance of obstacles and to homing. During the execution of the two basic motion tasks, unmapped objects may occur, which block the way and need to be avoided. Avoidance of obstacles implies the need for their detection. If the mobile robot can navigate accurately, and an obstacle is detected then, if desired its position can be inserted into the map at the 'true' coordinates. The results from a simulation and which moved the position and heading of a path curvature limited vehicle around a stationary object and then returned the vehicle back onto its original course are given.

1.5 The environment

A few general comments are made and then one element, the line segment is introduced to enable a very simple planar world model to be constructed. Four environmental examples are illustrated. They provide an elementary, but formal basis with which to model the environments used in the guidance experiments.

1.5.1 The connectivity and the observables

An environment can be viewed and classified in an indefinite number of ways. The main qualities of concern in mobile robotics are the routes that can be traversed, and the aspects of the environment that can be sensed. These qualities are the environments connectivity, and its observables.

The suitability of a route can be affected by the type of vehicle used. The kind of vehicle used can influence what may be regarded as traversable. Even though there may not be an obtrusion present the properties of the surface moved over can act as an effective barrier to movement. It was assumed that the tractive forces would always be sufficient to move the vehicle.

A quality that can be sensed and then measured may be regarded as a component within an observational space. The components of this space may be initially incommensurate, and some common metric needs to be adopted. The ability to sense and measure qualities of the enviroment places a limit on what may be regarded as an observable by the robot. If the robot cannot currently measure or reliably deduce information about say, the second spatial derivatives of a surface then there would be no immediate value in mapping this quality.

Since man-made highways are semi-permanent, a representation of the environments connectivity could be constructed. The elements to model the connectivity of an environment were line segments of zero curvature, of defined length, and orientation. The orientation of these segments

being defined so as to indicate the general direction of travel.

Associated with these paths were assumed to be observable elements that could be arranged around these paths to 'construct' an environment. These elements were also assumed to be composed of line segments of a defined length, position, and orientation. The orientation of these segments being perpendicular to the line defined by the length. With these segments, corners, corridors, T-junctions, and cross-roads can be constructed. Then these grouped segments can themselves be used to compose an environment.

1.5.2 A component to model the environment

The basic element proposed to model the environment is defined in the illustration below.

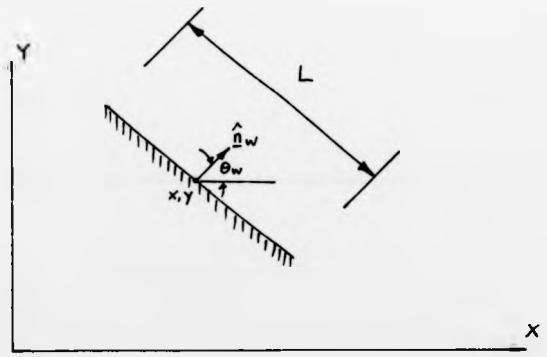

Figure 1.6 The line segment. The central coordinates of the line segment are, x , y , the length is L and the orientation is θ_w.

$$\hat{n}_w = [\cos(\theta_w) \sin(\theta_w)]^T.$$

A rationale for this type of proposed element forming part of the component basis of the map follows. With this single element structures to reflect the observables can be built. The implementation of such structures forms part of the evolving area of computer graphics. The techniques, methods, and mathematics to describe, input and manipulate such real world structures being developed there. This is taking the form of geometric data to reflect and to describe the real world. Since the

robot's basic navigation task is to determine what its position and heading are, and these are geometric concepts, then the research and results from computer graphics could be used by an autonomous mobile robot. The development of efficient and rapid hardware and the associated software, to manipulate the information contained in the 'data structures' to obtain different viewpoints, having its analog and use within the mobile robot needing to compute efficiently and rapidly, what its sensing 'viewpoint' will be, as it moves around. A few of the environmental 'constructs' that could be found in an industrial interior and could be constructed from line segments are illustrated (see figure 1.7). This aspect of the research was not pursued further.

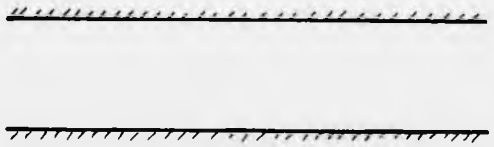

Figure 1.7 (a) The corridor or alley.

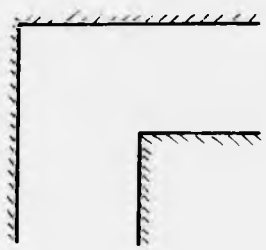

Figure 1.7 (b) The corner

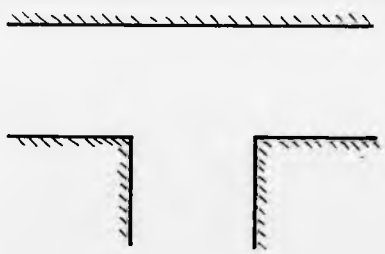

Figure 1.7 (c) The T-junction.

Figure 1.7 (d) The cross roads.

1.6 Methods of instructing robots in their tasks

1.6.1 'Traditional' methods

The command instructions to move a mechanism through space in some predetermined way, that is according to some rule, need some form of memory. Mechanical devices achieve this by using the relative arrangement of gears, linkages, and cams, to produce the kinematic motion. The 'memory' of the required motion being contained in the disposition of these devices. To produce another space motion requires the rearrangement of the parts. This task is laborious and time consuming. Thus, there arose the need to alter more rapidly the form of the kinematic motion. This led to the 'memory' of what to do, the command instruction, and when to do it, the timing, being stored in another medium, the contents of which could be modified more rapidly. These aspects were initially wired into the electronics and other hardware. The next stage was to allow a human operator to lead the mechanism through the desired sequence of actions. As this is done an electronic recording of the output of sensors is made to characterise the spatial arrangement of the mechanism. Then when the articulation needs to be used, servo systems are used to drive the articulation. The inputs to those servo systems being the difference between those made at the recording stage and the sensor values currently being fedback. This is the 'teach mode' of instructing a mechanism. This 'teach-mode' is frequently used to 'instruct' industrial manipulators. The sequence of actions being recalled and performed indefinitely. A further abstraction has been the substitution of the physical 'teach mode' by a computer language. Although a human still specifies each robot action, the robot is directed with a computer program instead of a manual device.

1.6.1 The necessity produce a 'plan'

Although the 'teach mode' approach may be relevant for a fixed base industrial manipulator, it would seem undesirable to have to drive a vehicle through all the combinations of its routes. Indeed, in some

circumstances, there may simply be to many. What is required is some means of automatically generating a 'plan' to enable the mobile robot to move from place to place. The problem identified by [Doran 1970; Munson 1973; Thompson 1977], is that although with perfect information a computer generated 'plan' might be able to provide a sequence of positions and headings to be adopted in sequence to the navigational accuracy of the mobile robot degrades with distance moved. The resulting positional uncertainty which results then requires that a 'new' plan be generated. One way to increase the interval between the times when this process needs to take place is to attempt to increase the spatial domain over which the position and heading estimate remain valid by improving the mobile robot's navigational 'abilities', and part of this thesis is spent in quantifying this aspect.

The time to produce a 'plan', by whatever method is eventually adopted, is preferably kept below the time taken for the vehicle to reach the location where that decision is needed. The term 'real time ' has a more acute meaning, distinct from that normally employed when discussing, for example, an air-line reservation system. This is especially true with a vehicle that can damage both itself and its environment, and would almost certainly be an undesirable action within most environments. The objective of 'planning' as discussed in the literature is to convert the sensed qualities via their electrical form into a condensed symbolic form. With the common 'measure' of these symbols and their relations, the aim is to manipulate the symbols and relations within this abstraction to produce decisions whose domain of validity would extend beyond the immediate sensor boundary, in a manner similar to route determination before setting off on a journey in a car. The automatic production of plans or task scheduling, to produce the sequence of (X , Y and Ψ) shown in figure 1.2, and that are one of the inputs to the guidance algorithms is not examined further.

circumstances, there may simply be to many. What is required is some means of automatically generating a 'plan' to enable the mobile robot to move from place to place. The problem identified by [Doran 1970; Munson 1973; Thompson 1977], is that although with perfect information a computer generated 'plan' might be able to provide a sequence of positions and headings to be adopted in sequence to the navigational accuracy of the mobile robot degrades with distance moved. The resulting positional uncertainty which results then requires that a 'new' plan be generated. One way to increase the interval between the times when this process needs to take place is to attempt to increase the spatial domain over which the position and heading estimate remain valid by improving the mobile robot's navigational 'abilities', and part of this thesis is spent in quantifying this aspect.

The time to produce a 'plan', by whatever method is eventually adopted, is preferably kept below the time taken for the vehicle to reach the location where that decision is needed. The term 'real time ' has a more acute meaning, distinct from that normally employed when discussing, for example, an air-line reservation system. This is especially true with a vehicle that can damage both itself and its environment, and would almost certainly be an undesirable action within most environments. The objective of 'planning' as discussed in the literature is to convert the sensed qualities via their electrical form into a condensed symbolic form. With the common 'measure' of these symbols and their relations, the aim is to manipulate the symbols and relations within this abstraction to produce decisions whose domain of validity would extend beyond the immediate sensor boundary, in a manner similar to route determination before setting off on a journey in a car. The automatic production of plans or task scheduling, to produce the sequence of (X , Y and Ψ) shown in figure 1.2, and that are one of the inputs to the guidance algorithms is not examined further.

2.0 NAVIGATION BY DEDUCED RECKONING

2.1 Introduction

The objective of this section is to show how the position, and heading of a vehicle can be determined by deduced reckoning and how these predictions compare to the position and heading determined experimentally.

2.2 Theory

The geometry of the tricycle vehicle is defined in Figure 2.1

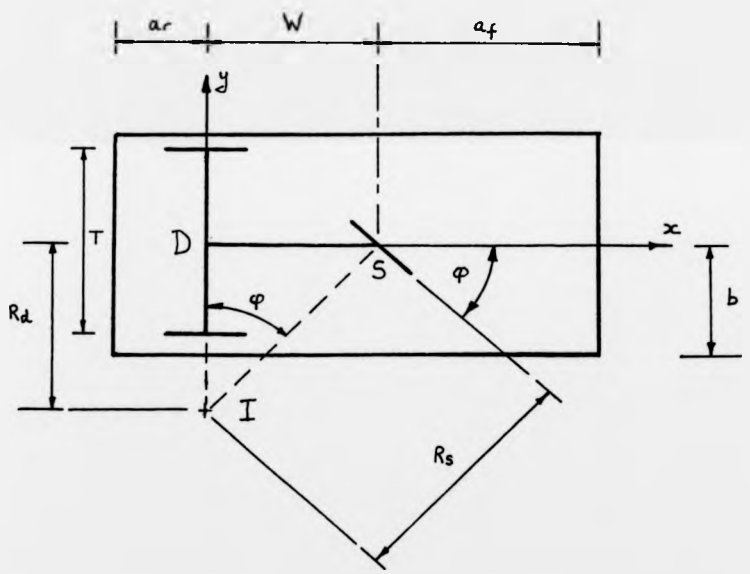

Figure 2.1 A plan view defining the geometry of the tricycle vehicle.

where W = The wheelbase of the vehicle T = The track of the vehicle

D = The differential point S = The steered point

a_r = The rear overhang a_f = The front overhang

b = The semi-width φ = The steer angle

x = The longitudinal axis of the local frame of reference

y = The lateral axis of the local frame of reference

R_s = The radius of the circle of the path traversed by the steered

wheel with a constant steer angle

R_d = The radius of the circle of the path moved over by the differential point with a constant steer angle

I = The point of intersection of R_s , and R_d .

The path of the steered wheel as it moves along one constant curvature segment is shown in Figure 2.2.

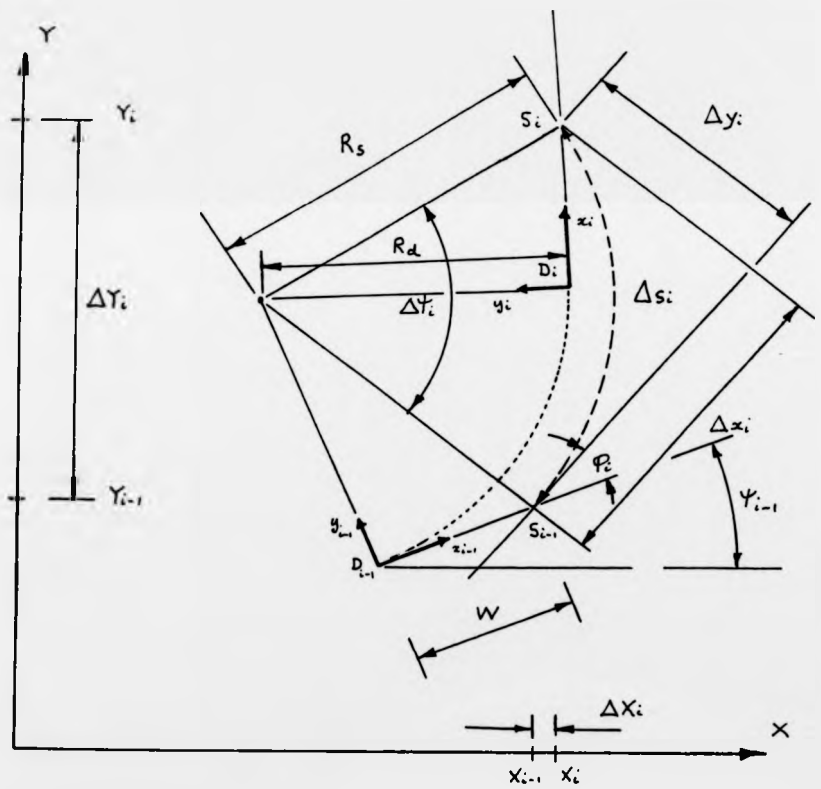

Figure 2.2 The path of the steered wheel as it traverses the ith segment.

where XY = The axes of coordinates of the global frame of reference

X_{i-1}, Y_{i-1} = The i-1 th position in the global frame of reference.

Ψ_{i-1} = The i-1 th heading in the global frame of reference.

ΔX_i = The ith incremental distance travelled by the steered wheel projected onto the X-axis.

ΔY_i = The ith incremental distance travelled by the steered wheel projected onto the Y-axis.

Δx_i = The ith incremental distance travelled by the steered wheel projected onto the x-axis of the vehicle frame of reference from where it was at the i-1 th stage.

Δy_i = The ith incremental distance travelled by the steered wheel projected onto the y-axis of the vehicle frame of reference from where it was at the i-1 th stage.

Δs_i = The ith incremental distance travelled by the steered wheel.

$\Delta\Psi_i$ = The ith incremental change in the body heading of the vehicle.

The heading can be computed from,

$$\Psi = \Psi_0 + \int_0^s K_s\,ds \qquad 2.1$$

and the position from

$$x = x_0 + \int_0^s \cos(\Psi).ds \qquad 2.2$$

$$y = y_0 + \int_0^s \sin(\Psi).ds \qquad 2.3$$

For the tricycle vehicle the curvature at the steered point is given by

$$K_s = \sin(\varphi)/W \qquad 2.4$$

when the along track distance s, and the steer angle φ, are quantised and discrete, the incremental distance moved is given by

$$\Delta x_{ci} = R_{si}.\sin(\Delta\Psi_{ci}) \qquad 2.5$$

and $$\Delta y_{ci} = R_{si}.[1 - \cos(\Delta\Psi_{ci})] \qquad 2.6$$

where $$R_{si} = W.\mathrm{cosec}(\varphi_{mi}) \qquad 2.7$$

and $$\Delta\Psi_{ci} = \Delta s_{mi}.\sin(\varphi_{mi})/W \qquad 2.8$$

The corresponding computed incremental distance moved in the global frame of reference is

$$\Delta X_{ci} = \Delta x_{ci}.\cos(\psi_{c(i-1)} + \varphi_{mi}) - \Delta y_{ci}.\sin(\psi_{c(i-1)} + \varphi_{mi}) \quad 2.9$$

$$\Delta Y_{ci} = \Delta x_{ci}.\sin(\psi_{c(i-1)} + \varphi_{mi}) + \Delta y_{ci}.\cos(\psi_{c(i-1)} + \varphi_{mi}) \quad 2.10$$

$$\Delta\psi_{ci} = \Delta s_{mi}.\sin(\varphi_{mi})/W \quad 2.11$$

When the steer angle is small, the cosecant term in (2.7) becomes large and in the limit when the steer angle is zero the steered radius becomes infinite. The following small angle approximations can be used.

$$\Delta X_{ci} = \Delta s_{mi}.[\ (1 - (z.z)/2.).\cos(\psi_{c(i-1)} + \varphi_{mi}) - 0.5.z.(1 - (z.z)/12).\sin(\psi_{c(i-1)} + \varphi_{mi})\ ] \quad 2.12$$

$$\Delta Y_{ci} = \Delta s_{mi}.[\ (1 - (z.z).2.).\sin(\psi_{c(i-1)} + \varphi_{mi}) + 0.5.z.(1 - (z.z)/12).\cos(\psi_{c(i-1)} + \varphi_{mi}) \quad 2.13$$

with $z = \Delta\psi_{ci}$ 2.14

The ith deduced position of the steered wheel is

$$X_{ci} = X_{c(i-1)} + \Delta X_{ci} \quad 2.15$$

$$Y_{ci} = Y_{c(i-1)} + \Delta Y_{ci} \quad 2.16$$

The ith deduced position of the differential point X_{di} , Y_{di} is

$$X_{di} = X_{ci} - W.\cos(\psi_{ci}) \quad 2.17$$

$$Y_{di} = Y_{ci} - W.\sin(\psi_{ci}) \quad 2.18$$

with the global heading given by

$$\psi_{ci} = \psi_{c(i-1)} + \Delta\psi_{ci} \quad 2.19$$

where $\psi_{c(i-1)} = \sum_{p=1}^{i-1} \Delta\psi_{cp}$ 2.20

As an alternative to the front steered wheel only being instrumented, both rear wheels may be equipped with odometers, to obtain an estimate of the intrinsic coordinates of the space path moved along. The rear wheels may be driven independently or through a differential. The along track speed for each rotating rear wheel is:-

$$v_1 = [\ R_d + 0.5.T\ ].\dot{\psi} \quad 2.21$$

and $$v_2 = [\ R_d - 0.5.T\ ].\dot{\psi} \quad 2.22$$

The speed at the differential point is then

$$v_d = 0.5.[\ r_1.\omega_1 + r_2.\omega_2\ ] \quad 2.23$$

where ω_1 , and ω_2 , are the angular speed of the rear port and starboard

wheels, and r_1 , and r_2 , are their rolling radii

The curvature of the track of the differential point is

$$K_d = [v_1 - v_2]/[v_1 + v_2].T \qquad 2.24$$

The oreintation of the structure is

$$\Psi (t) = [0.5/T].\int_0^t [v_1 - v_2] .dt \qquad 2.25$$

And the along track distance is

$$s_d = 0.5 \int_0^t [r_1 .\omega_1 + r_2.\omega_2].dt \qquad 2.26$$

2.3 Error analysis

The two sources of measurement error are contained in the distance travelled s, and the steer angle φ. At the ith stage, with the additional notation, t = true, c = computed, m = measured, and e = error, and where an error can be in either the measured or computed values, then the computed change in heading is from (2.8)

$$\Delta\psi_{ci} = \frac{\Delta s_{mi} \cdot \sin(\varphi_{mi})}{W} \qquad 2.27$$

but, $$\Delta s_{mi} = \frac{C}{n}\left\{1 + \frac{\Delta r_f}{r_f}\right\} \qquad 2.28$$

where C is the rolling circumference of the steered wheel, 'n' is the number of segments that C has been digitised into, r_f, is the rolling wheel radius, and Δr_f, is a small change in this radius. Also the measured steer angle has an error so with

$$\varphi_{mi} = \varphi_{ti} + \varphi_{ei} \qquad 2.29$$

substituting

$$\Delta\psi_{ci} = \frac{C}{n}\left\{1 + \frac{\Delta r_f}{r_f}\right\}\left\{\frac{\sin(\varphi_{ti}) + \varphi_{ei}\cdot\cos(\varphi_{ti})}{W}\right\} \qquad 2.30$$

$$= \frac{C\sin(\varphi_{ti})}{n.W} + \frac{C}{n.W}\left\{\cos(\varphi_{ti})\varphi_{ei} + \frac{\Delta r_f.\sin(\varphi_{ti})}{r_f} + \varphi_{ei}\frac{\Delta r_f.\cos(\varphi_{ti})}{r_f}\right\} \qquad 2.31$$

the true change in heading is

$$\Delta\psi_{ti} = \frac{C\sin(\varphi_{ti})}{n.W} \qquad 2.32$$

and the additional error is given by

$$\Delta\psi_{ei} = \frac{C}{n.W}\left\{\cos(\varphi_{ti})\varphi_{ei} + \frac{\Delta r_f.\sin(\varphi_{ti})}{r_f} + \frac{\Delta r_f.\cos(\varphi_{ti})\varphi_{ei}}{r_f}\right\} \qquad 2.33$$

If the steer angle was set to produce zero curvature motion then

$$\Delta\psi_{ci} = \frac{C\varphi_{ti}}{n.W}\left\{1 + \frac{\Delta r_f}{r_f}\right\} \qquad 2.34$$

and the accumulated error would be

$$\Delta\psi_{c(i-1)} \triangleq \sum_{p=1}^{i-1}\Delta\psi_{cp} = \frac{C}{n.W}\sum_{p=1}^{i-1}\varphi_{tp}\cdot\left\{1 + \frac{\Delta r_f}{r_f}\right\} \qquad 2.35$$

the change in position measured at each stage is

$$\Delta x_{ci} = \frac{W.\sin(\Delta\psi_{ci})}{\sin(\varphi_{ti} + \varphi_{ei})} \qquad \Delta y_{ci} = W.\frac{[1 - \cos(\Delta\psi_{ci})]}{\sin(\varphi_{ti} + \varphi_{ei})} \qquad 2.36$$

Assuming $\sin(\Delta\psi_{ci}) \doteq (\Delta\psi_{ci})$ and $\cos(\Delta\psi_{ci}) \doteq 1$. then

$$\Delta x_{ci} = \frac{C}{n}\left\{\frac{\sin(\varphi_{ei}) + \varphi_{ai}\cos(\varphi_{ei}) + \frac{\Delta r_i}{r_f}.\sin(\varphi_{ei}) + \frac{\Delta r_i}{r_f}.\cos(\varphi_{ei})}{\sin(\varphi_{ei} + \varphi_{ai})}\right\} \quad 2.37$$

but with the steer angle nominally set to zero this becomes

$$\Delta x_{ci} = \frac{C}{n}\left\{1 + \frac{\Delta r_i}{r_f}\right\} \quad 2.38$$

and $\Delta y_{ci} = 0$

Inserting (2.35) and (2.38) into (2.9) and (2.10) repeated directly below

$$\Delta X_{ci} = \Delta x_{ci}.\cos(\psi_{c(i-1)} + \varphi_{mi}) - \Delta y_{ci}.\sin(\psi_{c(i-1)} + \varphi_{mi}) \quad 2.39$$

$$\Delta Y_{ci} = \Delta x_{ci}.\sin(\psi_{c(i-1)} + \varphi_{mi}) + \Delta y_{ci}.\cos(\psi_{c(i-1)} + \varphi_{mi}) \quad 2.40$$

yields

$$\Delta X_{ci} = \frac{C}{n.W}\left\{1 + \frac{\Delta r_i}{r_f}\right\}\left\{\cos\left\{\frac{C}{n.W}\sum_{p=1}^{i-1}\varphi_{ep}\right\}\left\{1 + \frac{\Delta r_i}{r_f}\right\} + \varphi_{mi}\right\}\right\} \quad 2.41$$

$$\Delta Y_{ci} = \frac{C}{n.W}\left\{1 + \frac{\Delta r_i}{r_f}\right\}\left\{\sin\left\{\frac{C}{n.W}\sum_{p=1}^{i-1}\varphi_{ep}\right\}\left\{1 + \frac{\Delta r_i}{r_f}\right\} + \varphi_{mi}\right\}\right\} \quad 2.42$$

with the global heading given by equation (2.35)

Errors can appear in the measurement owing to elasticity and the changes in the wheel radius, the movement of the wheels in relation to the chassis, the finite wheel width, wheel slip, and 'bumps and indentations' in the surface moved over, and from the quantisation and discretisation of the steer angle.

Assuming $\sin(\Delta\psi_{ai}) \doteq (\Delta\psi_{ai})$ and $\cos(\Delta\psi_{ai}) \doteq 1$. then

$$\Delta x_{ci} = \frac{C}{n}\left\{\frac{\sin(\varphi_{ei}) + \varphi_{ei}\cos(\varphi_{ei}) + \frac{\Delta\eta}{\eta_f}.\sin(\varphi_{ei}) + \frac{\Delta\eta}{\eta_f}.\cos(\varphi_{ei})}{\sin(\varphi_{ei} + \varphi_{ei})}\right\} \quad 2.37$$

but with the steer angle nominally set to zero this becomes

$$\Delta x_{ci} = \frac{C}{n}\left\{1 + \frac{\Delta\eta_f}{\eta_f}\right\} \quad 2.38$$

and $\Delta y_{ci} = 0$

Inserting (2.35) and (2.38) into (2.9) and (2.10) repeated directly below

$$\Delta X_{ci} = \Delta x_{ci}.\cos(\psi_{c(i-1)} + \varphi_{mi}) - \Delta y_{ci}.\sin(\psi_{c(i-1)} + \varphi_{mi}) \quad 2.39$$

$$\Delta Y_{ci} = \Delta x_{ci}.\sin(\psi_{c(i-1)} + \varphi_{mi}) + \Delta y_{ci}.\cos(\psi_{c(i-1)} + \varphi_{mi}) \quad 2.40$$

yields

$$\Delta X_{ci} = \frac{C}{n.W}\left\{1 + \frac{\Delta\eta_f}{\eta_f}\right\}\left\{\cos\left\{\frac{C}{n.W}\sum_{p=1}^{i-1}\varphi_{ep}\left\{1 + \frac{\Delta\eta_f}{\eta_f}\right\} + \varphi_{mi}\right\}\right\} \quad 2.41$$

$$\Delta Y_{ci} = \frac{C}{n.W}\left\{1 + \frac{\Delta\eta_f}{\eta_f}\right\}\left\{\sin\left\{\frac{C}{n.W}\sum_{p=1}^{i-1}\varphi_{ep}\left\{1 + \frac{\Delta\eta_f}{\eta_f}\right\} + \varphi_{mi}\right\}\right\} \quad 2.42$$

with the global heading given by equation (2.35)

Errors can appear in the measurement owing to elasticity and the changes in the wheel radius, the movement of the wheels in relation to the chassis, the finite wheel width, wheel slip, and 'bumps and indentations' in the surface moved over, and from the quantisation and discretisation of the steer angle.

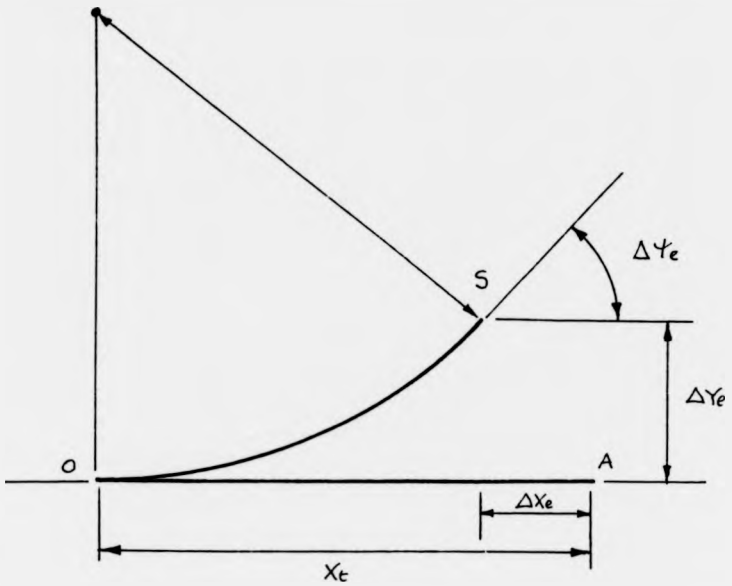

Figure 2.3 The definition of the longitudinal and lateral errors for a nominally zero curvature path. For a constant error in the steer angle the steered wheel traverses a circle. For a constant error the arc distance OS equals the distance OA.

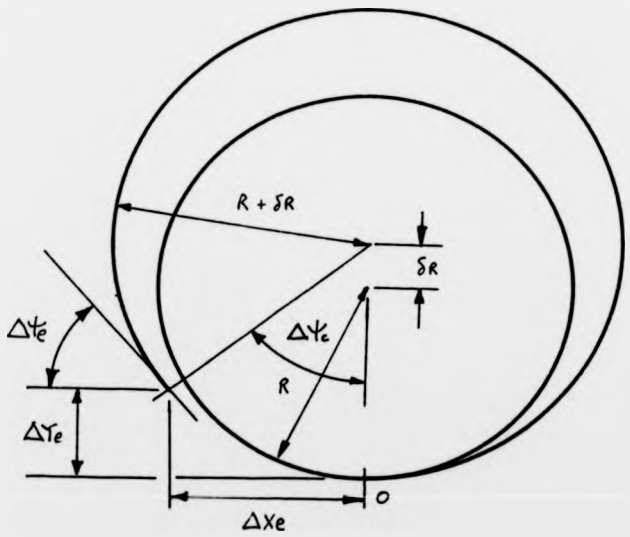

Figure 2.4 The definition of the errors for a path of nominally constant curvature. The point O is the origin.

2.4 Simulation

The equations of deduced reckoning were programmed. The inputs to this simulation were the steered wheel angle, and the along track distance moved by the vehicle for each step of the simulation. Based on these inputs the dead reckoned position and bearing were computed and displayed. This was done initially with simulated input to confirm the robot 'moved' to the expected positon and bearing. A simulated input of zero curvature, and a constant curvature 90 degree turn with the instantaneous centre of turning positioned on the port are shown below in Figure 2.5

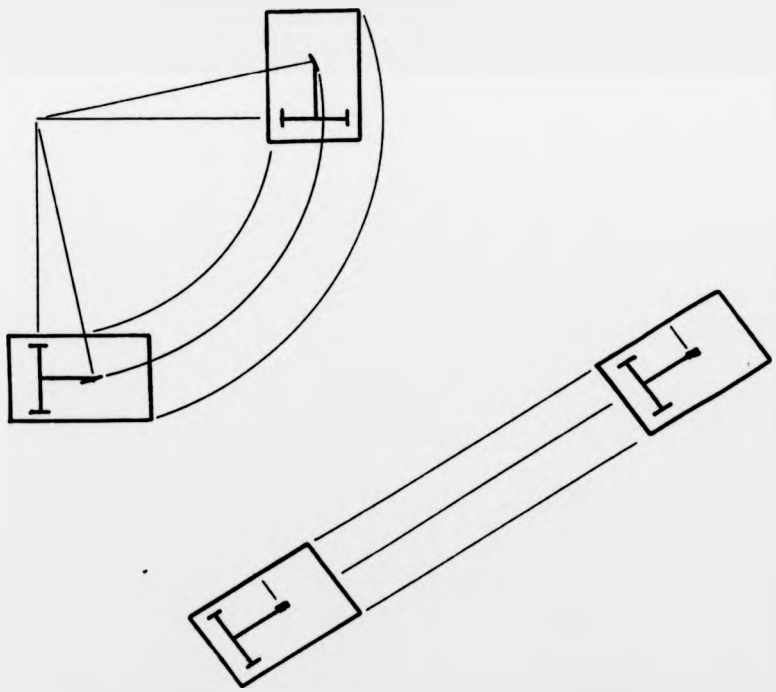

Figure 2.5 Example of the manoeuvres resulting from the input of simulated speed and along track distance moved, to the equations of deduced reckoning. The simulations verified that with these inputs the robot moved to its expected location.

The simulation was used to determine the effects of errors on the deduced position and heading. The results are graphed for a constant error in the measurement of the steered wheel angle.

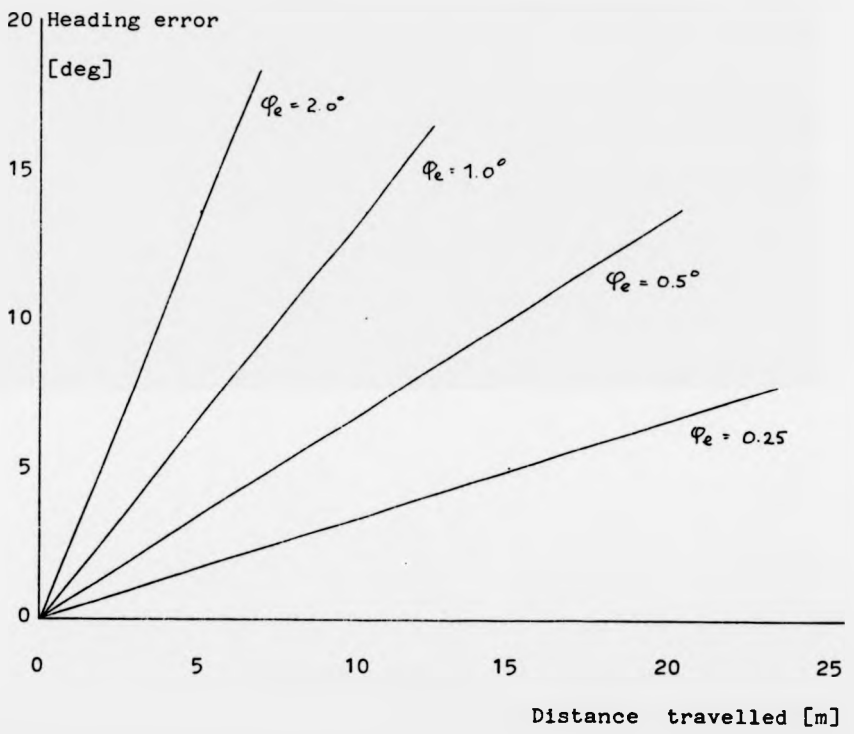

Figure 2.6 The linear growth of the error in the deduced heading versus distance moved for a constant error in the measurement of the angle of the steered wheel.

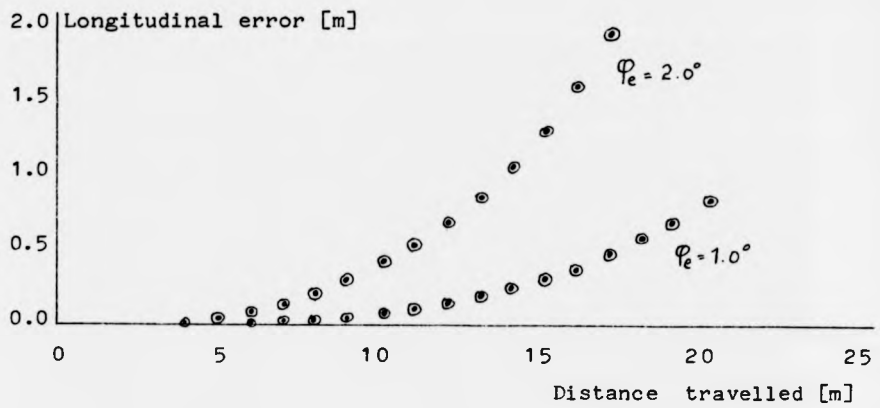

Figure 2.7 The growth of the error in the deduced x position versus distance moved for a constant error in the measurement of the angle of the steered wheel.

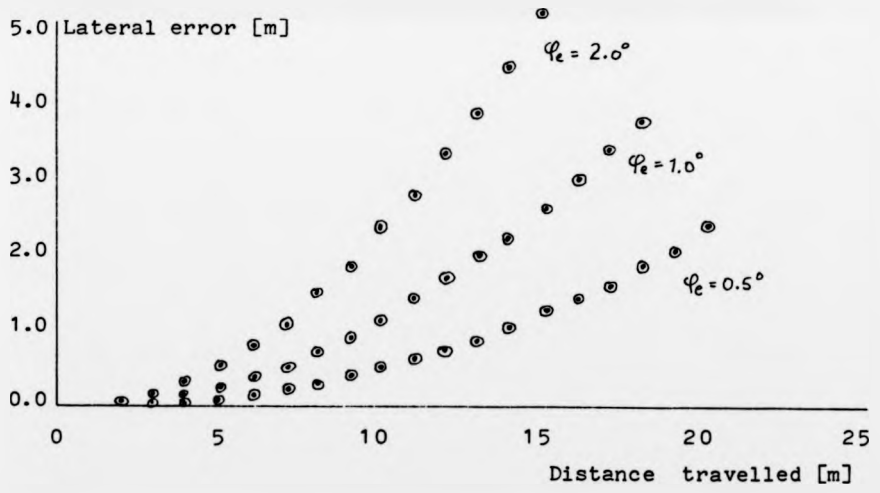

Figure 2.8 The growth of the error in the deduced y position versus distance moved for a constant error in the measurement of the angle of the steered wheel.

2.5 Experimental

The overall objective of these experiments was to obtain the sampled output of the odometer, the angle of the steered wheel, and to determine by deduced reckoning the computed location of the robot.

2.5.1 Calibration of the Odometer

The objective was to relate the true distance moved by the vehicle to the binary output of the odometer as the vehicle was moved between two points a known distance apart. The vehicle was driven manually along a zero curvature line. One odometer unit equalled 0.04 metres.

2.5.2 Calibration of the steered wheel angle

The objective was to relate the angle of the steered wheel set digitally by the control system to the true steer angle. The steered wheel was set to a non zero angle, and the vehicle was driven manually forward until the bearing had rotated by 360 degrees. The along track distance was measured by the odometer. The experiment was done turning both port and starboard. The circumference C_i , of the circle moved along by the steered wheel is given by the formula

$$C_i = [\ 2.pi.W\ ]/\sin(\varphi_i) \qquad 2.43$$

and was used to obtain the steer angle. Figure 2.9 and Figure 2.10 are the experimentally determined relations from Table 2.1.

2.5.3 Calibration results

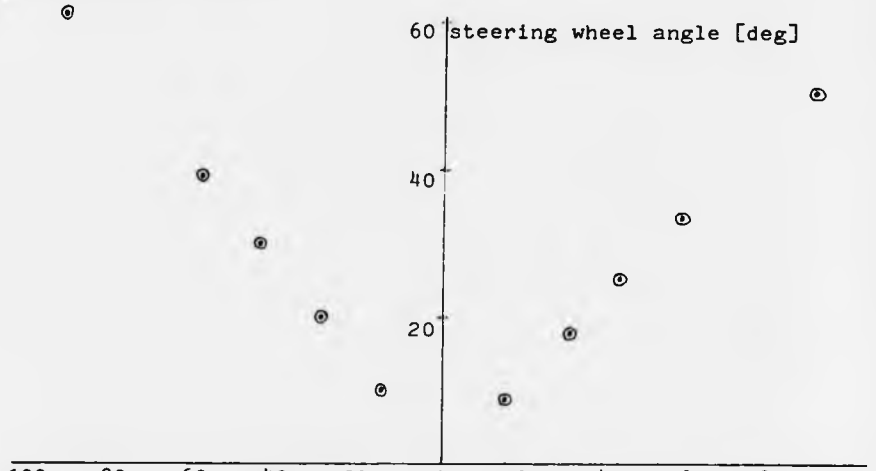

Figure 2.9 The relation between the digital steer demand and the resulting steer angle in degrees. Slope of graph to the port is 0.61, and to the starboard 0.64.

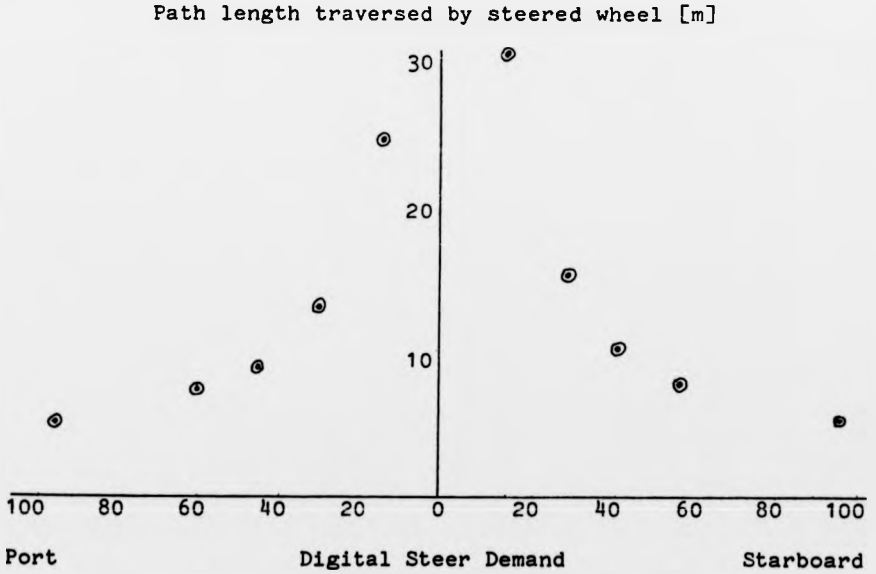

Figure 2.10 The relation between demanded steer angle and the length of the path travelled by the steered wheel.

Steering wheel angle [digital units]		Path length [deg]	traversed [m]		Steer radius [m]	
demanded	achieved	achieved	mean	std.dev	mean	std.dev
-95	-96	-62.4	5.08	± 0.04	0.81	± 0.00
-60	-60	-38.7	7.20	± 0.08	1.14	± 0.01
-45	-45	-30.0	9.00	± 0.08	1.43	± 0.01
-30	-31	-20.1	13.08	± 0.28	2.08	± 0.04
-15	-16	-10.9	23.88	± 0.16	3.80	± 0.03
+15	+14	+8.5	30.32	± 0.28	4.83	± 0.04
+30	+28	+17.3	15.16	± 0.28	2.42	± 0.05
+45	+41	+25.6	10.44	± 0.08	1.66	± 0.01
+60	+56	+33.9	8.08	± 0.12	1.29	± 0.02
+95	+93	+54.7	5.52	± 0.04	0.88	± 0.02

Table 2. 1 Summary of results from experiments to obtain the relationship between digital steer demand, the steer angle of the steered wheel, and the resulting path length of the steered wheel while the vehicle was driven forward until the body of the vehicle had rotated through 360 degrees. Also shown is the steer radius corresponding to that steering angle.

2.6 Motion with zero curvature

The vehicle was manually driven forward with zero curvature. The odometer, and the steering wheel angle were recorded. These data were input to the computer simulation.

2.6.1 Results

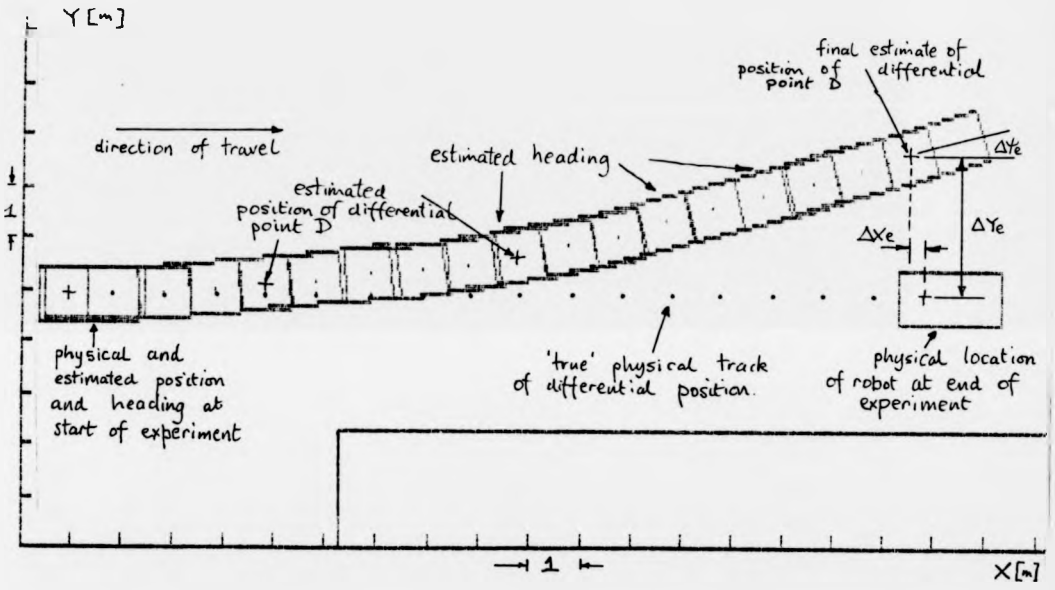

Figure 2.11 Displays the position of the differential point computed by dead reckoning using measurements of the steer angle and along track run distance. Also shown is the computed orientation of the robot, and its relation to the known environmental feature at the start and finish of the simulation. The scale is marked at 1 metre intervals. The dotted horizontal from the start position is the path the vehicle actually followed as determined by external measurement.

2.6.2 Discussion

Although the vehicle was manually driven in a straight line the sampled measurements of the steered wheel show offset from the demanded zero value. As a result the computed heading diverges from the real heading, which increases in proportion to the distance travelled, as given

by (2.34) This error increases without bound. Since the i-1th computed heading is used in the ith computed position estimate, this accumulated heading error increasingly distorts the computed position. This is in addition to the ith measurement errors. Without another means to determine the true heading no correction is possible.

2.7 Motion with constant curvature

The vehicle's speed and the steering wheel angle were controlled by the computer, and set to a constant value. The speed demand was constant. The experiment started and ended with the vehicle stationary. The distance to be travelled, to obtain a rotation in body heading of 360 degrees, was obtained by manually driving the vehicle through one complete circle with a constant steer angle and recording the odometer count. As the vehicle moved forward under computer control, the odometer and steer angle were sampled until the odometer count matched the manually determined distance. The vehicle was then stopped as rapidly as possible using the vehicle's braking system. The experiment was performed five times for each of the steer angles used. The experiments were performed by refreshing the transit interface at 1200 ms intervals, and effectively maintaining a constant input to the traction motor. The graphed results comparing the position and orientation based on the deduced reckoning equations and the actual observed location follow the tabulated results.

2.7.1 Results

Longitudinal error		lateral error		heading error	
measured	computed	measured	computed	measured	computed
-0.15	-0.25	-0.19	-0.22	8.1	-9.1
-0.21	-0.67	-0.12	-0.45	-7.3	-22.0
-0.17	-0.19	-0.20	-0.18	8.0	-7.2
-0.16	-0.14	-0.16	-0.13	6.7	-5.1
-0.22	-0.61	-0.12	-0.43	-8.2	-20.2
correlation 0.92		-0.83		0.96	
mean -0.19	-0.37	-0.16	-0.28	1.5	-12.7
s.d. ± 0.03	± 0.22	± 0.03	± 0.13	± 7.5	± 7.0

Table 2.2 Measured and deduced position and heading of the robot after moving in a 'circle' with a deduced along track distance of 7.20 [m].

Longitudinal error		lateral error		heading error	
measured	computed	measured	computed	measured	computed
-	-	-	-	-	-
-0.27	-0.35	-0.25	-0.24	-7.0	-11.1
0.00	-0.20	0.00	-0.18	0.0	-6.6
-0.32	-0.51	-0.12	-0.35	-7.9	-14.6
-0.49	-0.92	-0.25	-0.46	-17.0	-25.0
correlation 0.92		0.60		0.97	
mean -0.27	-0.50	-0.15	-0.31	-8.1	-14.3
s.d. ± 0.18	± 0.27	± 0.10	± 0.12	± 7.0	± 6.8

Table 2.3 Measured and deduced position and heading of the robot after moving in 'circle' with an along track distance of 9.08 [m].

Longitudinal error		lateral error		heading error	
measured	computed	measured	computed	measured	computed
-0.30	-0.09	-0.12	-0.07	-4.9	-2.3
-1.23	-0.94	-0.26	-0.34	-22.8	-18.6
-0.85	-0.67	-0.22	-0.27	-16.8	-13.8
-0.97	-0.79	-0.21	-0.30	-19.2	-15.7
-0.86	-1.05	-0.26	-0.35	-17.1	-20.6
correlation 0.87		0.98		0.91	
mean -0.84	-0.71	-0.21	-0.27	-16.2	-14.2
s.d. ± 0.34	± 0.37	± 0.06	± 0.11	± 6.7	± 7.2

Table 2.4 Measured and deduced position and heading of the robot after moving in 'circle' with an along track distance of 13.88 [m].

Longitudinal error		lateral error		heading error	
measured	computed	measured	computed	measured	computed
0.15	2.92	0.10	2.64	0.0	48.0
1.30	3.07	0.55	3.09	16.6	53.7
1.75	3.10	0.84	4.25	21.7	69.8
2.21	3.10	1.30	4.44	31.0	72.1
0.81	2.84	0.34	3.09	10.8	55.6
correlation 0.81		0.94		0.91	
mean 1.24	3.00	0.63	3.50	16.0	60.0
s.d. ± 0.72	± 0.12	± 0.42	± 0.71	± 10.4	± 9.4

Table 2.5 Measured and deduced position and heading of the robot after moving in 'circle' with an along track distance of 29.52 [m].

Deduced distance moved forward	mean value of measured heading	deduced distance to bring robot heading to 360 degs	nominal steer radius	$\Delta\Psi_c$ mean value of Deduced change in heading	corrected value of body heading
29.52	16.0	-1.28 ± 0.84	3.80	-19.3	-3.3
13.88	-16.2	0.68 ± 0.28	2.08	18.7	2.5
9.08	-8.1	0.18 ± 0.15	1.43	7.2	-0.9
7.20	1.5	-0.04 ± 0.16	1.14	-2.0	-0.5

Table 2.6 Constant curvature experimental results. The mean additional distance moved either forward or backwards was used to compute the additional deduced heading change consequent from moving the vehicle manually until its body heading had rotated around to 360 degrees. The corrected error in body heading is the difference between the mean 'true' measured and deduced change in heading.

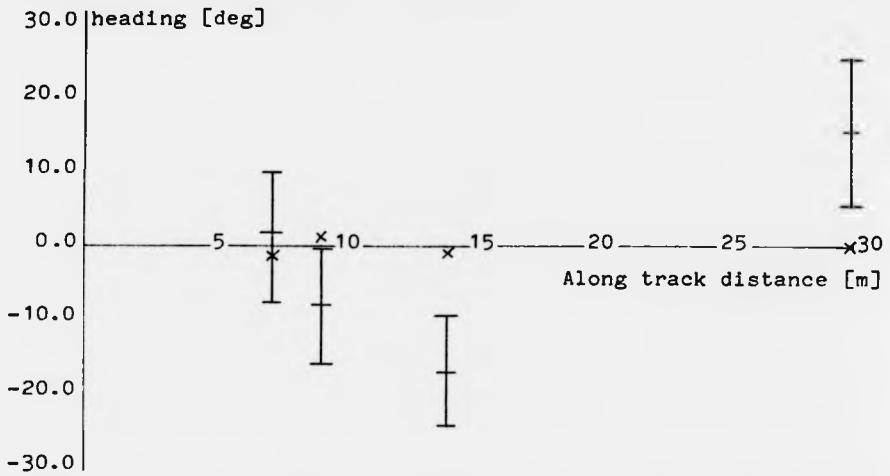

Figure 2.12 'True' vehicle heading versus along track distance. The crosses are the corrected values from Table 2.6. column 7

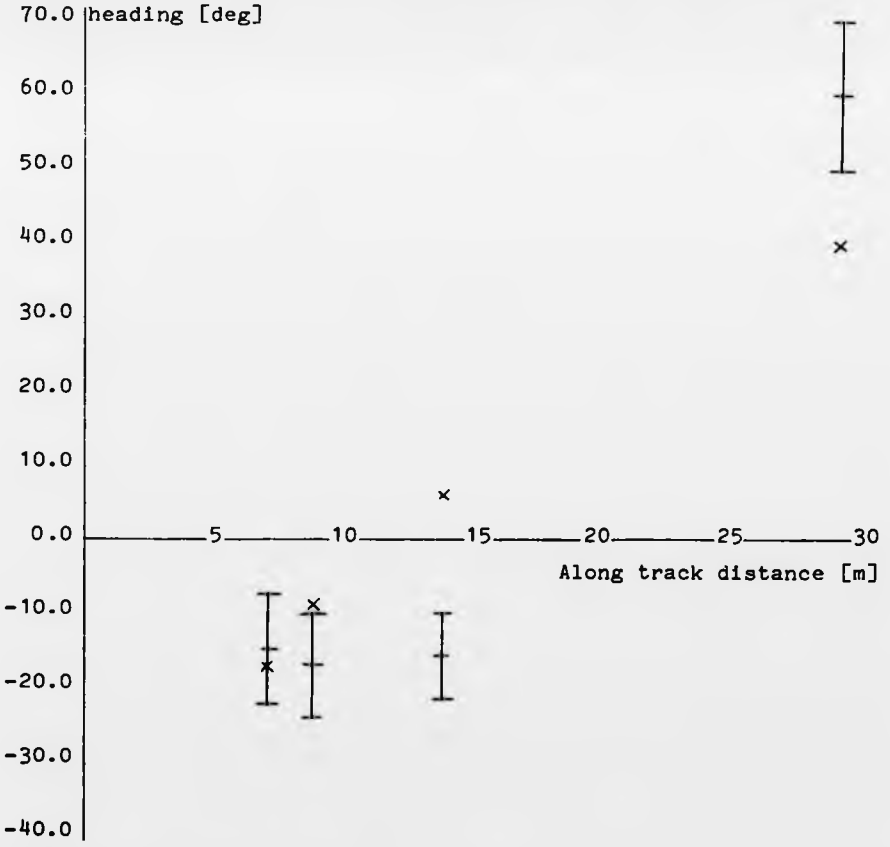

Figure 2.13 Deduced vehicle heading versus along track distance based on manual calibration. The solid lines show the deduced heading that would be obtained if the computations used a steer angle calibration based on the experiment itself. These are indicated by the crosses.

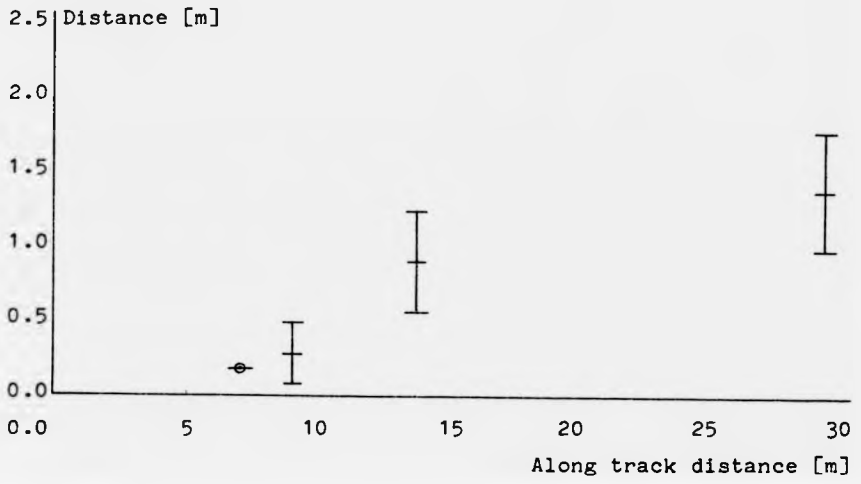

Figure 2.14 'True' measured Euclidan distance from vehicle to the start point.

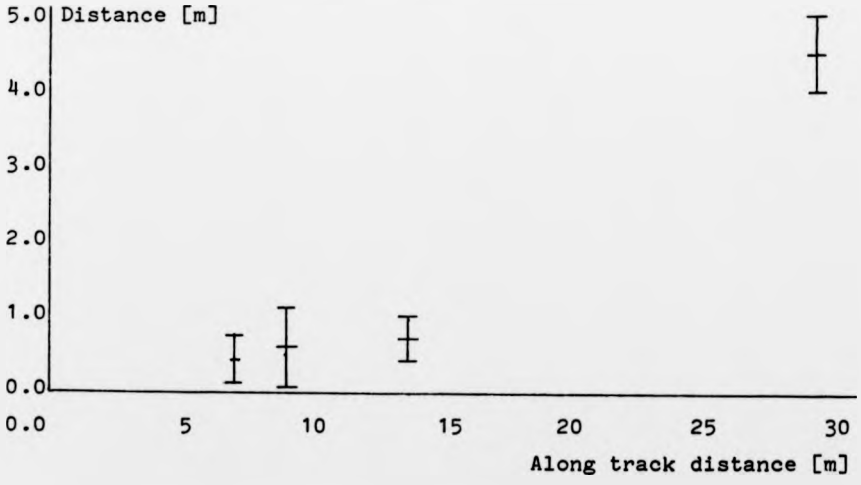

Figure 2.15 Deduced Euclidian distance to the origin based on the manual calibration. Note the change of the vertical scale from figure 2.14

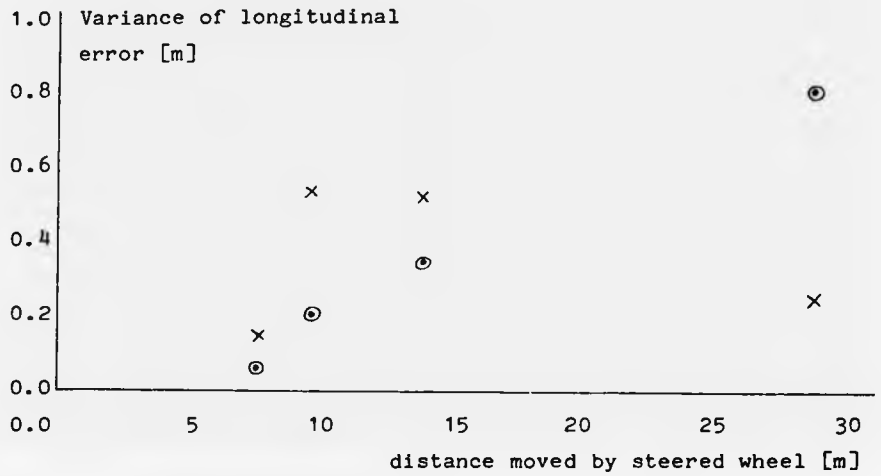

Figure 2.16 'True' and deduced variance of the longitudinal error versus distance moved by steered wheel.

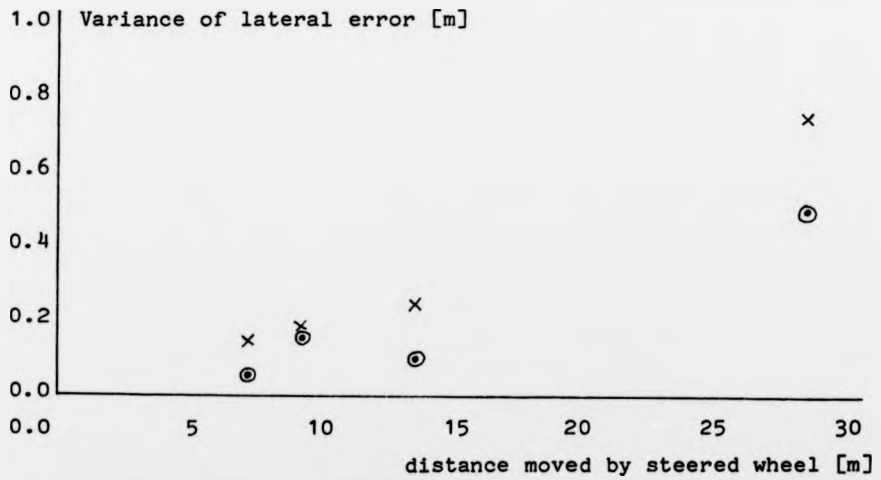

Figure 2.17 'True' and deduced variance of lateral error versus distance moved by steered wheel.

key

⊙ = 'true'

x = deduced

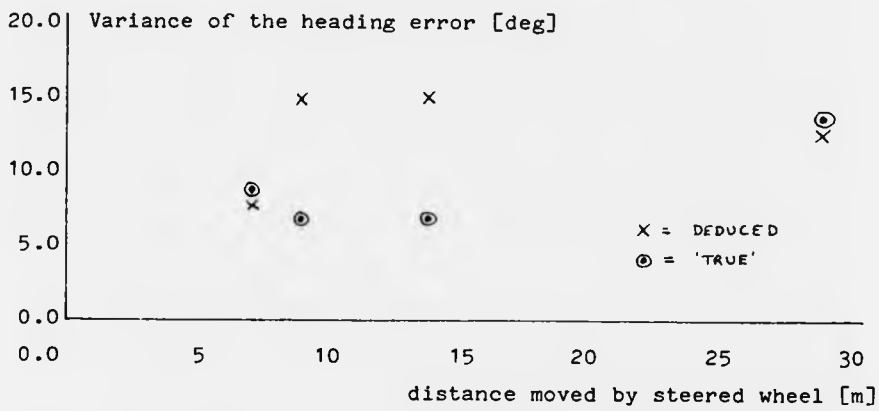

Figure 2.18 'True' and deduced variance of the heading error versus distance moved by steered wheel.

2.7.2 Discussion of results

Experimentally the distance to the origin increased linearly with the distance moved, or equivalently with decreasing steer angle. For the three largest steer angles, (18 to 40°), their is good agreement. The difference between the deduced reckoned and the experimental values was < 0.3 [m], after one complete 'circle'. The variance of the experimental values increased linearly with distance moved. This variance remained below 3% of the distance moved, for all steer angles used. The variance of the error in ΔX_e, and ΔY_e, both increased linearly with distance moved. The slope of increase in ΔX_e, was 0.35s, where s is the along track distance moved, and the slope of the increase in variance of ΔY_e, was 0.19s. With the smallest steer angle the agreement between theory and experiment was low, 4.6 [m] to 1.4 [m] respectively.

The final heading obtained experimentally is graphed (see figure 2.12). When the vehicle had halted it was moved so as to bring the body heading around to 360°. The distance moved to achieve this, along with the relevant steer angle, was used to compute the consequent change in heading $\Delta\psi_e$. This change in the heading was used to modify the results of figure 2.12 so as to obtain the heading values shown by the crosses. The magnitude of these heading errors after this correction were all less than 4°. The computed heading values are constant and about the same value, the difference is less than 2°, for the three largest steer angles. The computed heading for the smallest steer angle was 60°, and this compares with 16°, obtained experimentally. However, if these dead reckoned heading estimates are adjusted by the mean value of the deduced change in heading of Table 2.6 the relation becomes linear and increases with distance moved. For small steer angles and large distances moved the deduced heading is an over estimate, while for large steer angles and small distances moved the heading is an underestimate. From (2.33) the heading error has a minimum value at each stage given overleaf by

$$\tan(\varphi_{t_i}) = \frac{1}{\varphi_{e_i}}\left\{\frac{\frac{\Delta r_{f_i}}{r_{f_i}}}{1 + \frac{\Delta r_{f_i}}{r_{f_i}}}\right\} \qquad 2.44$$

and for Δr_f = 0.005 and r_f = 0.203, the value of the steer angle error at each stage would need to be about 0.06 of a degree at each stage to obtain the minimum value of about 20 degrees corresponding to a distance moved around the circle of 11 [m]. The variance of both the computed and experimentally determined heading remained constant and less than 15°, for all distances moved.

A computer simulation that varied the constants of calibration showed that small changes in these values would produce large variations in the dead reckoned heading (see figure 2.19). A 5% change in the odometer to count relation, and a change from 0.62 to 0.65 in the steer angle to digital calibration results in a final heading error for the smallest steer angle of 35°.

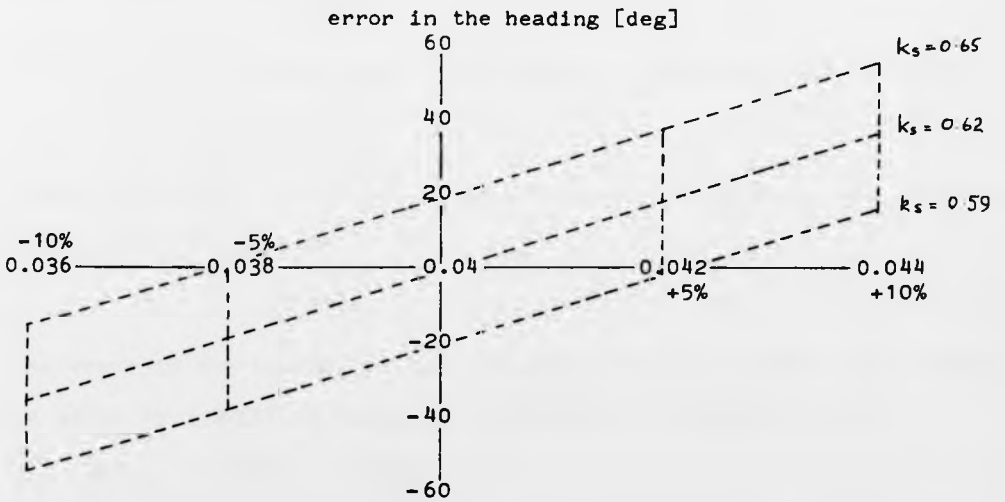

Figure 2.19 Variation in body heading obtained by simulating a change in the calibration constants for the steer angle k_s, and odometer k_o.

These errors led to a comparison between the dual rear wheel odometer system, and the implemented front wheel odometer and steer angle system. The along track distance moved by each of the rear wheels is

$$\Delta s_1 = [R_d + 0.5.T].\Delta\Psi \quad 2.45$$

$$\Delta s_2 = [R_d - 0.5.T].\Delta\Psi \quad 2.46$$

with

$$\Delta s_i = r_i . \Delta\theta_i \quad i = 1,2 \quad 2.47$$

where r_i is the rolling radius of the rear wheels, and $\Delta\theta_i$, is the angle turned through. Rearranging, the heading angle turned through is

$$\Delta\Psi = \frac{r_1 . \Delta\theta_1 - r_2 . \Delta\theta_2}{T} \quad 2.48$$

If the vehicle actually moves with zero curvature then with the same tyre radius $\Delta\theta_1$, and $\Delta\theta_2$, will be the same. If however the radius of one wheel is different from the other then

$$r_2 = [\, r_1 - \Delta r_1 \,]. \Delta\theta_1 \quad 2.49$$

Substituting into (2.48) the error in the heading is

$$\Delta\Psi = \frac{\Delta r_1 . \Delta\theta_1}{T} \quad 2.50$$

For the rolling circumference of the wheel C , quantised into 'n' segments

$$\Delta\theta_1 = \frac{C}{r_1 . n} \quad 2.51$$

substituting (2.51) into (2.50) the error in the bearing for the dual rear wheel odometer system is

$$\Delta\Psi = \frac{C\,\Delta n . 1}{n\, r_1\, T} \quad 2.52$$

The error in the heading at each stage with the front wheel instrumented is given by (2.33) and equating with (2.52) and cancelling gives

$$\frac{\Delta r_1}{r_1}\frac{1}{T} = \frac{\varphi_e}{W}\left\{1 + \frac{\Delta r_f}{r_f}\right\} \quad 2.53$$

If the change in tyre radius was the same for both rear wheels the heading error would be zero, but a longitudinal error would exist. If the change in radius of one of the rear wheel tyres and the front tyre on the tricycle was the same the heading error would become equal only if the steer angle error was equal to (2.54), given overleaf.

$$\varphi_e = \frac{W}{T}\left\{\frac{\frac{\Delta r_1}{r_1}}{1 + \frac{\Delta r_f}{r_f}}\right\} \qquad 2.54$$

For the experimental vehicle with $\Delta r_f = 0.005$, $r_f = 0.203$, and $W = 0.717$ $T = 1.0$, all in metres, the steer angle error would need to be < 0.21 degrees. With the single odometer, and steer angle measurement there appears to be no way for the control system to independently measure when the steered wheel is pointed exactly parallel with the longitudinal axis of the vehicle. There is no inbuilt zero curvature 'reference' for the steer angle. This analysis suggests the dual rear wheel system will be superior to the front wheel system. The problem is now to ensure even loading of the rear wheels. If the rear wheels were driven separately then it would be necessary to ensure identical speeds for zero curvature motion to result.

The use of deduced reckoning to compute the position and heading of a vehicle can be performed by using a number of different system configurations. [Myer 1970], identified the use of an inertial compass and odometer system, or a magnetic compass and an odometer system to compute position and heading. The use of rear wheel odometers is proposed by [Myer 1970; Lezniak 1976; Tsumura 1978]. These workers introduce the simple rules contained in (2.1),(2.2), and (2.3). That the technique of deduced reckoning introduces errors into the position and heading estimates and that these errors accumulate can be seen to varying degrees in this work. An analysis of the source and effect of these errors, was not available in the literature. From his experimental work Myer identified tyre pressure differences and the consequent systematic errors these introduced into the dual rear wheel odometer system, as being of more importance than the computational inaccuracies, but with no supporting theory.

The theory of deduced reckoning has been extended to enable the effect of errors in the front tyre rolling radius, and the steer angle,

for a tricycle vehicle moving along a nominal zero curvature line to be quantified. An expression for the error in the vehicle's heading as it moves with nominally zero curvature for a dual rear wheel system has also been obtained. The location estimate has been shown to be sensitive to small changes in the calibration constants.

2.8 Conclusions

The technique of deduced reckoning can be used to estimate the position and heading of a tricycle vehicle, whose front wheel has been instrumented to measure the steer angle and the along track distance.

This can be done for both constant curvature and zero curvature motion.

The further the wheels travel the more uncertain these estimates become.

For zero curvature motion the lateral positional error accumulates more rapidly than the longitudinal error.

The heading error with the front steered wheel instrumented is proportional to the error between the 'true' steer angle and the measured steer angle.

For constant curvature motion there is a steer angle which results in a minimum value for the heading error.

A mobile robot using deduced reckoning to locate itself will require other means to reduce the effect of the accumulated location errors.

If a mobile robot is to navigate using deduced reckoning and the needed accuracy in the location estimate, for some given travel distance, can be specified, then this specification of the accuracy, will determine the necessary resolution that the measuring instruments must possess for this specification to be met. The 'noise statistics' in the measurement will also place a limit to the spatial extent over which the mobile robot can move and still be assured that its estimated position and heading can be relied upon.

A dual rear wheel odometer system has been analysed and its associated heading error compared with a front wheel odometer, steer angle system. For equal error in the rolling radius, the dual rear wheel system accumulates a smaller heading error.

3.0 NAVIGATION with an ODOMETER and a COMPASS

3.1 Introduction

The objective of this section is to show how the position and heading of the vehicle as determined by deduced reckoning can be augmented by the measurement of the robot's bearing to reduce the error associated with the deduced heading The experimental results that show this is possible are given. The compass measurement as has already been indicated in Chapter 1.0 should be made prior to performing the range based navigation.

3.2 Theory and error analysis

The incremental change in position and heading in the global frame can now be written as,

$$\Delta X_{ci} = \Delta x_{ci} . \cos(\psi_{m(i-1)}) - \Delta y_{ci} . \sin(\psi_{m(i-1)}) \quad 3.1$$

$$\Delta Y_{ci} = \Delta x_{ci} . \sin(\psi_{m(i-1)}) + \Delta y_{ci} . \cos(\psi_{m(i-1)}) \quad 3.2$$

with $$\Delta x_{ci} = R_{si} . \sin(\Delta\psi_{mi}) \quad 3.3$$

and $$\Delta y_{ci} = R_{si} . [1 - \cos(\Delta\psi_{mi})] \quad 3.4$$

with the change in measured bearing

$$\Delta\psi_{mi} = \psi_{mi} - \psi_{m(i-1)} \quad 3.5$$

Assuming a constant change in bearing at each stage, then

$$R_{si} = \Delta s_{mi} / \Delta\psi_{mi} \quad 3.6$$

substituting (3.6) into (3.3) and (3.4) and then substituting (3.3) and (3.4) into (3.1) and (3.2) and rearranging gives

$$\Delta X_{ci} = \Delta s_{mi} . \mathrm{sinc}(\Delta\theta_{mi}) . \cos(\bar{\theta}_{mi}) \quad 3.7$$

and $$\Delta Y_{ci} = \Delta s_{mi} . \mathrm{sinc}(\Delta\theta_{mi}) . \sin(\bar{\theta}_{mi}) \quad 3.8$$

where $$\bar{\theta}_{mi} = (\psi_{mi} + \psi_{m(i-1)})/2 \quad 3.9$$

and $$\Delta\theta_{mi} = (\psi_{mi} - \psi_{m(i-1)})/2 \quad 3.10$$

the distance d_i moved at each stage being

$$d_i = (\Delta X_{ci}^2 + \Delta Y_{ci}^2)^{1/2} \quad 3.11$$

$$= \Delta s_{mi} . \mathrm{sinc}(\Delta\theta_{mi}) \quad 3.12$$

The errors at each stage for 'zero' curvature motion are

$$\Delta X_{ei} = \Delta s_{mi} \cdot \bar{\theta}_{ei} \cdot \sin(\bar{\theta}_{mi}) \qquad 3.13$$

and $$\Delta Y_{ei} = \Delta s_{mi} \cdot \bar{\theta}_{ei} \cdot \cos(\bar{\theta}_{mi}) \qquad 3.14$$

3.3 Simulation

The effect of a constant bias in the measurements on the lateral and longitudinal errors is shown

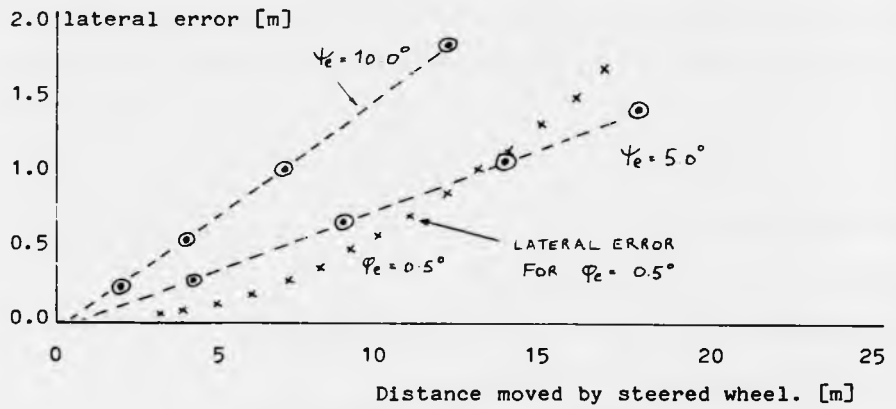

Figure 3.1 Growth in lateral error for a constant error from the true value of the bearing versus the along track distance travelled by the steered wheel. Also shown is the lateral error for a constant error in the measurement of the steered wheel angle.

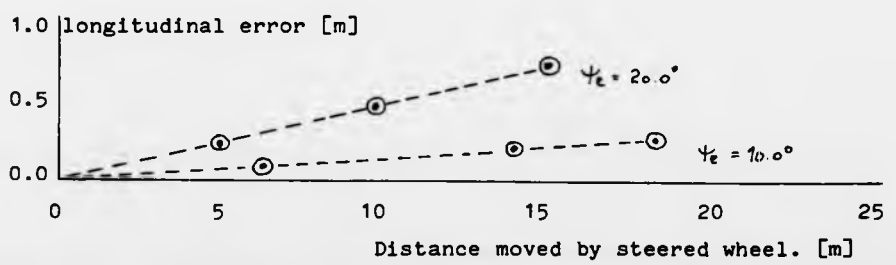

Figure 3.2 Growth in longitudinal error for a constant error from the true value of the bearing versus the along track distance travelled by the steered wheel.

3.3 Simulation

The effect of a constant bias in the measurements on the lateral and longitudinal errors is shown

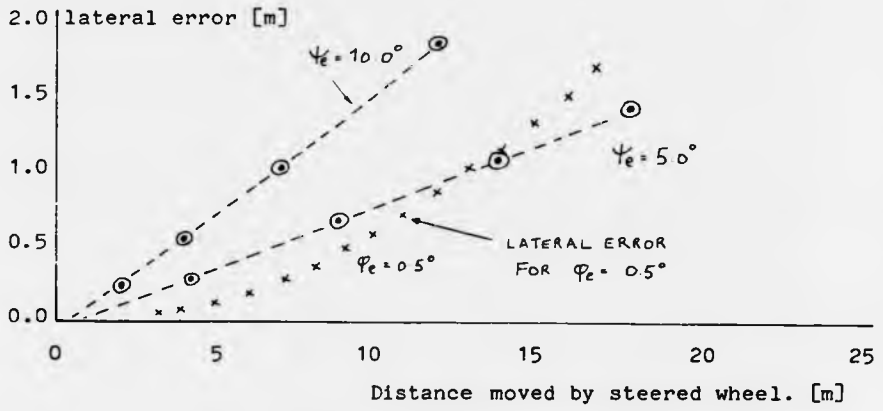

Figure 3.1 Growth in lateral error for a constant error from the true value of the bearing versus the along track distance travelled by the steered wheel. Also shown is the lateral error for a constant error in the measurement of the steered wheel angle.

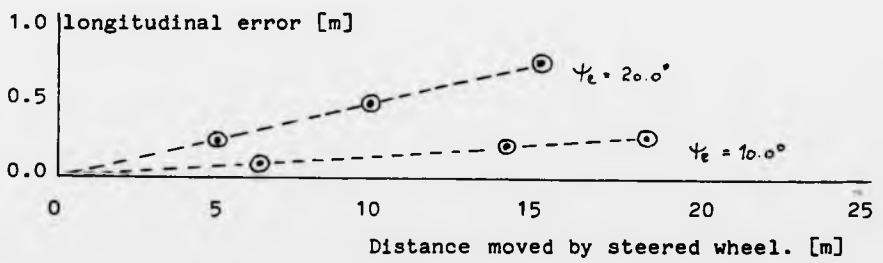

Figure 3.2 Growth in longitudinal error for a constant error from the true value of the bearing versus the along track distance travelled by the steered wheel.

3.4 Experimental

The vehicle was driven to the start position. The along track distance and compass readings were taken as the vehicle was manually driven forward with the 'best' zero curvature line that could be obtained by eye.

3.4.1 Results

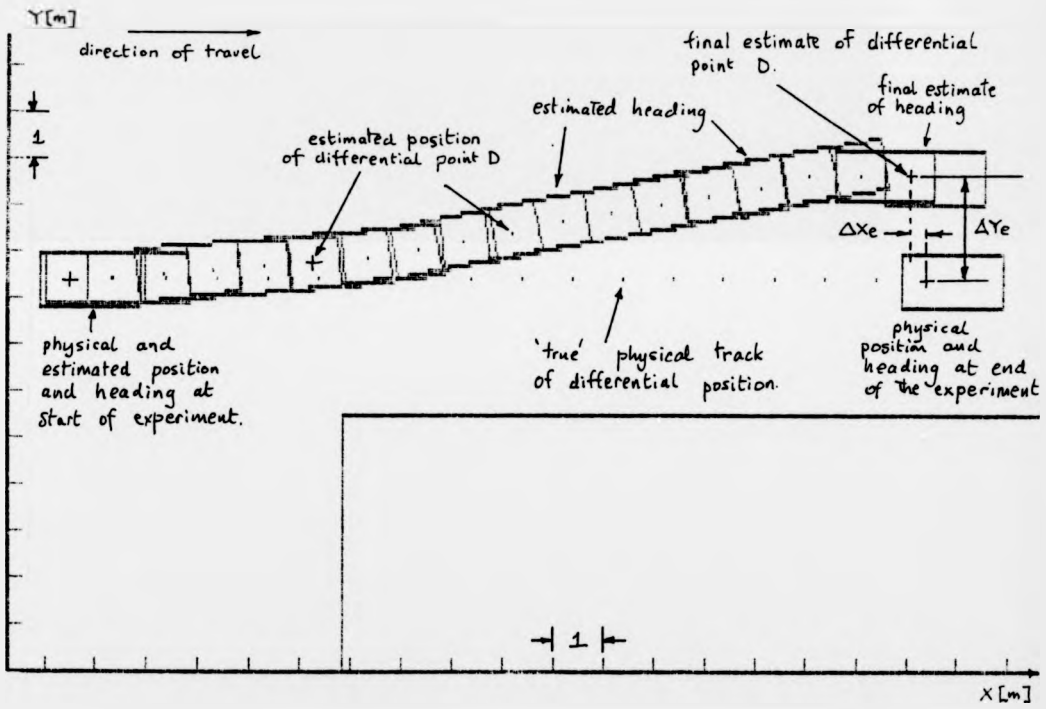

Figure 3.3 The longitudinal and lateral errors that actually arose using a direct measurement of the robot's bearing. The scale on the X and Y axes are marked at 1 metre intervals.

3.4.2 Discussion

Without filtering, and with a resolution of $\pm$ 5 degrees the compass odometer system was able experimentally to locate the robot more precisely than with the odometer and steer angle system. The lateral error obtained experimentally was 0.75 [m] less than with the odometer steer angle system. The dynamic behaviour of the compass needle as it rotates can be expected to be at least second order. There will be a delay in the measurement of the bearing, and the computation to produce the "best" estimate of the robot's heading. Thus the estimated heading will lag behind the "true" heading of the robot. The effect of this delay requires further investigation, and it is evident that there will be some adverse influence on the stability. A comparison of the growth in error between the odometer steer angle and compass odometer systems show that in some circumstances the odometer steer angle system errors can be smaller then the compass. Even with a compass the lateral positional errors remain, and these have to be corrected by other means.

3.5 Conclusions

The direct measurement of the vehicle's heading with a magnetic compass has been used to maintain the positional and bearing uncertainty below the level achieved experimentally with the steer angle, and odometer measurements alone. These measurements can be used to reorientate the local frame of reference and thereby combat the otherwise irreducible accumulated uncertainty in the heading, if only deduced reckoning were used. More work would be needed to characterise the noise in the measurements as the vehicle moved over a surface not perfectly 'flat' and design an appropriate filter that would minimise the effects of the unwanted forces and torques acting on the compass.

4.0 NAVIGATION with SONAR

4.1 Introduction

The objective of this section is to provide the theory and the experimental evidence to show how range measurements to objects in the environment can be used to reduce the accumulated uncertainty associated with the estimated global position of the robot.

4.2 Theory

The environment of the robot is modelled as line segments whose midpoint, semi-length, and orientation in the global frame of reference are known. The robot is modelled as possessing length, width, a local zero for its frame of reference, and a-priori information about the positioning and orientation of its ranging sensors. The orientation of the outward pointing normal from the sensors is calculated with respect to the longitudinal axis x axis. The zero of the local coordinate frame of reference is the differential point with the x axis parallel to the heading.

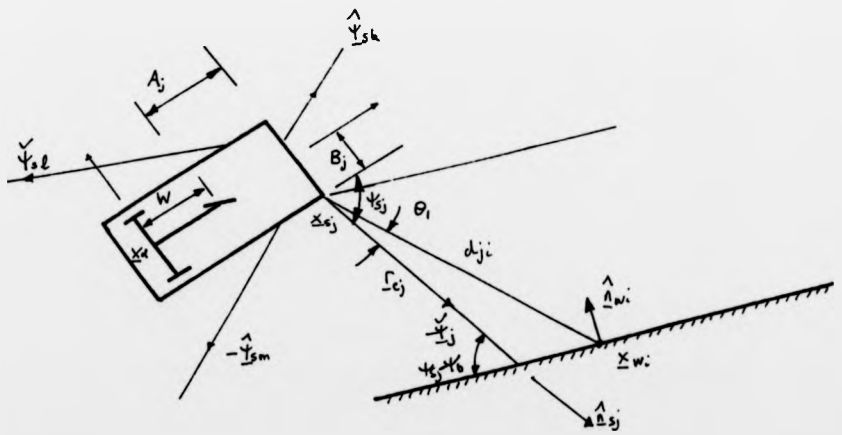

Figure 4.1. The geometrical arrangement of the robot-vehicle near to a feature in the environment that was physically a wall.

The wall was represented in the robot's "map" as a line segment. Four range sensors with their orientations are shown in the four quadrants relative to the heading. The symbols have the following meaning.

$\underline{x}_d$ = The estimated coordinates of the differential point.

ψ_h = The estimated heading of the vehicle.

$\underline{x}_{s_j}$ = The coordinates of the jth sensor position as determined from the differential point.

$\hat{\underline{n}}_{s_j}$ = The outward pointing unit vector of the jth range sensor whose direction cosines are with respect to the central longitudinal axis of the vehicle.

$\underline{x}_{w_i}$ = The position coordinates of the line segment.

$\hat{\underline{n}}_{w_i}$ = The outward pointing unit vector of the ith line segment whose direction cosines are with respect to the global frame of reference.

p_{j_i} = The distance from the position of the jth sonar sensor perpendicular to the ith line segment.

h_{j_i} = The projection onto the ith line segment of the distance from the estimated position of the jth sonar head to the central coordinates of the ith line segment.

r_{m_j} = The range measurement made by the jth sonar ranger.

r_{c_j} = The computed distance from the jth sonar to the ith segment.

θ_s = The effective beamwidth of the sonar.

$\| d_{j_i} \|$ = The computed distance from the jth sonar to the central coordinates of the ith line segment.

The range measurement is assumed to be made from a 'true' position which is near to the estimated position. The measured range is assumed to lie along the outward pointing normal from the sonar ranger for orientations with respect to the wall of less than $\pm$25 degrees. This

assumption is based on experimental evidence that was obtained in an earlier phase of the research and which is described later. The positional error is defined to be

$$e_{ji} = r_{mji} - r_{cji} \qquad 4.1$$

The distance from the sensor position $\underline{x}_{sj}$ to the central wall coordinates is computable, and for the ith identified segment

$$\underline{d}_{ji} = \underline{x}_{wi} - \underline{x}_{sj} \qquad 4.2$$

with $$\underline{x}_{sj} = \underline{x}_{d} + [W + A_j].\hat{\underline{\psi}}_h \pm B_j.\check{\underline{\psi}}_h \qquad 4.3$$

The unit vector in the direction of the central coordinates of the identified segment can be computed by substituting (4.3) into (4.2). This is possible since $\underline{x}_d$, W, A_j, B_j, $\hat{\underline{\psi}}_h$, and $\underline{x}_{wi}$, are either a-priori known or estimated values. The angle θ_1, between the normal from the sensor and the direction of the central wall coordinates can then be computed.

$$\cos(\theta_i) = -\hat{\underline{d}}_{ji} \cdot \hat{\underline{n}}_{sji} \qquad 4.4$$

The angle the computed range makes with line segment is

$$\pi - (\psi_{sj} - \psi_h) \qquad 4.5$$

The computed range to the ith segment is then given by

$$r_{cji} = \|d_{ji}\|.\sin(\psi_{sji} - \psi_h)/\sin(\psi_{sji} - \psi_h - \theta_1) \qquad 4.6$$

The difference between this computed range and the measured range can now be used as the error in whatever algorithm is chosen to reposition the notional coordinate frame so as to reflect more accurately where the robot really is. Two possible methods of correcting the positional error were considered. The first is

$$\underline{x}_{di} := \underline{x}_{di} + C_1.e_{ji} \qquad 4.7$$

where ":=" means "is replaced by", and the second correction algorithm is

$$\underline{x}_{di} := \underline{x}_{di} + C_2.e_{ji} + C_3.e_{j(i-1)} \qquad 4.8$$

and C_1, C_2, and C_3, are suitably chosen gain constants. The application of (4.7) is illustrated in figures 4.4 and 4.5. The application of (4.8) is shown in figure 4.6. Before a line segment may realistically be included

in the range based adjustments to the computed position three conditions need to be satisfied, these are

r_{cji} < = The maximum range measurable by the range sensor.

h_{ji} < = The semi-width of the candidate line segment.

$\hat{n}_g \cdot \hat{n}_{wi}$ < = The cosine of the effective beamwidth, where effective means that a range signal will be returned. This will vary with the acoustic reflecting properties of the material.

4.3 Experimental

The vehicle was driven manually forward. The steering wheel was held so as to result in 'zero' curvature motion. At one metre intervals range readings were taken. At the same time, compass, and odometer, and steer angle readings were taken. The 'real' path the vehicle followed is illustrated in figure 4.2.

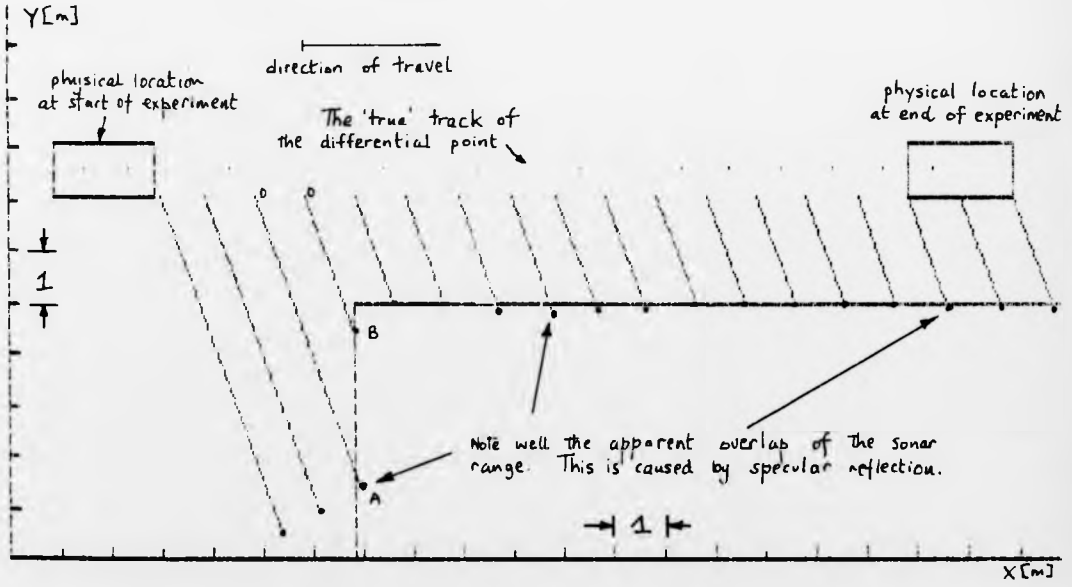

Figure 4.2 The 'true' path followed by the robot. The scale on the X and Y axes is marked at 1 metre intervals. The orientation of the normal direction to the sonar ranger is represented by the slanting dotted lines that represent the sound pulse travelling away from and back to the transducer after having been reflected from the wall.

4.3.1 Results

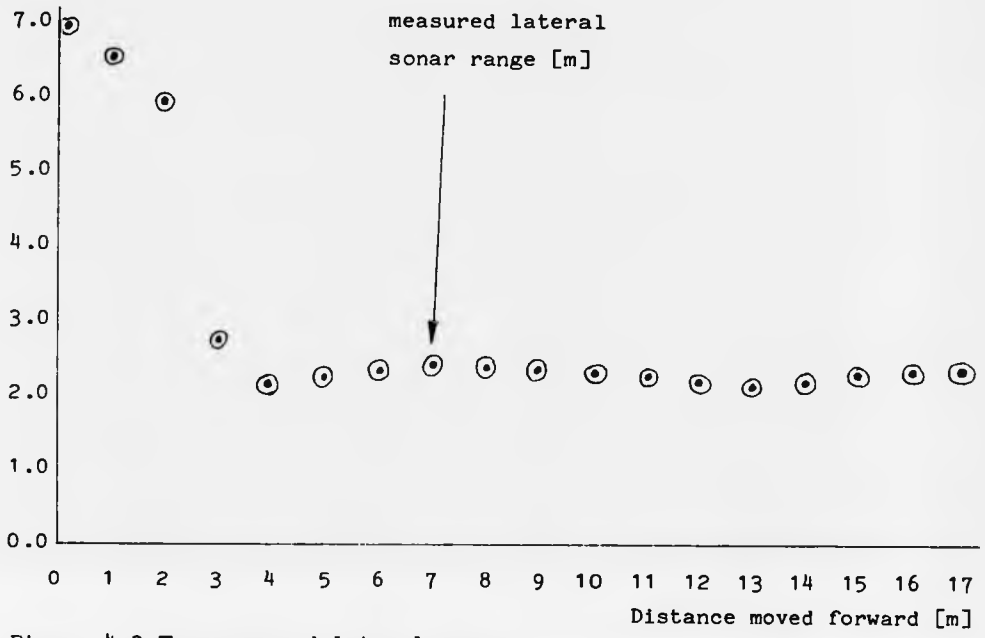

Figure 4.3 The measured lateral range.

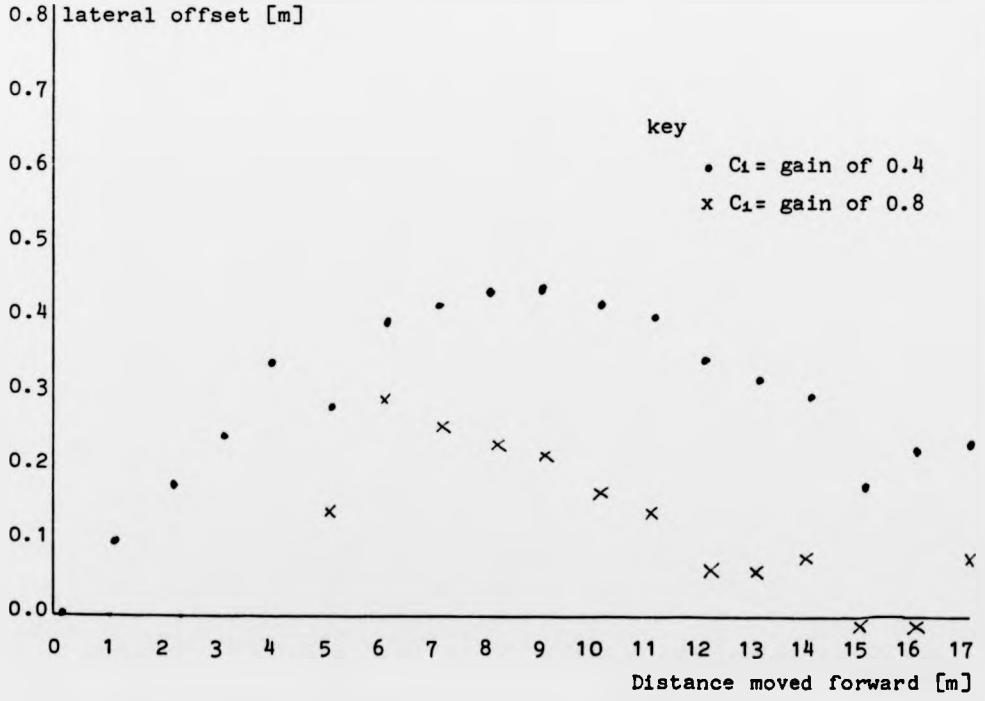

Figure 4.4 The computed lateral position versus the distance moved forward. This repositioning is based on the measured lateral range carried out by the lateral sonar ranger as graphed in Figure 4.3 above.

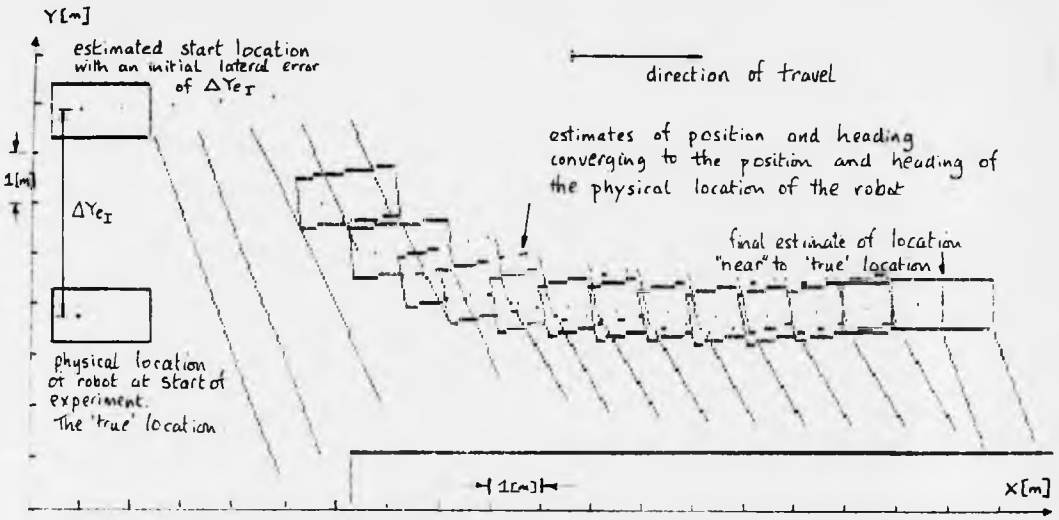

Figure 4.5 The illustration shows the mobile robot starting with an initial error in the estimate of its lateral position. As the vehicle is moved forward the range measurements, that were obtained experimentally, are shown as being able to correct the robot's position estimate. The correction algorithm on which this example is based, used the latest expected and actual range. The proportion of the error used, at each stage, to correct the vehicle's estimated position influences the rate at which the position estimate converges to its 'true' value.

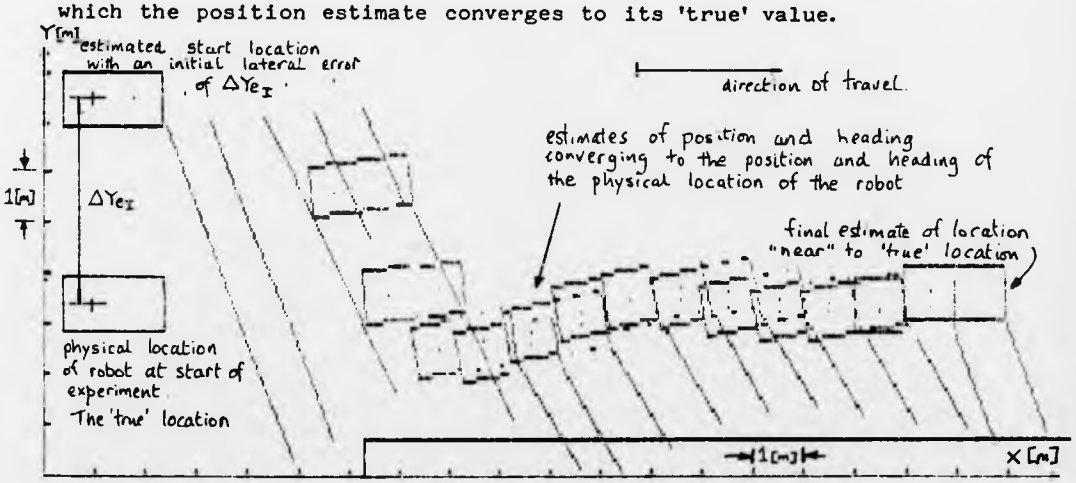

Figure 4.6 The effect of laterally repositioning the mobile robot's computed position based on the range measurements obtained experimentally. The correction is based both on the latest and the previous computed and measured range. Other schemes are possible.

4.3.2 Discussion

The sequence of experimentally obtained lateral ranges graphed in figure 4.3 were used in conjunction with the computed range calculated using (4.6) to form the error in (4.1). These were used in conjunction with the estimated position and heading based on the odometer, steer angle and compass to reposition the mobile robot. The repositioning was proportional to the error. The effect of varying the constant of proportionality on the rate at which these measurements reposition the mobile robot is graphed in figure 4.4. This graphs the initial increase in the estimated lateral offset of the differential point from the initial position. This increases to a value of 0.3 [m]. This lateral drift being caused by the accumulated errors in the navigation by deduced reckoning and with the bearing measurement. The environmental segment was used as the 'local reference' as soon as it became validly available. There was a known initial longitudinal and lateral offset from the wall segment. These were the mobile robot's initial world coordinates. The estimated lateral position is shown at about 5 [m] starting to converge to the 'true' value as illustrated by the offset converging to the 'true' value. Although the vehicle had been driven with the intention of travelling along a zero curvature path, an external measurement of the lateral offset at the end of the experiment revealed a measured offset of 0.14 [m]. This change is reflected in the estimated offset with a gain of 0.4. Figure 4.5 illustrates the effect of introducing an initial error into the lateral position. The algorithm used only the latest range error.

With the error signal thus defined, it would now be possible to utilise it in other algorithms. For example, figure 4.6 illustrates the effect of using both the latest and the previous range error to reposition the robot. The sequence of corrected positions produced by this algorithm are shown oscillating around the final 'true' value. The time for the estimated lateral position to settle within an acceptable tolerance band

of the 'true' solution can be altered by changing the 'numerical damping'. With these other algorithms there will be a convergence rate to the 'true' value. Their convergence rate can be expected in general to be different. Further work would be required to identify appropriate algorithms and then to quantitatively compare their convergence.

The expected range measurement is based on the computed heading of the robot. If this computed heading is in error from the 'true' heading then the computed range will contain this heading error. Even if there were no error in the computed heading the measured range could be in error. The measured range error increases as the distance from the object to the sensor increases. The measured range error also increases as the angle along which the returned signal energy actually travels increases. This phenomenon is related to the amount of acoustic energy which is reflected from the feature. This effect is graphed in Figure 4.7.

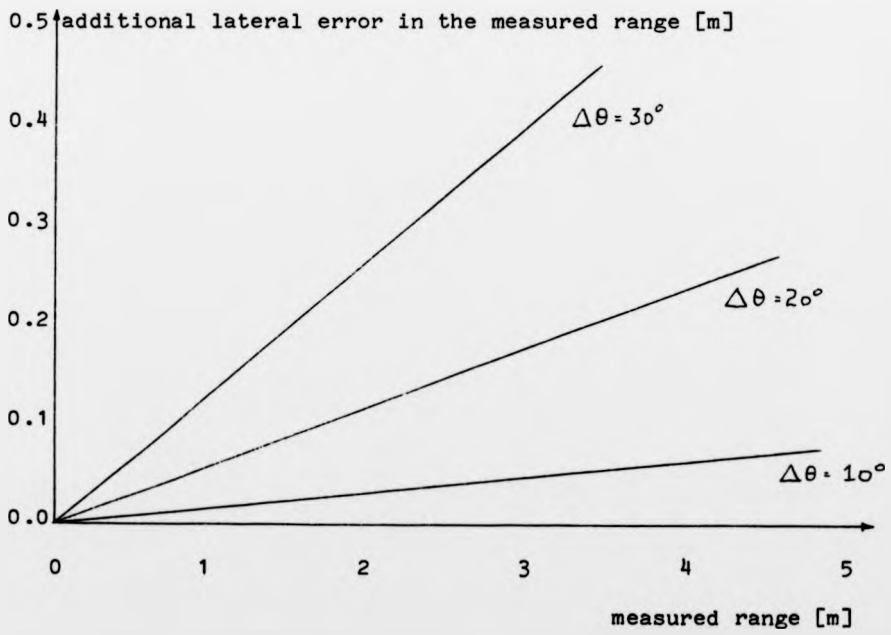

Figure 4.7 The additional lateral error ΔY_e caused by variations in the angle along which the echo arrives from, for various distances from sensor to feature.

The measured ranges with the vehicle moving along its 'true' track is shown in figure 4.2. As the vehicle approached the wall perpendicular to its heading the first two ranges were received prior to the line segment being validly available. The next two ranges at OA , and OB , are intended to illustrate that 'good' acoustic reflecting features in the environment at angles greater than the beamwidth of the sonar 'true' range can be obtained.

The acoustic reflecting properties of the environment, combined with the polar diagram of the transducer in its transmit and receive mode, can therefore alter this angle at which a range measurement is valid. A variation in this angle would need to be taken into account to avoid the introduction of additional uncertainty caused by the uncertainty in the orientation of the sonar sensor from this cause. In these regions there were the indented corners of a doorframe, a 'good' acoustic reflector.

The ranges to the wall parallel to the heading show variation. Since in the colloquial sense the wall was flat, these variations may be expected to arise from the non-uniformity of the acoustic reflecting properties of the wall. Since the wall was painted brickwork with indentations and protusions this hypothesis seems likely. Further work would be required to quantify these effects. A "map" that contained a-priori information about the acoustic properties of its surroundings, for the different materials expected, could assist the navigation process and could take advantage of this 'extra' information.

The measured range used, was the first range echo received. No attempt was made to use the other echoes which the Polaroid ranger provides. Indeed, before this phase of the research is reached many more 'test' environments and surfaces need to be examined to establish the limitations of using just the first range.

A complete model of all the environmental segments is required. If part of the world is not modelled, then unexpected range measurements

caused by a real change in the world will cause the 'navigator' to recompute the position based on an erronious correlation owing to missing map data.

A laboratory 'bench study' of the Polaroid Sensor as used in this research has recently been made by [Clemence 1983]. The characteristics of the ultrasonic range sensors were examined for their application to acoustic ranging for the automatic control of a ground vehicle. They identified the variation in sound velocity with temperature as being able to introduce errors in the range measurement if no method is employed to compensate for it. They report a variation of 5.5 ^{o}C theoretically able to cause an error in the range measurement of 0.06 [m]. No experiments were performed to verify this expected change. The use of a local reference target was identified as being able to reduce this effect. The loss of signal due to target offset, and incidence angle effects also degraded the accuracy of the measured ranges, and this is in general agreement with the results in this thesis.

Although range information obtained from acoustic ranging devices transmitting in air and attached to a robot have until recently been technically inhibited by the lack of a robust reliable ranging sensor, [Affinito 1976], proposed their attachment to a robot manipulator. Their use on a mobile robot in the 'terrain comparison' mode as outlined in this thesis was proposed by [Larcombe 1981]. The ROBNAV study [Cahn 1975], contains an algorithm that uses range only information to navigate, but since their study was a simulation, the need to maintain a 'true' position and heading estimate did not arise. The work of [Bauzil 1981] is the most comprehensive study and it shows their robot in a variety of configurations with respect to environmental features. However, no mention is made of any problems encountered with their finite beam width, which was 30 degrees, or specular reflection altering the direction of the returned echo. Indeed no experimental results are given in this or any

other paper examined with which to be able to compare my results. [Maffadat 1983], describes a mobile robot with two independently driven wheels. The navigation system is a single scanning sonar sensor, and this is driven by a stepper motor. The project's aim was to provide a teaching aid, and a vehicle for further research which remains to be reported.

4.4 Conclusions

The accumulated uncertainty in the deduced position can be reduced by environmental sensing using a single sonar ranger.

To do this the position and orientation of the environmental segment in the global frame of reference needs to be known a-priori, and an estimate of the vehicle's position and heading are required.

If the direction associated with the range measurement is not that assumed then this error will alter the accuracy of the estimated position. This error has two sources. One source is the uncertainty in the orientation of the frame, used to calculate the computed range. The other is from the uncertainty associated with the real direction from along which a returned echo can be received from.

5.0 LATERAL GUIDANCE with the SONAR

5.1 Introduction

The problem is to determine whether, whilst moving along a nominally zero curvature path, the sensing of an environmental feature can be used to ensure that stable lateral motion of the robot's structure ensues. A simple model of the lateral spatial and temporal movement of the differential point is examined. The application of the Routh-Hurwitz criteria to this simple model suggests there are geometric contraints on placing range measuring devices on such a vehicle. To assess the need for more exact knowledge about the process to be controlled a proportional controller was implemented in experiments. The steered wheel angle was varied in proportion to the error between a measured and a desired lateral range. A closed loop transfer function of the experimental arrangement is derived.

5.2 Theory

The vehicle's differential point, D, is positioned at a distance, y_d , from one of the walls of the corridor, (see figure 5.1). The heading, ψ , is relative to the local zero bearing defined by the orientation of the wall. The range sensor is positioned a distance W + A, ahead of the differential point. The distance A , of the range sensor ahead of the steered point can be varied. The lateral offset of the sensor from the longitudinal axis is B. The measured range to the environmental line segment is y_m . The error ϵ is f - y_m where f is the desired offset. The assumptions are that the angle of the body heading, and the steer angle are small, the range measurement is normal to the wall, and the forward speed V_x, of the vehicle is constant.

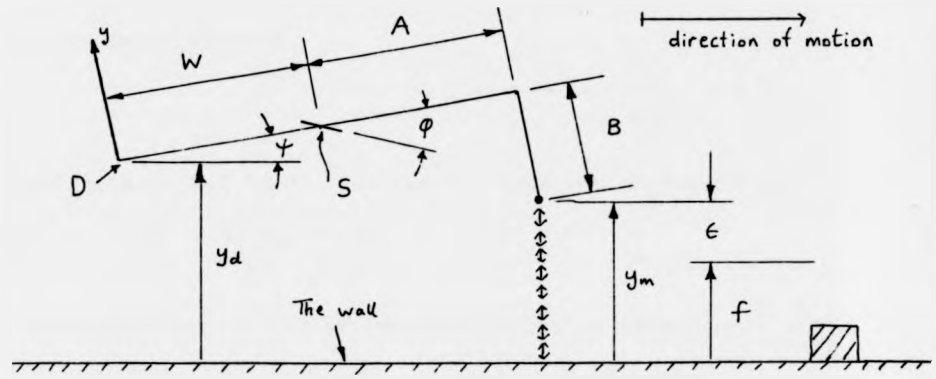

Figure 5.1 The vehicle and its starting relation to the wall.

The curvature K_d , at the differential point D is defined to be

$$K_d = \frac{\frac{d^2 y_d}{dx^2}}{\left\{1 + \left\{\frac{dy_d}{dx}\right\}^2\right\}^{\frac{3}{2}}} \qquad 5.1$$

When the angle of the body heading with respect to the wall is small, this curvature can be approximated by

$$K_d \doteq \frac{d^2 y_d}{dx^2} \qquad 5.2$$

The curvature of the path of the steered wheel and the curvature at the differential point are about the same, for small steer angles, that is

$$K_s = \frac{\sin(\varphi)}{W} \doteq K_d = \frac{\tan(\varphi)}{W} \qquad 5.3$$

Now if K_d , is made proportional to the error then

$$K_d = k.\epsilon \qquad 5.4$$

and using (5.2)

$$\frac{d^2 y_d}{dx^2} = k.\epsilon \qquad 5.5$$

Now the measured range is

$$y_m = y_d + (W + A).\sin(\psi) - B.\cos(\psi) \qquad 5.6$$

and since the heading is assumed small so that

$$\frac{dy_d}{dx} \doteq \tan(\psi) \doteq \sin(\psi) \qquad 5.7$$

then the error becomes.

$$\epsilon = f - [\, y_d + (W + A).\frac{dy_d}{dx} - B \,] \qquad 5.8$$

Equating (5.5) and (5.8), the lateral equation of motion is

$$\frac{d^2 y_d}{dx^2} + k.(W + A).\frac{dy_d}{dx} + k.y_d = k.(B + f) \qquad 5.9$$

In the steady state, the differential point is offset by

$$(B + f) \qquad 5.10$$

Using the Routh-Hurwitz rules for stability

$$\text{sgn}[k.(W + A)] = \text{sgn}[\, k \,] \text{ and} \qquad 5.11$$

$$k.(W + A) > 0 \qquad 5.12$$

Also

$$\frac{dy_d}{dx} = \frac{dy_d}{dt}.\frac{dt}{dx} \qquad 5.13$$

so

$$\frac{dy_d}{dx} = \frac{1}{V_x}\frac{dy_d}{dt} \qquad 5.14$$

and if V_x , is constant the equation becomes

$$\frac{d^2 y_d}{dt^2} + k.(W + A).V_x.\frac{dy_d}{dt} + k.V_x^2 y_d = k.V_x^2(B + f) \qquad 5.15$$

For stability $\text{sgn}[\, k.(W + A).V_x \,] = \text{sgn}[\, k.V_x^2 \,]$ 5.16

and $k.(W + A).V_x > 0$ 5.17

If V_x is positive in the forward direction, k and (W + A) positive, then both conditions for stability are satisfied. If however V_x is negative then to obtain these conditions the sensor should be placed behind the differential point,

Equation (5.15) may be Laplace transformed, with V_x assumed constant

$$\frac{y_d(s)}{u} = \frac{k.V_x^2}{(s^2 + k.V_x.(W + A)s + k.V_x^2)} \qquad 5.18$$

Where B + f has been redefined as u. The track of the vehicle as it moves in response to environmental features may be determined by subjecting the

system to the expected operational inputs. In state space form

$$\dot{\underline{x}} = \underline{F}.\underline{x} + \underline{G}.\underline{u} \qquad 5.19$$

and the output is assumed to be a linear combination of the state x

$$\underline{y} = \underline{H}.\underline{x} \qquad 5.20$$

converting to the difference equation form we obtain

$$\underline{x}(n+1) = \underline{E}.\underline{x}(n) + \underline{T}.\underline{u}(n) \qquad 5.21$$

$$\underline{y}(n) = \underline{K}.\underline{x}(n) \qquad 5.22$$

If now the vehicle is offset from the desired track and not orientated correctly, then these equations may be solved to determine the distance and time required to bring them to their desired values. The special case of bringing the differential point to the desired offset, in a critically damped fashion requires that

$$k = \frac{4}{(W + A)^2} \qquad 5.23$$

If this condition is satisfied then at the steered point the damping ratio

$$\zeta = \frac{A}{(W + A)} \qquad 5.24$$

Since both A , and W are positive this value is less than unity. This demonstrates that if the differential point is critically damped then the steered point must be underdamped. This accords with the common experience of driving into a parking space while moving forward, such that the rear of the vehicle is just correctly aligned that the front of the vehicle overshoots, and the front wheels can mount the pavement. A similar analysis shows that if the steered point is critically damped, then the differential point becomes overdamped. This may be understood in terms of parking a car, to stop the front wheels from mounting the pavement requires a greater length of parking space than that required to bring the rear end into line. For the vehicle used in these experiments, W = 0.7 [m], and with A = 0.7, then the damping ratio is about 0.49, which corresponds to 20% overshoot.

5.3 Experimental

In order to examine the bounds of validity of the previous analysis a simple proportional control loop was implemented and tested. This control scheme is illustrated in figure 5.2. The contents of the transfer function blocks shown below are derived in the discussion in view of the experimental results obtained.

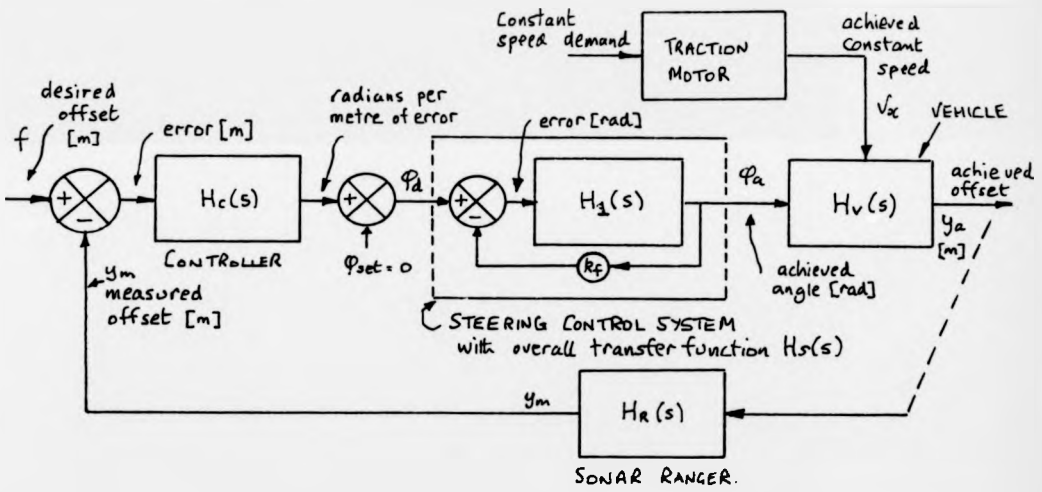

Figure 5.2 Block diagram of the control scheme proposed as being able to use distance feedback from a lateral pointing sonar to enable the robot to maintain its orientation parallel to a 'flat' wall whilst moving forward.

The assumption that the vehicle moved forward at a constant speed is indicated by the constant speed into the vehicle block $H_v(s)$. The vehicle was manually driven to its start position. At the start of the experiments the steer angle was set under computer control so that if there had been no lateral error and the steer angle had actually remained pointing 'dead ahead' zero curvature motion would have ensued.

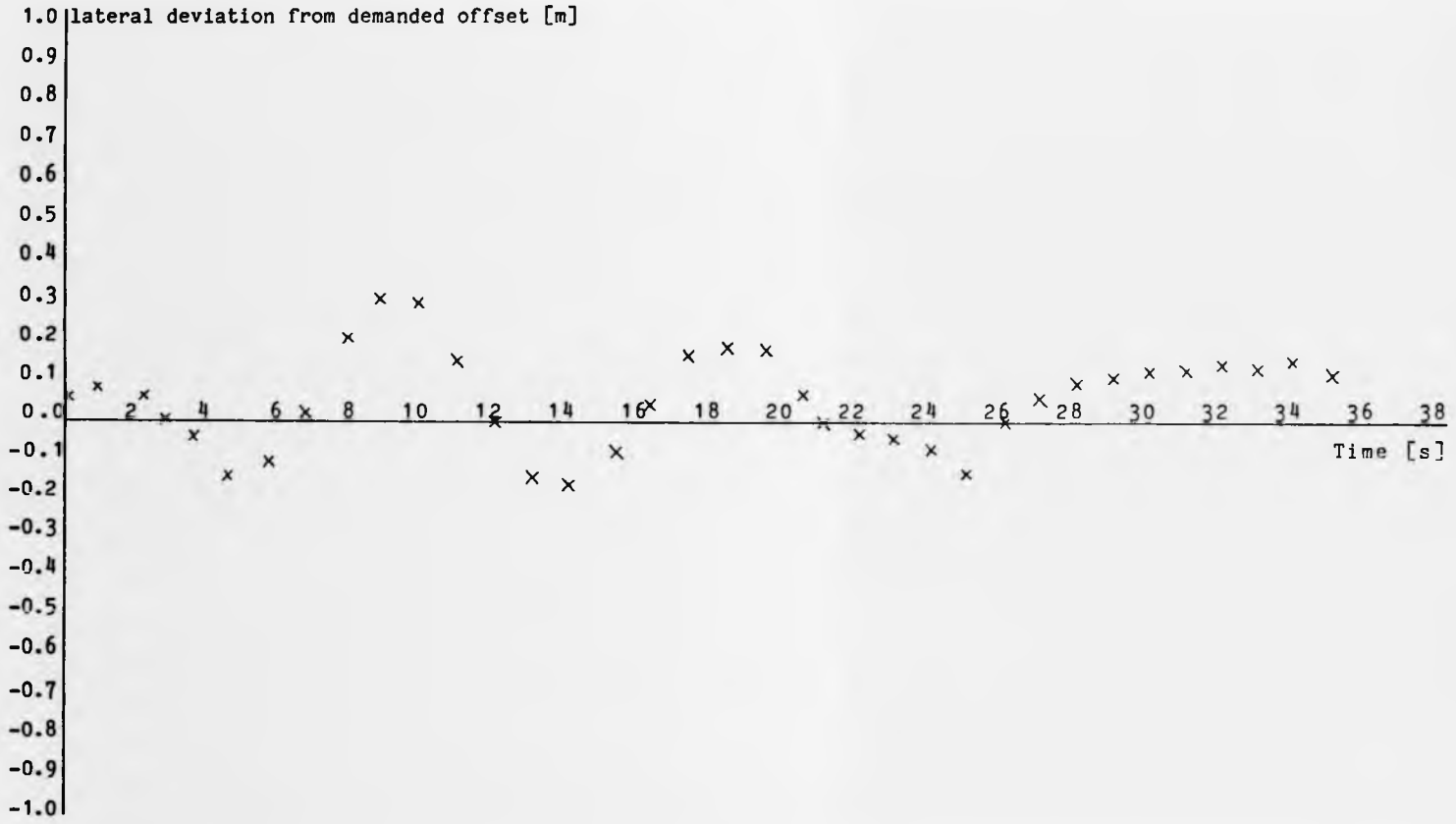

Figure 5.3 The deviation of the measured lateral sonar range from the demanded range, whilst the vehicle attempted to move forward with zero curvature. v = 0.33 ms^{-1}. G = 0.2

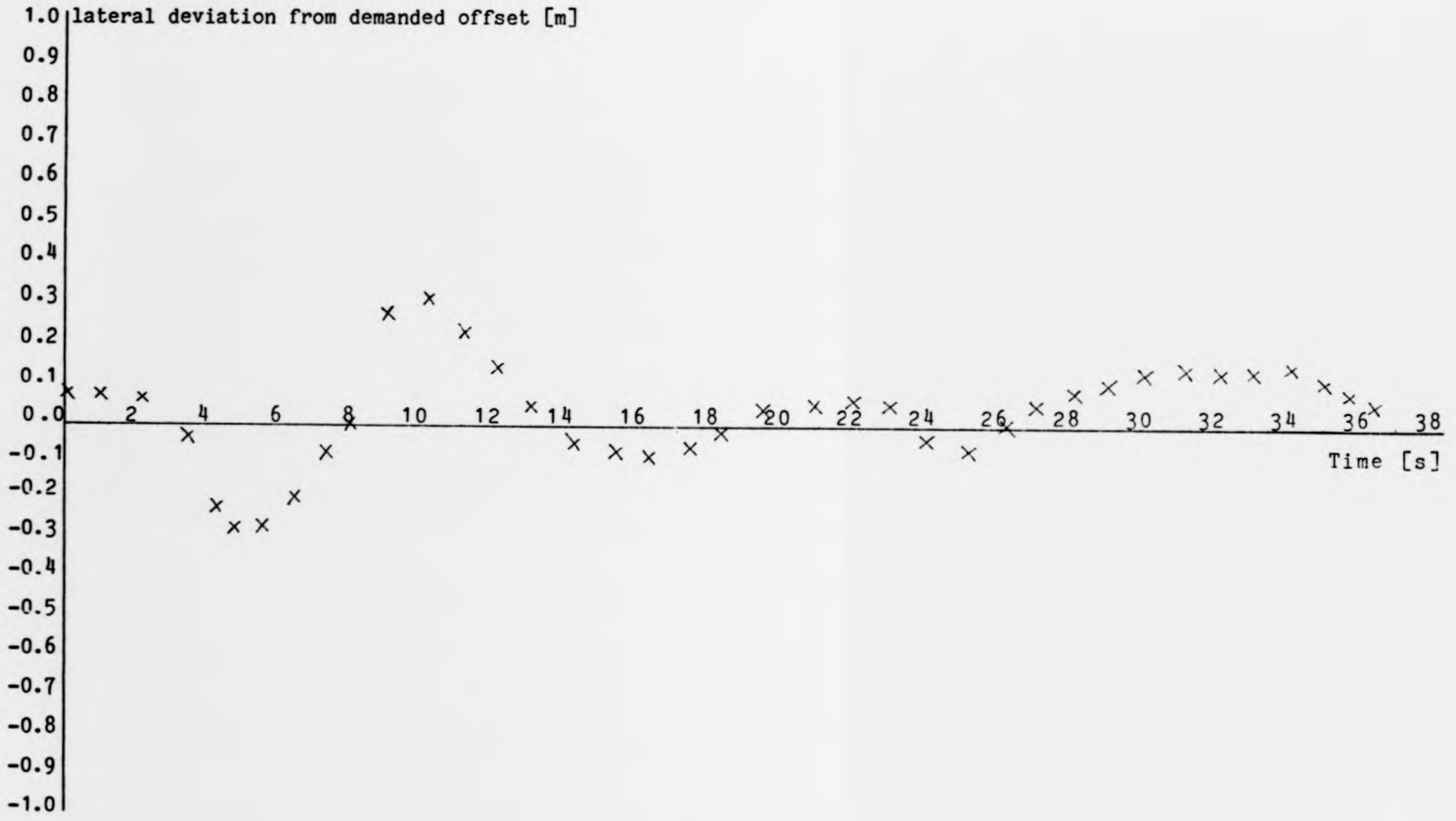

Figure 5.4 The deviation of the measured lateral sonar range from the demanded range, whilst the vehicle attempted to move forward with zero curvature. $v = 0.33\ ms^{-1}$ $G = 0.35$

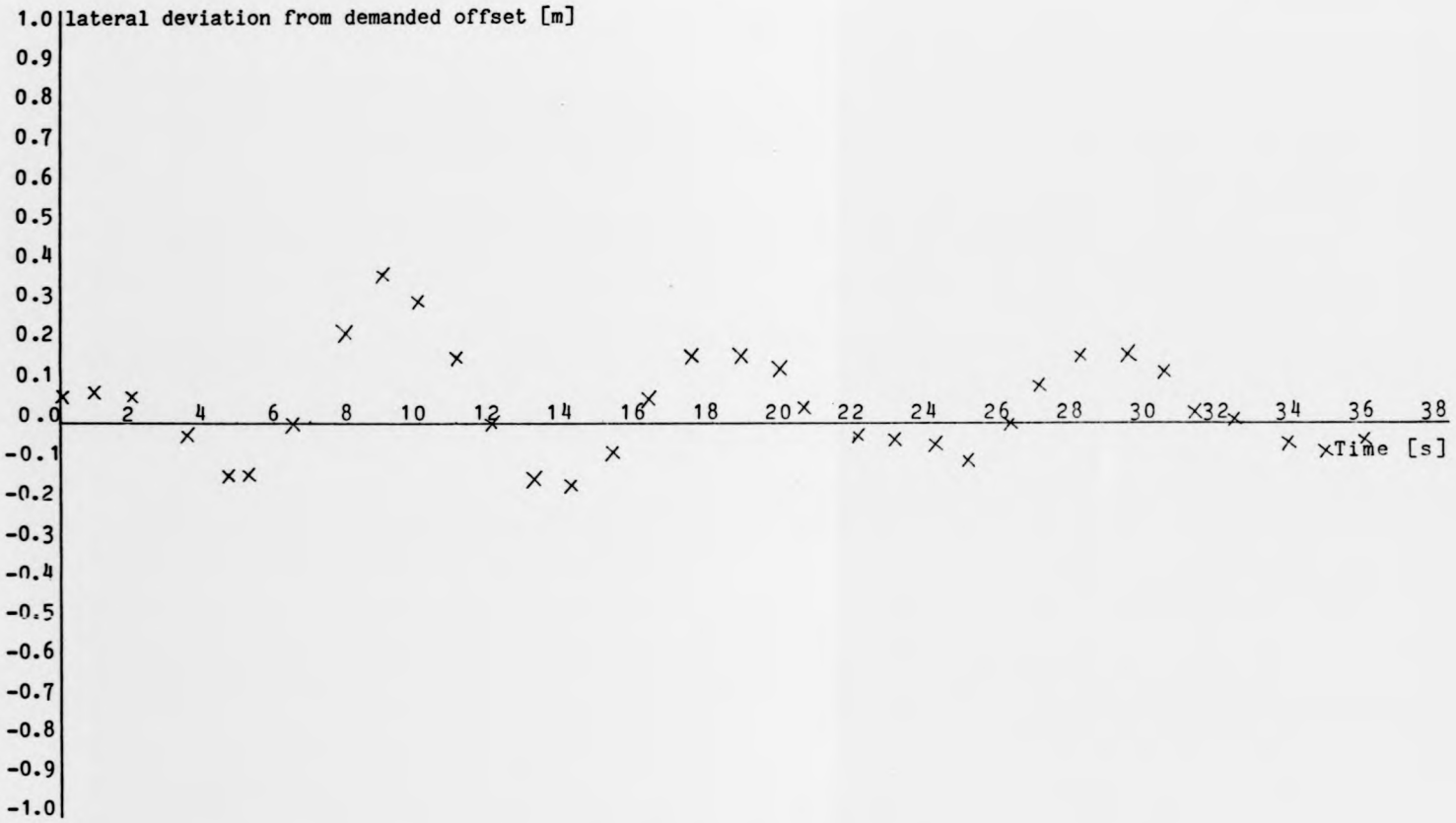

Figure 5.5 The deviation of the measured lateral sonar range from the demanded range, whilst the vehicle attempted to move forward with zero curvature. v = 0.33 ms^{-1}. G = 0.5

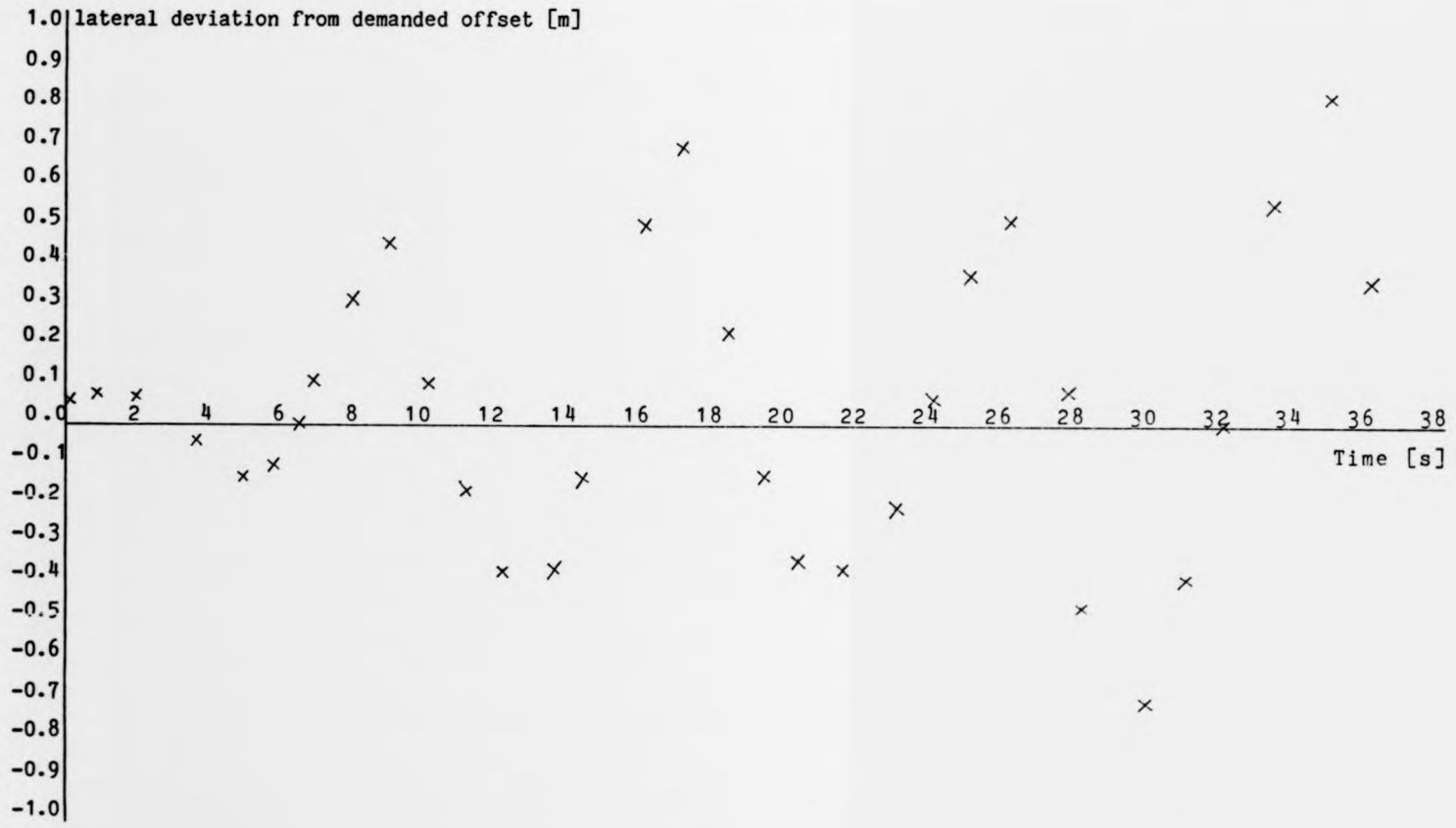

Figure 5.6 The deviation of the measured lateral sonar range from the demanded range, whilst the vehicle attempted to move forward with zero curvature. v = 0.33 ms^{-1}. G = 1.0

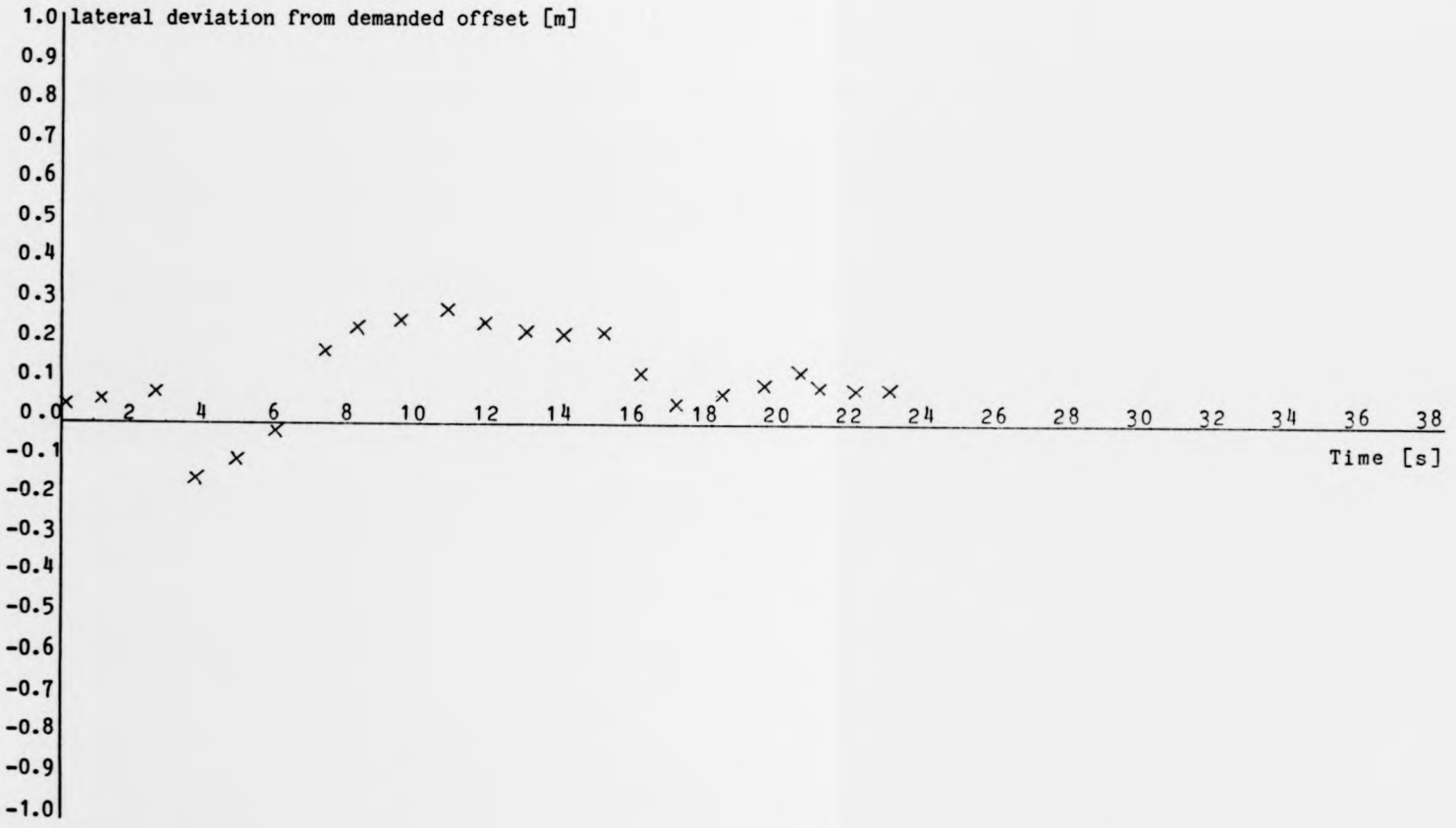

Figure 5.7 The deviation of the measured lateral sonar range from the demanded range, whilst the vehicle attempted to move forward with zero curvature. $v = 0.5\ ms^{-1}$. $G = 0.1$

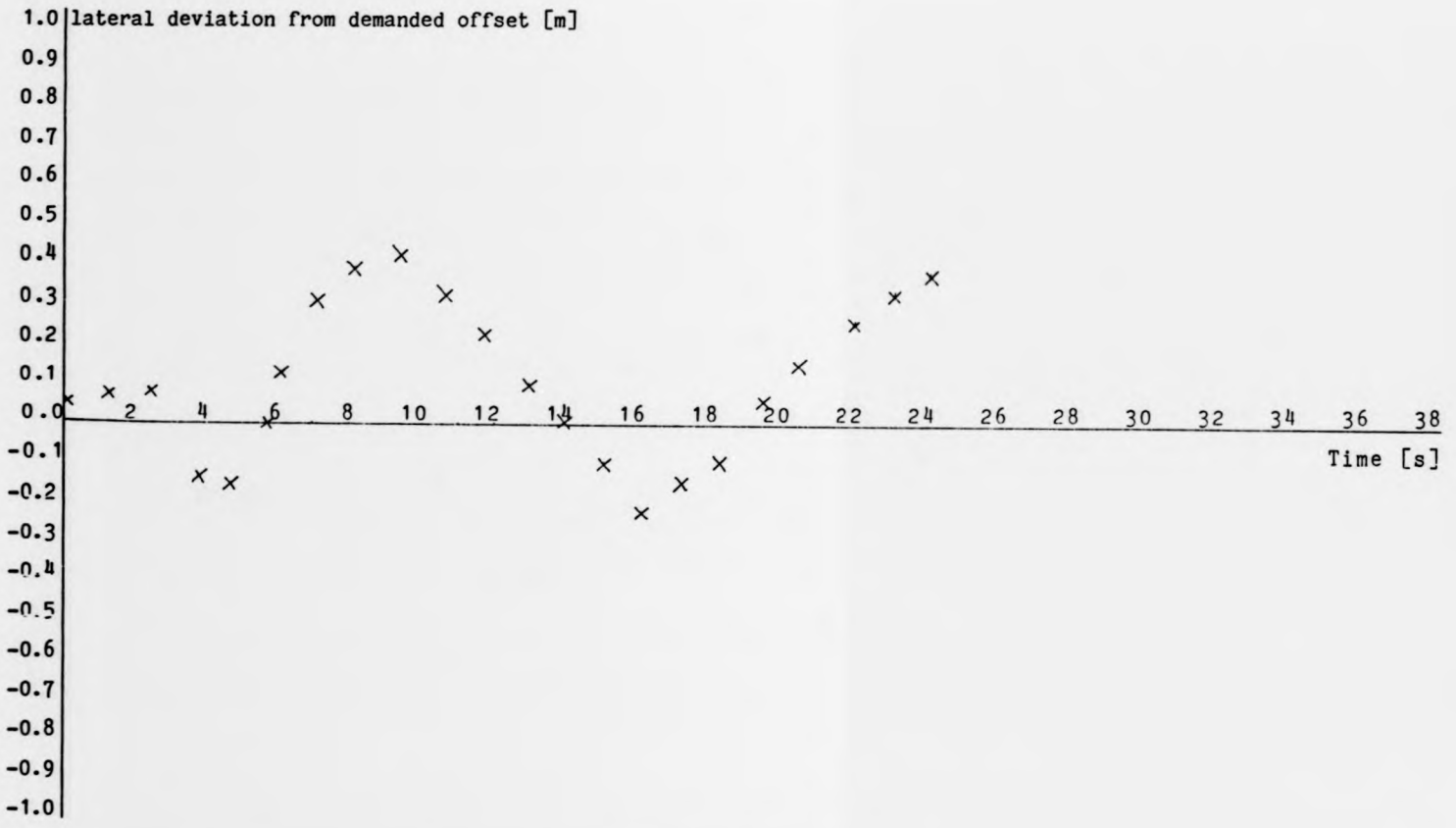

Figure 5.8 The deviation of the measured lateral sonar range from the demanded range, whilst the vehicle attempted to move forward with zero curvature. v = 0.5 ms^{-1}. G = 0.2

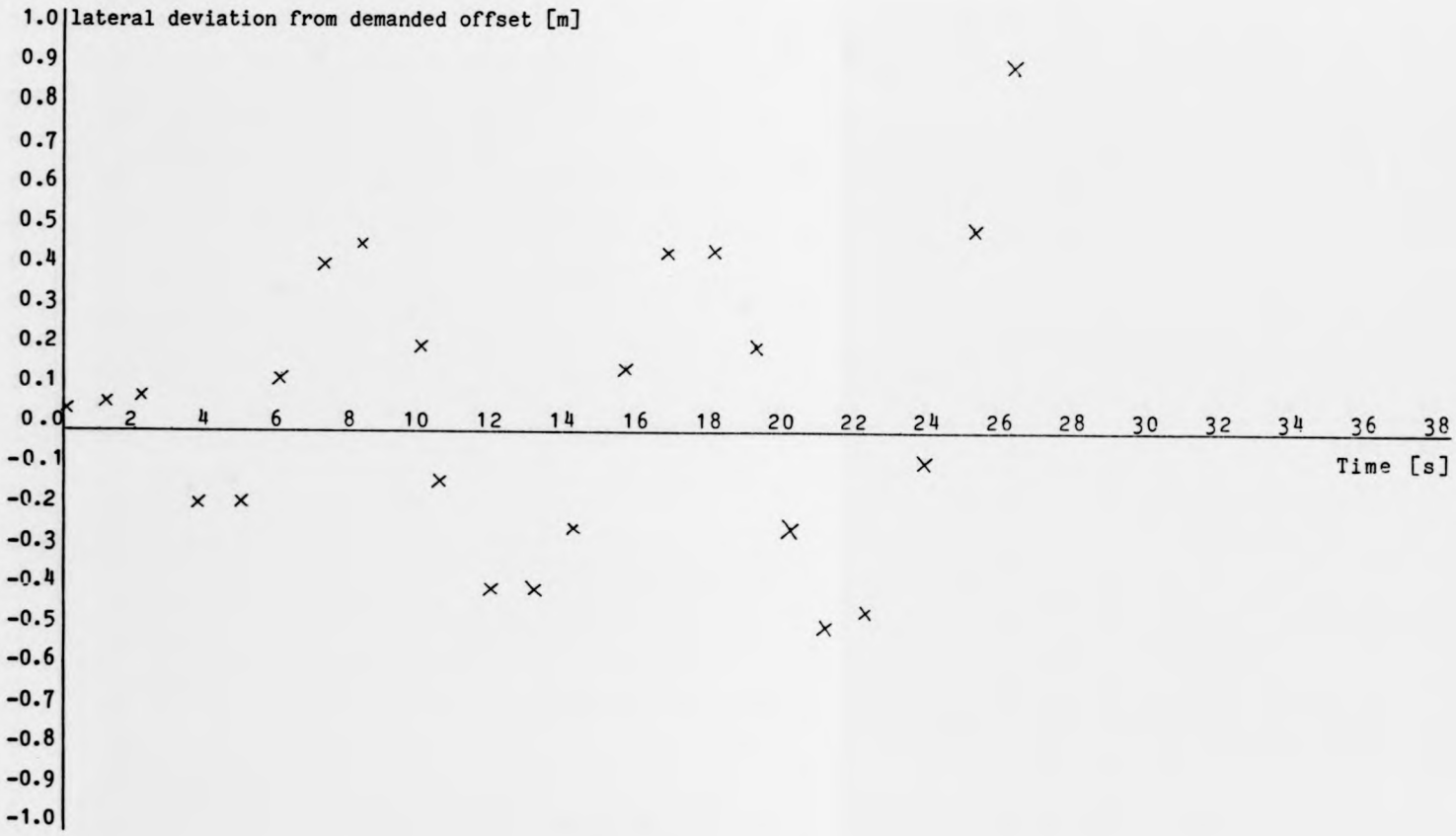

Figure 5.9 The deviation of the measured lateral sonar range from the demanded range, whilst the vehicle attempted to move forward with zero curvature. v = 0.5 ms^{-1}. G = 0.5

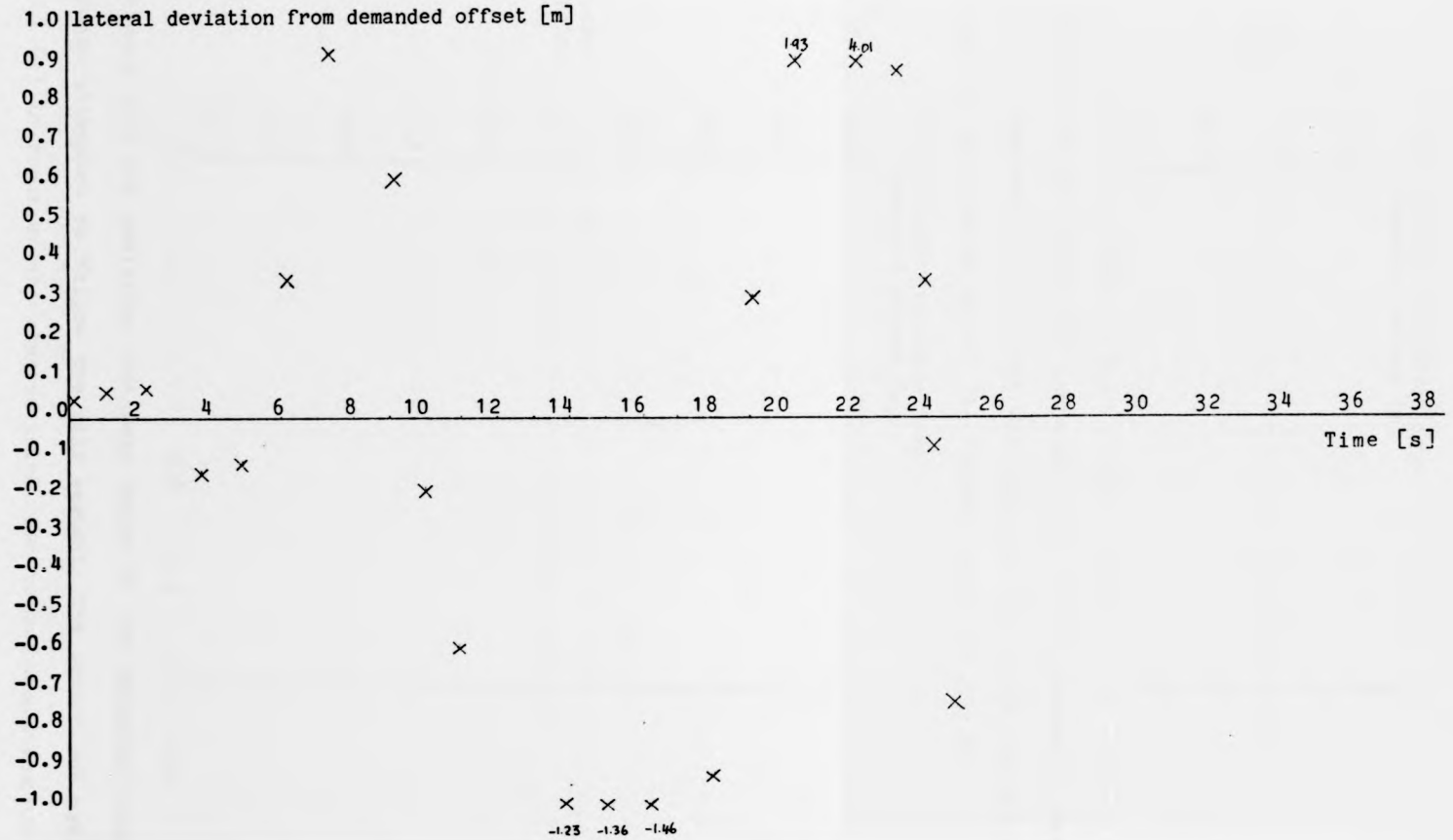

Figure 5.10 The deviation of the measured lateral sonar range from the demanded range, whilst the vehicle attempted to move forward with zero curvature. v = 0.5 ms^{-1}. G = 1.0

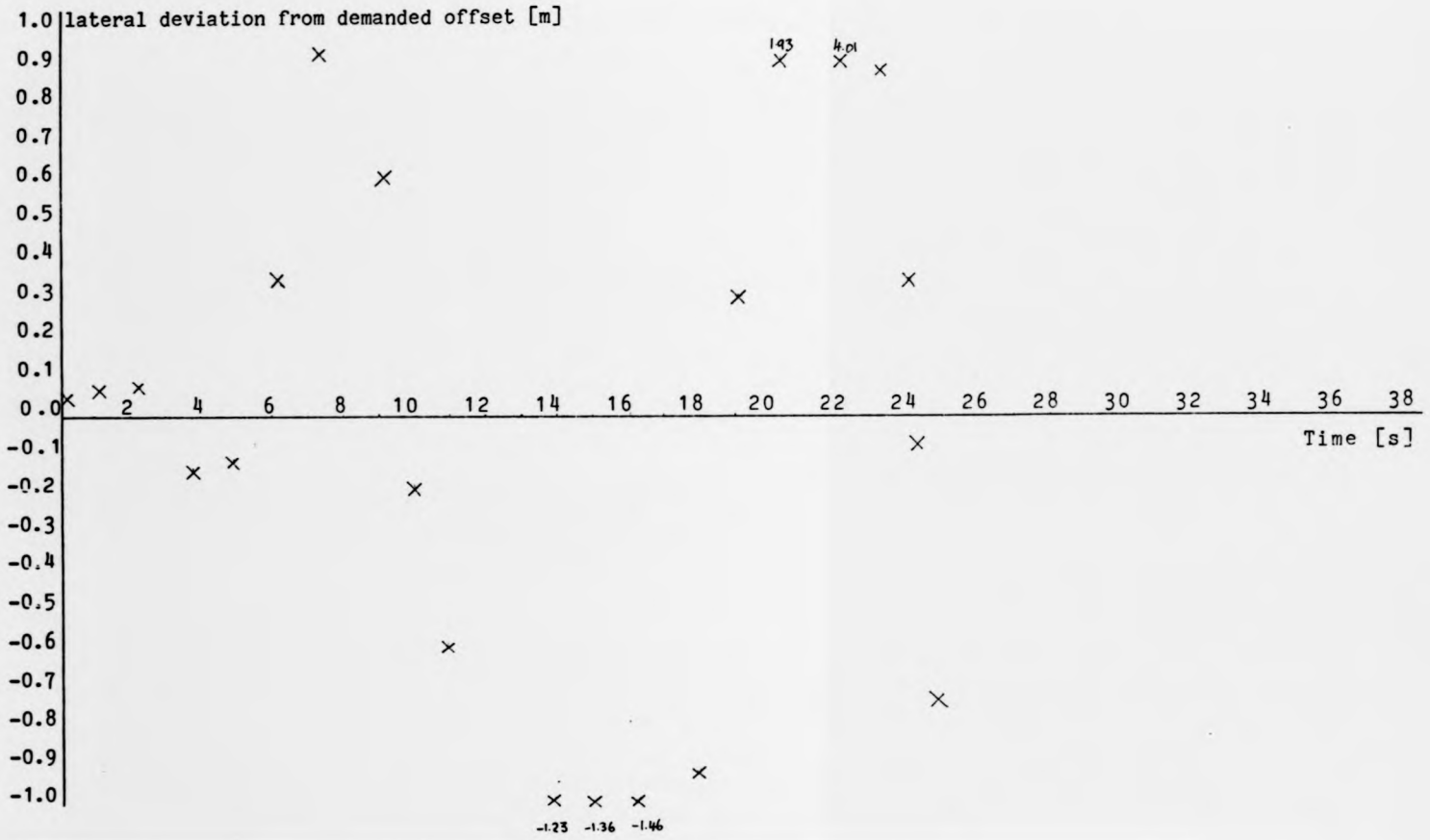

Figure 5.10 The deviation of the measured lateral sonar range from the demanded range, whilst the vehicle attempted to move forward with zero curvature. v = 0.5 ms^{-1}. G = 1.0

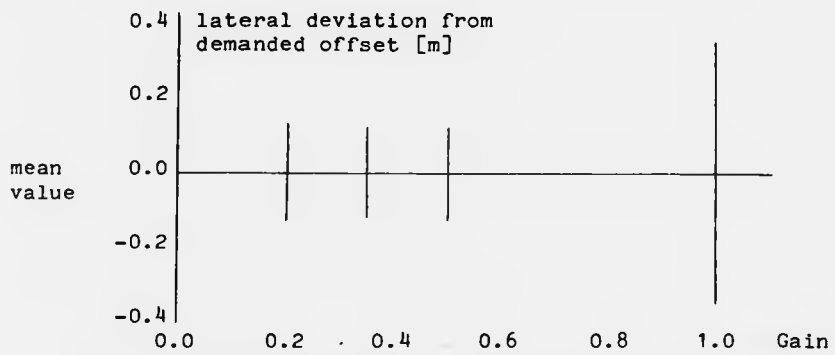

Figure 5.11 The deviation and mean value of the measured range as the robot attempted to follow the wall segment. The sensor was placed 1.7 [m] ahead of the steered 'point' The forward speed was 0.33 ms^{-1}.

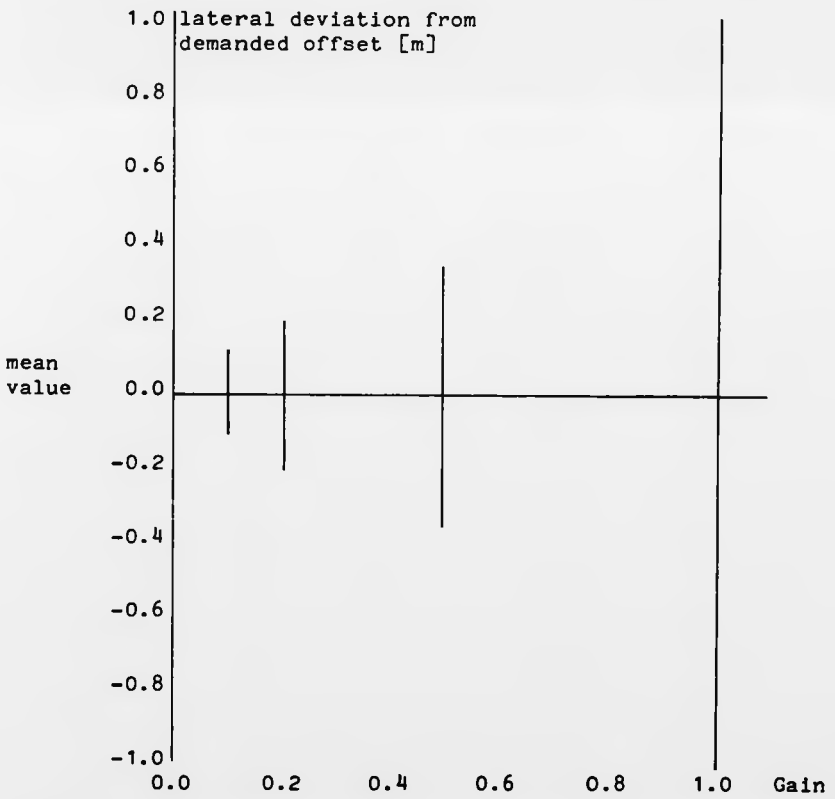

Figure 5.12 The deviation and mean value of the measured range as the robot attempted to follow the wall segment. The sensor was again placed 1.7 [m] in front of the steered point. The forward speed was 0.5 ms^{-1}.

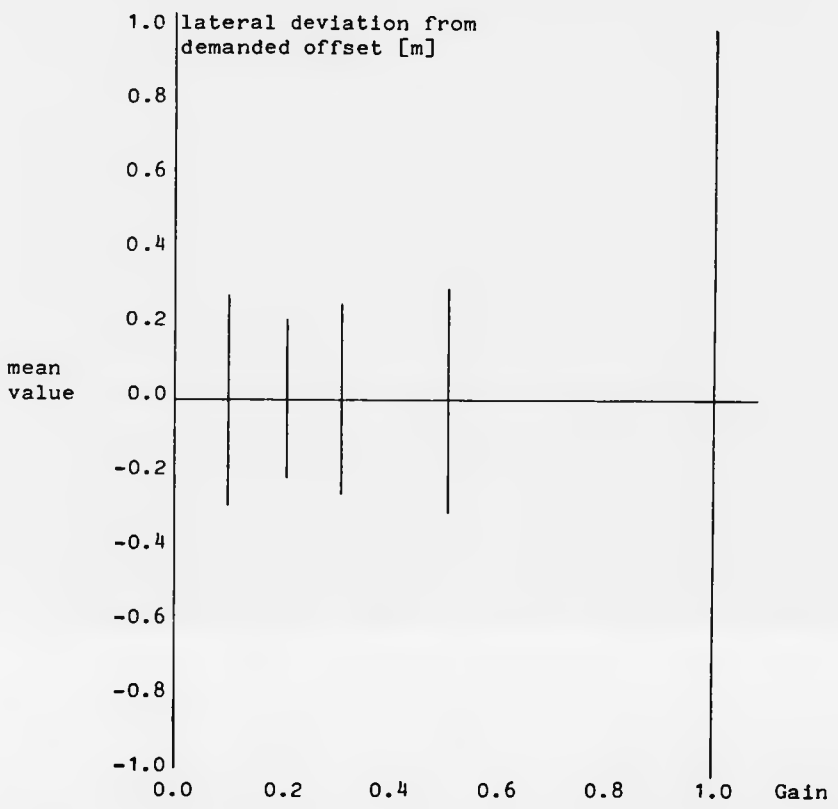

Figure 5.13 The deviation and mean value of the measured range as the robot attempted to follow the wall segment. The sensor position ahead of the steered point was reduced by 1 [m] to 0.7 [m]. The forward speed was maintained at 0.5 ms^{-1}.

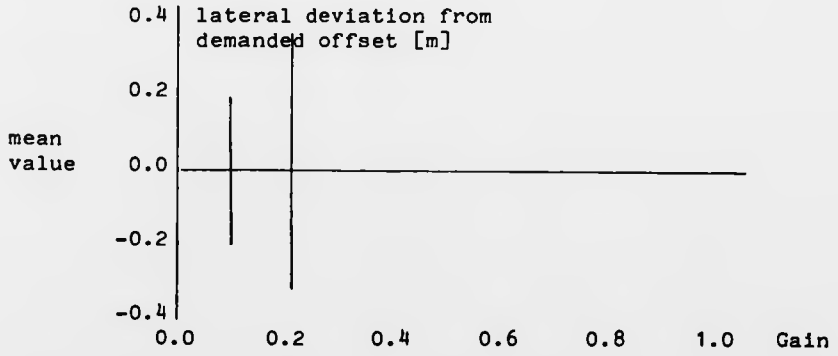

Figure 5.14 The deviation and mean value of the measured range as the robot attempted to follow the wall segment. The sensor was placed 1.7 [m] ahead of the steered 'point' The forward speed was increased to 0.8 ms^{-1}.

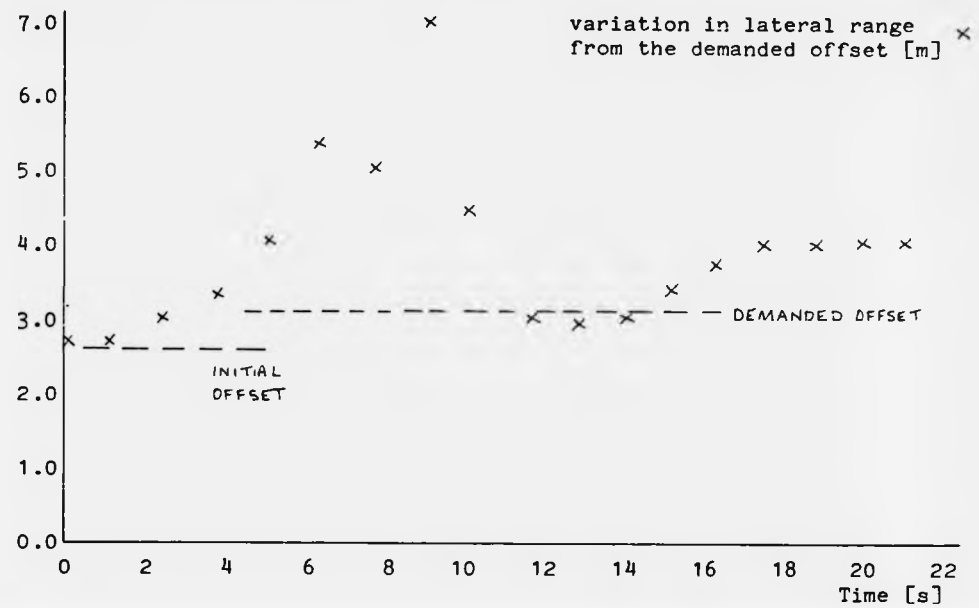

Figure 5.15 The robot's measured lateral range whilst moving away from the wall under the guidance of the saturating proportional control scheme. The objective of the experiment had been to turn and move the vehicle away from its offset by 0.5 [m] as it moved forward. The destabilising effect of the sonars finite beam width, and the discontinuity caused in the range measurements by the specular reflection of the sound can be seen about 6 seconds into the experiment. Increasing the gain simply increased the amount of overshoot, and subsequent oscillation. The speed was 0.5 ms^{-1}.

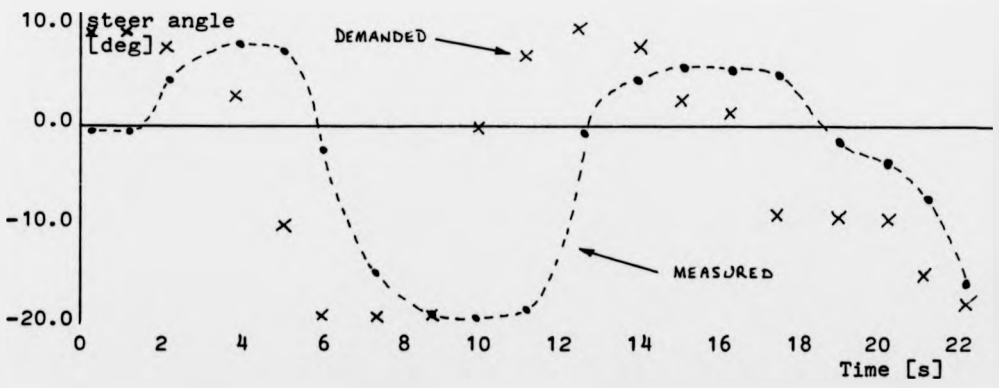

Figure 5.16 The variation in the measured and demanded steer angle. The experimental conditions were the same as above in Fig 5.9. The delay between the demand and the measured was the result of the delay imposed by pulsing the transit motor, making the measurement, performing the calculations, and the dynamic of the steering control system.

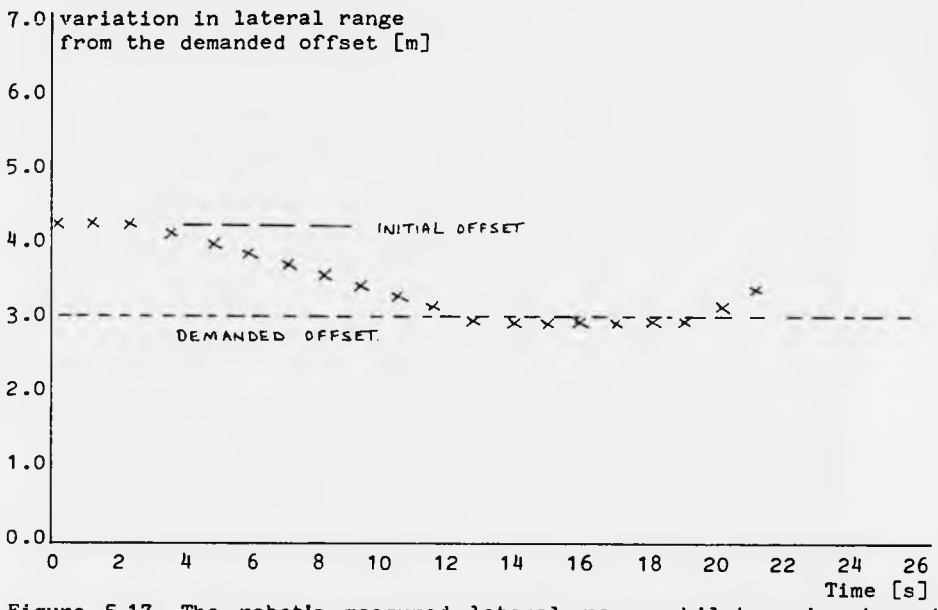

Figure 5.17 The robot's measured lateral range whilst moving toward the wall under the guidance of the saturating proportional control scheme. The robot had been displaced by 1.0 [m] away from from its previous offset. The speed here was 0.5 ms^{-1}. The destabilising effect of the finite beam width, and the specular reflection of the sound as the robot moved toward the wall are not now apparent. This may be explained as follows. The measurement sonar pointed 20 degrees ahead of the normal from the longitudinal axis of the vehicle, and, as the robot turned toward the wall, the measured range was obtained from the main lobe of the sonar, because this lobe is of a finite width, about $\pm$ 20 degrees, the sonar can vary its orientation angle made with the wall, and yet there still be a 'smooth', change in the measured range. Since the range varied smoothly so too did the steer angle.

5.3.2 Discussion

The software initially written to control the vehicle's movement revealed the effect that was later to be examined theoretically and is discussed in the chapter on deduced reckoning. Namely that the externally observed track of the robot would 'drift' away from the desired zero curvature path. The 'following' of an environmental feature in this case a 'smooth and flat' wall, was proposed as means of overcoming this deficiency.

Although a non-linear kinetic model (derived in Appendix A.4.0), had been obtained to model this ground vehicle's lateral and yaw motion, the work of [Russell 1981], indicated that the depth of an underwater vehicle, itself a complex non-linear system, could be stabilised by using simple proportional and integral control. The kinetic model contains parameters which are difficult to obtain without specialist equipment. This equipment was not available. For example, the coefficient relation between the slip angle of the tyre (Appendix A.4.0) and the lateral forces developed when the wheel turns and moves. For these reasons, it was decided to go directly to the experimental robot and make a preliminary assessment of the stability using a simple proportional controller. At the stage of understanding, at that time, these experiments needed to be performed to identify which of the system elements were significant to the lateral stability.

The sensitivity of the lateral control algorithm to changes in the measured range, was tested by using a natural feature that extended from the 'flat' of the wall by 0.15 [m] and was 0.20 [m] in length. This was used as a 'pulse' disturbance to the lateral control scheme, outlined in figure 5.2

As the robot passed this 'environmental pulse' the measured lateral range reduced and to maintain the demanded distance away from the 'wall' the controller altered the steering angle so as to move the

structure in the appropriate direction, This was observed as the structure of the robot veering away from, and then returning to its original offset, overshooting and then oscillating with varying amplitude around the constant demanded offset.

At time t = 0 the following situation holds

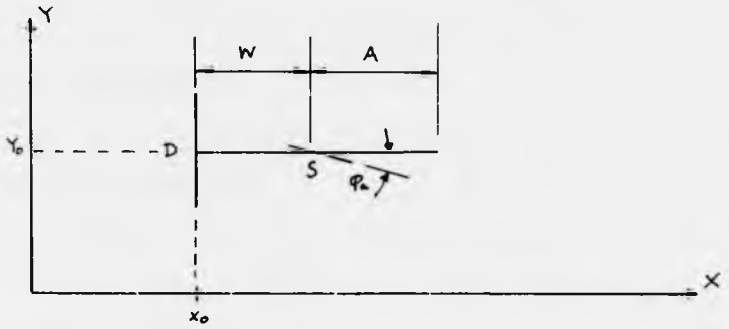

Figure 5.18 Experiment starting with vehicle parallel to the wall

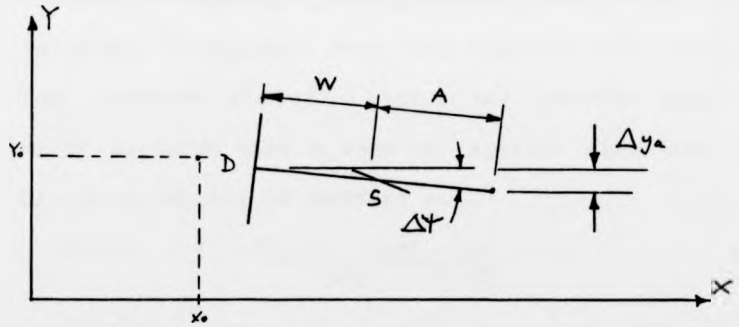

Figure 5.19 At a t = Δt the vehicle has moved and turned to the following position and orientation.

The change in lateral offset is for small changes in $\Delta\Psi$,

$$\Delta y_a = (W + A).\Delta\Psi \qquad 5.25$$

For small angles of steer

$$R_s = W/\varphi_a \qquad 5.26$$

and the distance moved ΔS is

$$\Delta S = R_s . \Delta\Psi \qquad 5.27$$

substituting for R_s in (5.27) rearranging and substituting into (5.25) then

$$\Delta y_a = (W + A).\Delta S.\varphi_a/W \qquad 5.28$$

Since ΔS is proportional to V_x, for the constant speed assumed then

$$\Delta S = V_x .\Delta t \qquad 5.29$$

so that the change in achieved offset Δy_a is

$$\Delta y_a = (W + A).V_x.\Delta t.\varphi_a/W \qquad 5.30$$

dividing by Δt, yields, with the notation that "." above the symbol means differentiation

$$\dot{y} = (W + A).V_x.\varphi_a/W \qquad 5.31$$

so that in Laplace form

$$H_v(s) = \frac{y_a(s)}{\varphi_a(s)} = \frac{(W + A)}{W}.\frac{V_x}{s} \qquad 5.32$$

Now from the steer step response tests (see Appendix A.3.0) the form of the steer angle response has an initial transient with a time constant of T_1, followed by a ramp of slope G_s, to the final achieved steer value φ_a. In Laplace form the ramp is $1/s^2$ and when the steer angle has achieved its final value the constant steer angle may be modelled by assuming that a ramp of negative slope starts at a delayed time T_d, this can all be expresed as

$$H_s(s) = \frac{G_s.[1 - \exp(-sT_d)]}{[s^2(1 + sT_1)]} \qquad 5.33$$

The sonar ranger is assumed to have a simple transfer function of unity. The offset error into the controller $H_c(s)$ was related to the angular demand into the steering control system by a slope of G_c. In the open loop the relation between measured offset y_m, and the error ϵ, is

$$\frac{y_m(s)}{\epsilon(s)} = G_c.\,G_s.\frac{[1 - \exp(-sT_d)]}{[s^2(1 + sT_1)]}.\frac{[W + A]}{W}.\frac{V_x}{s} \qquad 5.34$$

and in the closed loop becomes

$$\frac{y_m(s)}{f(s)} = \frac{G_c.\,G_s.[1 - \exp(-sT_d)].[W + A].V_x/W}{[s^3(1 + sT_1] + G_c.\,G_s.[1 - \exp(-sT_d].[W + A].V_x/W} \qquad 5.35$$

The delay T_d, is proportional to the angle demanded φ_d. Using the

approximation that $\exp(-sT_d) = 1 - sT_d$, then 5.35 becomes

$$\frac{y_m(s)}{f(s)} = \frac{G_c \cdot G_s \cdot [1 - (1 - sT_d)] \cdot [W + A] \cdot V_x / W}{[s^3(1 + sT_1)] + G_c \cdot G_s \cdot [1 - (1 - sT_d)] \cdot [W + A] \cdot V_x / W} \quad 5.36$$

which becomes

$$\frac{y_m(s)}{f(s)} = \frac{G_c \cdot G_s \cdot sT_d \cdot [W + A] \cdot V_x / W}{[s^3(1 + sT_1)] + G_c \cdot G_s \cdot sT_d \cdot [W + A] \cdot V_x / W} \quad 5.37$$

and cancelling the s from the numerator and denominator yields

$$\frac{y_m(s)}{f(s)} = \frac{G_c \cdot G_s \cdot T_d \cdot [W + A] \cdot V_x / W}{[s^2(1 + sT_1)] + G_c \cdot G_s \cdot T_d \cdot [W + A] \cdot V_x / W} \quad 5.38$$

and this analysis has revealed what was observed experimentally that the lateral motion for the higher values of G_c, resulted in essentially saturated oscillatory motion. By simplifying the transfer function $H_s(s)$

$$H_s(s) = G_s / s(1 + sT_1) \quad 5.39$$

then the closed loop transfer function becomes

$$\frac{y_m(s)}{f(s)} = \frac{G_c \cdot G_s \cdot (W + A) \cdot V_x / W}{s^2(1 + sT_1) + G_c \cdot G_s \cdot (W + A) \cdot V_x / W} \quad 5.40$$

Even if the control systems could have been designed so that the transient response of the steered wheel was very rapid the response would still have been inherently unstable. On the basis of this further analysis and the experimental results, equation (5.18) can now be viewed only as a very crude model of the lateral motion. To produce lateral motion with improved stability and less oscillations would require further work, and the sensing of other information. For example, it may be advantageous to sense rate and acceleration terms so that these could be introduced appropriately into the denominator.

A comparison of figures 5.12 and 5.13 and for the lower values of gain show a decrease in lateral deviation caused by reducing the sensors position ahead of the steered point. This is in agreement with the factor of (W + A) in the vehicle transfer function. A further comparison between

figures 5.11 and 5.12 shows an increase in deviation caused by increasing the speed of the vehicle. This is also in general agreement with the use of this transfer function. A further increase in speed to 0.8 ms^{-1}, (see figure 5.15), and for gains higher than 0.2, there was virtually uncontrollable motion.

The speed of sound in air places a bound on the rate at which range samples can be obtained. For the Polaroid ranger designed for a 10 [m] range, the sampling rate is fixed at 10 Hz. The samples in these experiments were obtained at intervals of about 1 second. An order of magnitude increase is possible. Three delays can be identified. The range measurement, the computation to produce the appropriate steering wheel commands, about 0.05s and, the lag between issuing the command to the steer control system and the wheel achieving the desired value. With the control system used and an error of 10 degrees in the steer angle resulted in a delay of about 0.5 s, between the demand and the steer angle achieving that demand.

The theory had assumed that the measured range would be the normal from the feature, and for the experimental surroundings this is not justified. The transfer function needs to be modified by the orientation between the sensor and the wall. Some experiments were performed with the vehicle laterally displaced from the desired offset both toward and away from the wall. However, as the vehicle moved and turned there were discontinuities in the measured range. The phenomenon of specular reflection combined with the finite beamwidth, results, as the vehicle turns, in relative orientations at which the returned echo does not indicate the true range normal from the feature. One means to obtain a better measure of this normal from some point on the vehicle would be to increase the number of sensors and place them at different orientations. The relevant range to be used in the controller being obtained from the sensor whose angle θ , with respect to the feature is a minimum, that is,

min $[\hat{n}_j \cdot \hat{n}_i]$ over the j sensors, and for the ith feature.

The lateral deviations observed experimentally even at the lower speeds would almost certainly not be acceptable in an industrial interior. To improve the quality of the control improved knowledge about the process dynamic could be of used. Other workers, [Fenton 1976; Cormier 1980] employ a modified two degree of freedom model of the vehicle's lateral dynamics and measurement system. These early experiments carried out with this vehicle indicate that such process knowledge is desirable and needs to be incorporated in the mobile robot's a-priori knowledge.

The dynamics of rubber-tyred vehicle's have been described by three degree of freedom, 3-DOF [Segal 1956-1957], and two degree of freedom 2-DOF models used by [Fenton 1976; Schladover 1978]. If the body roll of the vehicle can be neglected, then a 2-DOF model can be adequate.

The kinetic equations are given in appendix A.4.0, and based on the states defined in these the full state feedback would make φ be dependent on [y , $\dot{y}$, $\dot{\psi}$, ψ], that is

$$\varphi = -K_y[y - y_r] - K_{\dot{y}}[\dot{y} - \dot{y}_r] - K_{\dot{\psi}}[\dot{\psi} - \dot{\psi}_r] - K_{\psi}[\psi - \psi_r] \quad 5.41$$

where K_y, $K_{\dot{y}}$, $K_{\dot{\psi}}$, and K_{ψ}, are the gains of the respective differences between the vehicle state variables and the reference values for those variables. The design of the full state feedback controller requires the selection of the four gains in (5.41). The implementation of the full state feedback controller requires the measurement or, the estimation of each state variable. The addition of lateral pointing range sensor at the rear, would enable, in principle, the lateral error and yaw angle to be obtained directly. However to obtain the yaw rate and the lateral velocity would be more difficult. To obtain improved performance, estimates of the yaw rate and the lateral velocity could be formed.

5.4 Conclusions

Experiments to control the lateral motion of a tricycle vehicle as it moves forward by turning the steered wheel angle in proportion to the difference between a desired and a measured offset and the results obtained have shown that this method of control is only just adequate. As a result a 2nd order linear differential equation that was proposed as a simple model of the lateral motion has been shown to be inadequate. This conclusion is based both on the experimental results, and on the predictions of a further model based on the experiments performed on the actual vehicle.

In experiments decreasing the distance between where the sensor made its measurements and the steered wheel has been observed experimentally to result in smaller deviations from a mean value. Increasing the speed of the vehicle has been observed to result in less stable lateral motion.

Simulations to establish the effect of the other system elements involved in this 'following' process, showed that, for example, the finite beam width of the sonar, and the sampling rates, all contribute to a decrease in the lateral stability.

6.0 'HYBRID' GUIDANCE to REORIENTATE

6.1 Introduction

With a control algorithm marginally able to stabilise and solely able to move the vehicle 'parallel' to a wall the experimental attention focussed on the problem of how the speed and steer angle demands to the vehicle should be altered to enable it to make the transition from one zero curvature segment to another. Two methods of achieving this are examined in theory, for a vehicle whose mimimum path curvature is limited by the maximum steer angle. The experiments actually performed to move the experimental vehicle from one orientation to another, defined by an environment that was a 'T-junction' is described. The relation of the vehicle to these surroundings is illustrated and the sensor readings obtained during the experiment are graphed. The main conclusion is that a tricycle vehicle with feedback about its ambient from sonar range measurements, and navigational input from the deduced reckoning system can be used to negotiate such an intersection whilst moving.

6.2 'Theory' and Task Description

Two modes of passing through the intesection are examined either the curvature is changed only when the vehicle is stationary, (see figures 6.1 and 6.2.) or the changes in curvature are made with the vehicle moving, (see figure 6.4)

Referring to figure 6.1. with the robot initially at A, and then moving along the corridor, with its lateral motion stabilised by the two lateral sonars s_1, and s_2. The robot's forward speed is reduced from V , to zero, as it approaches the intersection. The intersection is 'recognised' by the transition in the lateral ranges, from the expected short ranges when moving in the corridor, to the longer range as illustrated by the increase in s_2, coupled with the decreasing forward range r_f. This pattern is used as the initiating information to start this 'braking process'.

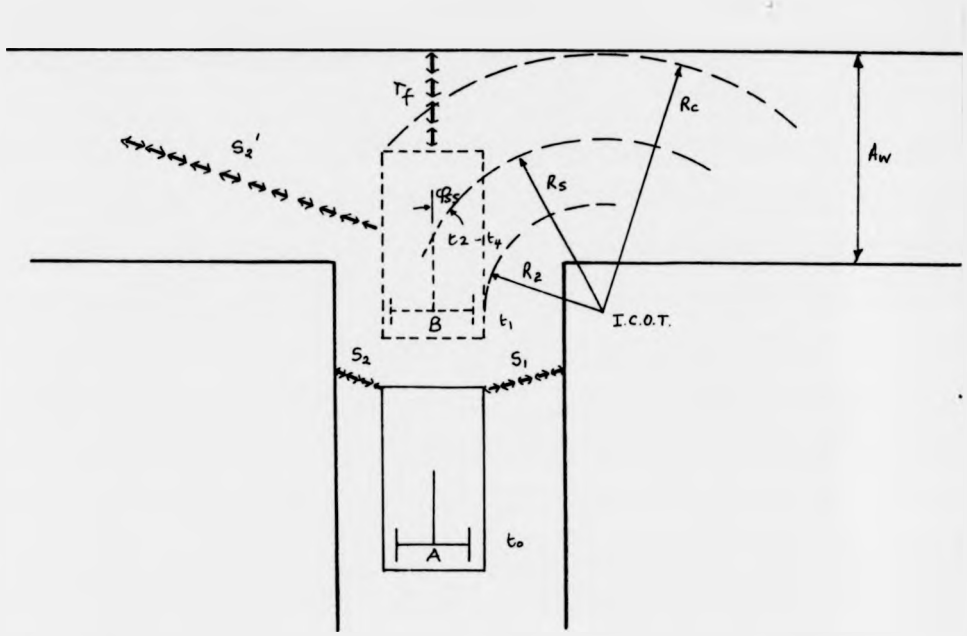

Figure 6.1 The tricycle vehicle in relation to the 'T-junction'

With the vehicle halted at B , the steer angle is then turned through some angle φ_{ss}, to result in the turning radius R_s. This radius being selected to avoid impact with the forward constraint. When the steer angle has reached its steady state, the speed increases from zero to V , and the heading rotates through an angle determined by the area under the curve from t_3, to t_6, and the steer angle φ_{ss}. The completion of the desired heading angle turned through can be monitored by measuring how far the steered wheel has travelled, and the required distance having been moved, used to initiate the 'braking process'. With the vehicle halted the steered wheel is then returned to its 'dead ahead' position. This is shown as location C. in Fig 6.2. The speed is then increased to V . The vehicle is shown at location D having moved along another segment and corridor and being guided again by the 'following' algorithm that enabled the lateral tracking of the wall to take place.

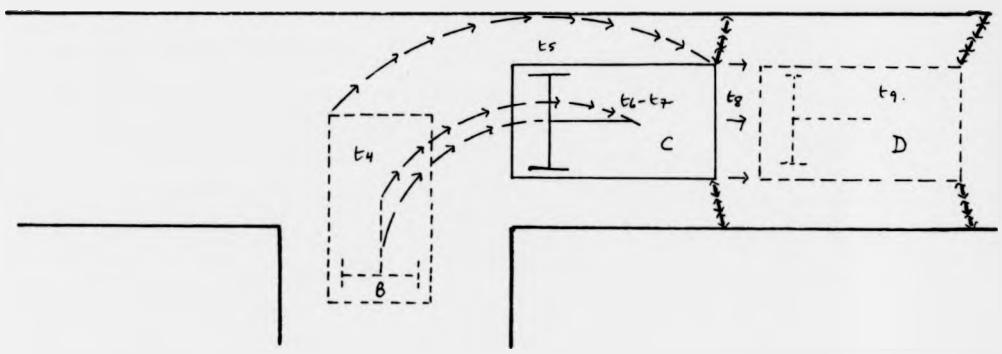

Figure 6.2 The vehicle and its subsequent relation to the intersection after moving from B, to C, with a constant steer angle. At D the vehicle is moving at a constant speed down the 'corridor' stabilised and guided by the lateral sonar.

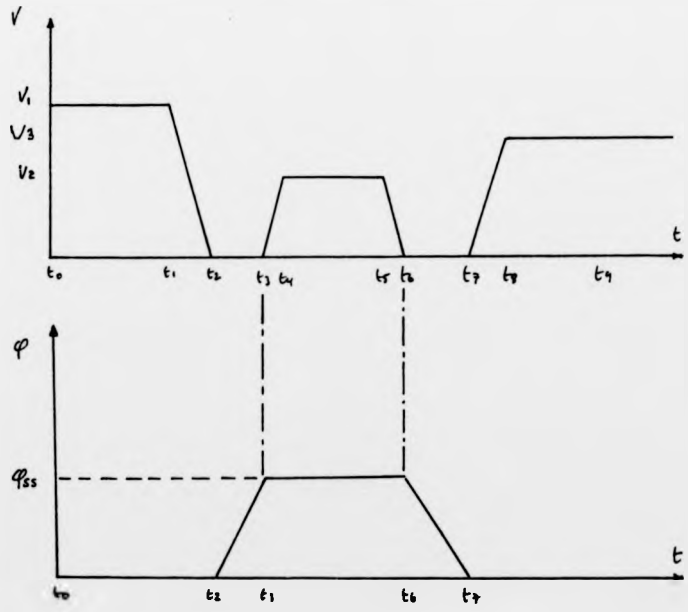

Figure 6.3 The scheduling of (a) the speed, and (b) the steer angle, to enable the vehicle to negotiate the 'T-junction'.

An alternative to this mode (see figure 6.4) is to turn the steered wheel as the vehicle moves. The approach phase is the same as before (see figure 6.1.). The vehicle's speed remains constant. The finite time taken to change the curvature of a vehicle means that there will be positional and heading differences between this mode of turning and the previous method. The extra distance is $\Delta X_e, \Delta Y_e$, and the additional heading $\Delta\psi_e$. This reduces the total distance required to bring the vehicle's heading around to that of location C, (see figure 6. 2).

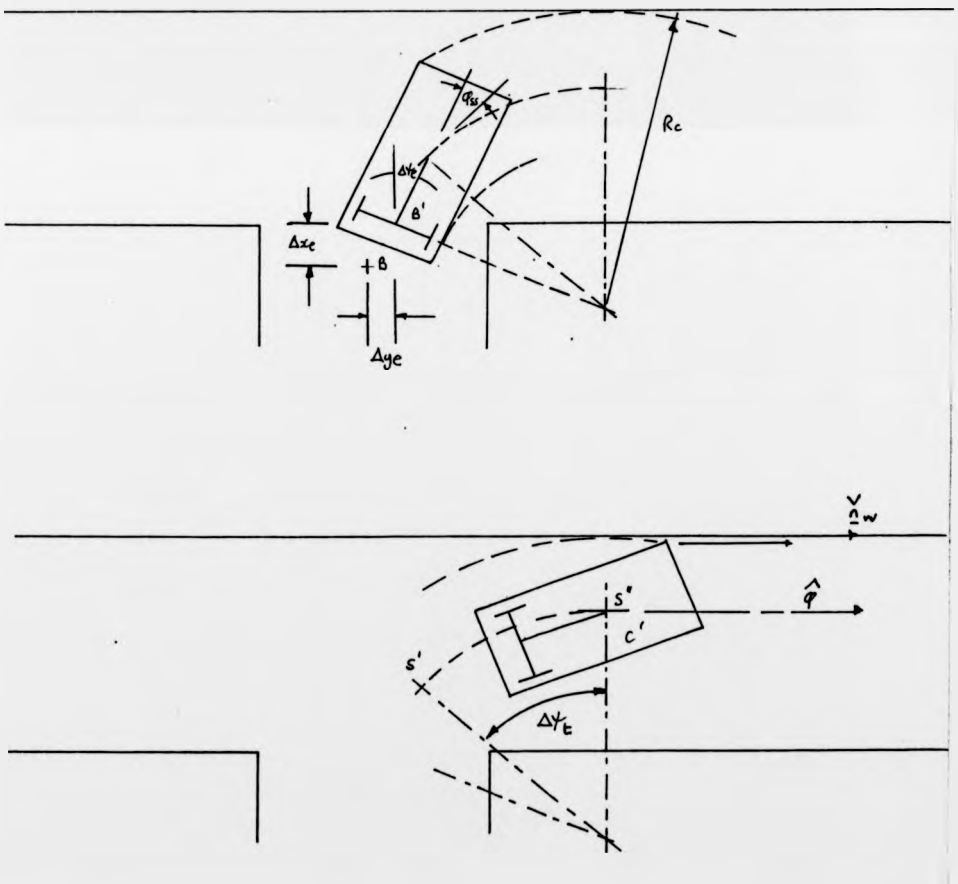

Figure 6.4 Turning whilst moving at an intersection, (a) initial 'offset' location, (b) final location with steered wheel parallel to the exit wall.

The wheel can then be turned at a rate so as to remain parallel with the exit wall as the vehicle continues to move forward.

With a particular steer angle, there is an exit corridor width, A_w, and longitudinal and lateral offset of the beginning of the turn into the exit which can be tolerated so as to allow the vehicle to pass through and to have turned through 90 degrees. The radius of turn with a particular steer angle φ, is R_s and, $A_w <= R_c - [R_d - b]$ where $R_c^2 = [W + \alpha]^2 + [R_d + b]^2$, and $R_d = W.\cot(\varphi)$. Substitution and rearrangement gives that the corridor width A_w, must be greater than

$$[(W + \alpha)^2 + (R_d + b)^2]^{\frac{1}{2}} - (R - b) \qquad 6.1$$

And, the minimum lateral offset for a constant curvature turn is $R_d - b$, The effect of these relations on the lateral offset and exit width required for two constant curvature turns are illustrated in figure 6.5.

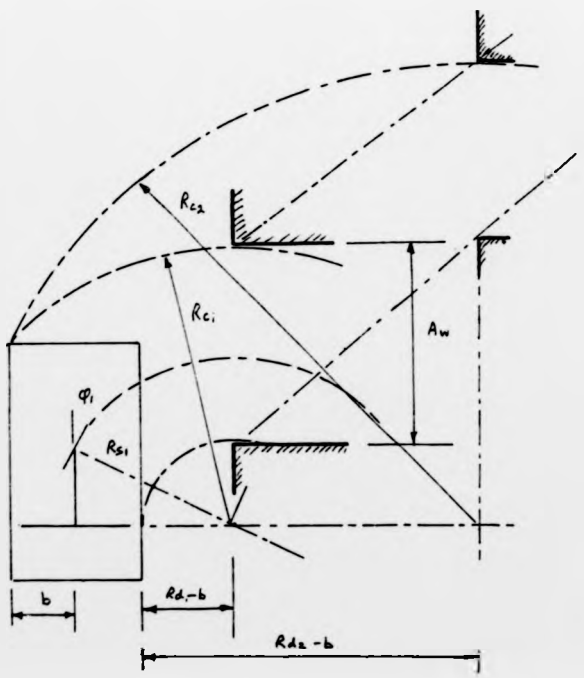

Figure 6.5 The relation between exit corridor width and lateral offset.

6.3 Experimental

The vehicle was manually driven to the starting position illustrated as location A , (see figure 6.1). The forward constraint was initially placed beyond the maximum range detectable by the forward pointing sonar. The lateral motion was assumed to be stabilised by the flank sonars and the robot was set in motion under control of the computer, the forward range was sampled to determine when the steer angle needed to be turned, and whilst the vehicle continued to move forward. The distance to be moved in order that the body heading would rotate by 90 degrees, was determined from $s = R.\frac{\pi}{2}$, and the odometer output was sampled to measure when that distance had been traversed. At that point the following process was once more intitiated. The following process was used to stabilise the vehicle's motion as it moved along the 'exit' corridor. Experimentally, at this point the vehicle was permitted to continue to move forward. This caused the body heading to rotate too far. To correct this the steer angle was not simply returned to its central position, but was taken past the central position and then returned to the 'dead ahead' position, this all being done whilst the robot continued to move forward. Doing this enabled the integrated heading error that had been caused by the time taken for the steering wheel to return to its zero position to be removed.

6.3.1 Results

Three measurements are graphed. The sampled forward range. The steer angle dynamic whilst the robot continued to move forward, and the lateral range measurements in the 'exit' corridor. The step response of the steering control system had been initially obtained with the vehicle stationary, (see appendix A.3).

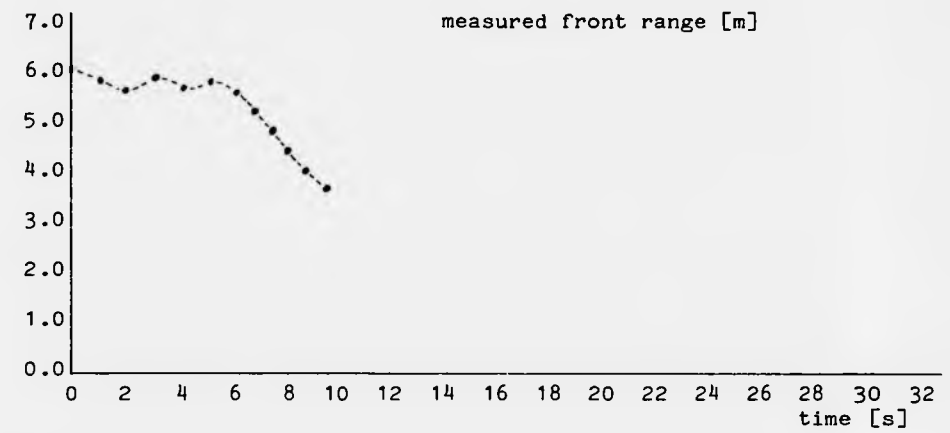

Figure 6.6 Measured sonar range from the front constraint.

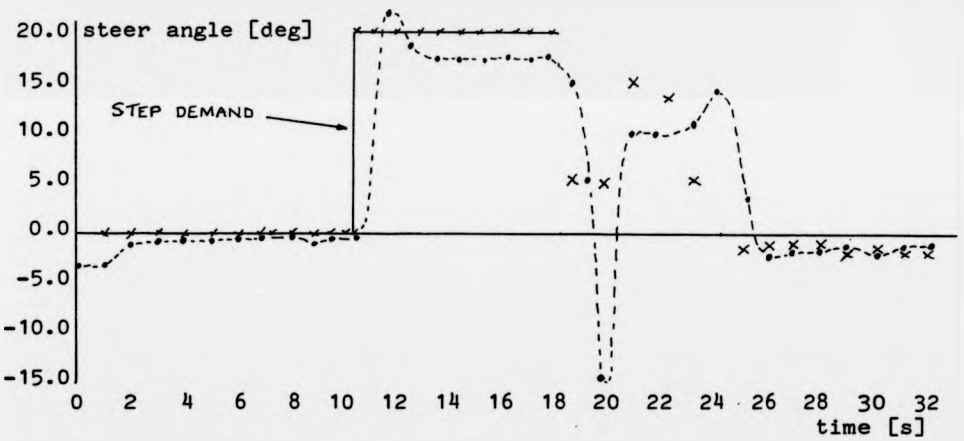

Figure 6.7 The steer angle dynamic. The vehicle was moving forward and turning. × = demanded, -•- = measured.

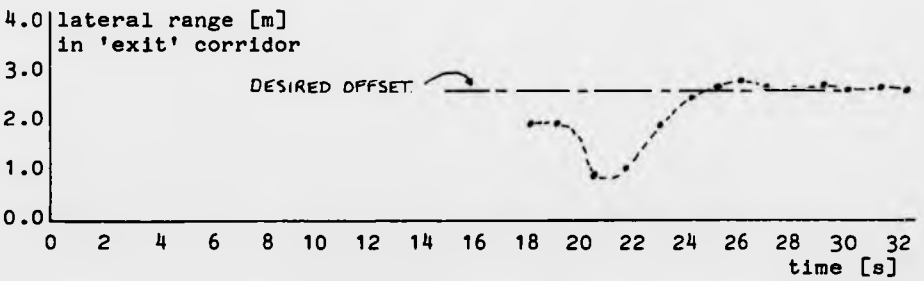

Figure 6.8 Lateral sonar range measurements as the following algorithm and the lateral range measurements were used to guide the steered wheel and stabilise the lateral motion.

6.3.2 Discussion

During motion the steered wheel response is underdamped. This is in constrast to the overdamped response obtained with the vehicle stationary, (see Appendix A.3). As the tyre rolls a reduction in the frictional forces between the tyre and the surface it moved over would be expected. The response also shows a steady state error. A constant load torque would produce this effect.

The sonar range pattern and the expected changes in these ranges, when entering a 'T-junction' were used to initiate task rescheduling. This can be done in principle with each of the other environmental 'components', since a unique range pattern exists. The 'dead end', 'cross-roads', 'corner' and 'corridor' range pattern are shown below.

F = Front, P = Port, R = Rear S = Starboard.

sensors	corresponding environmental element
F R P S	
1 1 1 1	crossroads (X)
0 1 1 1	T-junction (T)
0 0 1 1	Corner (K)
1 0 1 0	Corridor (C)
1 0 0 0	Dead end (D)

Figure 6.9 Range patterns associated with prototypical environments. The value 1 indicates a long range, 0 a short range. The exact range would depend on the dimensions of a particular environment.

With four sensors there are sixteen possible patterns. (0 0 0 0) is invalid, it corresponds to the robot being boxed in. The pattern for the crossroads occurs once. The remaining four patterns can each be cyclically permuted and still correspond to the same environmental element. If the world was composed of these basic building blocks, and given the uniqueness of the range measurements associated with each

intersection, then they could be used in conjunction with the navigated position and heading to enable the type of intersection to be identified. The range transitions from one environmental component (defined in section 1.5.1 figure 1.6) could be used as feedback to a task scheduler that would use this information to initiate the next task. In this case for a T-junction this subsequent task consists of reorientating to take the robot from its current path onto the next path identified by a 'path planning' process, as being able to take the robot from its original location to its goal position. The problem of representing the connectivity and then automatically producing a sequence position coordinates that can form the basis of a task schedule has not been considered here. This represents further work.

The finite number of range sensors used, combined with their finite beam width, places a limit on the variety in the environmental configurations that can be uniquely detected. An estimate of this variety can be obtained if it is assumed that for the object to be detectable it must lie within the 3db locus of the sonar in its receive mode, and that the angle between the outward pointing normal from the wall and the sonar ranger be less than B degrees. To obtain panoramic coverage with a 3db beamwidth of $\pm$B degrees then naively 360/2.B = p sensors are required If the range resolution is r [m] and the maximum range is R [m], then the information in one full panoramic sample assuming random placement of the features returning the signal is

$$I = \log_2(p \cdot R / r)$$

and for B = $\pm$10 , p = 18, with R = 10 [m], r = 0.01, then I = 14.13 bits.

When the vehicle was in motion the steer angle versus time had the appearance of a 2nd order linear system responding in an underdamped manner to a step input. When the vehicle was stationary the response was overdamped. Although a study of the control system to 'improve' its performance could have been undertaken this was not done, and, as a result of not examining traditional technique, an alternative method of modulating the steered wheel angle with time was discovered. The technique to be outlined enables the heading control variable, for this vehicle, the steered wheel, or for example, on an oil tanker, the rudder, to be controlled so that a change in heading can be achieved whilst moving without 'overshoot and smoothly'. Since the alteration is based on a mathematical function whose values can be precomputed, the technique could be automated. A further application of this function to the heading control, with the control variable made to be the negative of the first, enables the vehicle to perform a transfer smoothly and without overshoot from one parallel path to another. With the vehicle moving in reverse the application of this technique permits the automatic parking of a wheeled vehicle. The use of this function would also enable other 'complex' manoeuvres to be programmed off-line and the results of the mobile robot displayed graphically prior to executing the task for real.

The desirable characteristics of a modulating function are that it should have a defined area and be smooth over the range of times it is active. Ideally it should start and finish at zero value. After some experimentation with various candidate functions the one that had some attractions was the Gaussian.

The change in steer angle is now assumed to be governed by a control system that can change the steer angle according to

$$\varphi(t) = A.\exp[- (t - m)^2/(2.s^2)] \qquad 6.6$$

where A is the maximum angle of the steered wheel, m is the time that the

When the vehicle was in motion the steer angle versus time had the appearance of a 2nd order linear system responding in an underdamped manner to a step input. When the vehicle was stationary the response was overdamped. Although a study of the control system to 'improve' its performance could have been undertaken this was not done, and, as a result of not examining traditional technique, an alternative method of modulating the steered wheel angle with time was discovered. The technique to be outlined enables the heading control variable, for this vehicle, the steered wheel, or for example, on an oil tanker, the rudder, to be controlled so that a change in heading can be achieved whilst moving without 'overshoot and smoothly'. Since the alteration is based on a mathematical function whose values can be precomputed, the technique could be automated. A further application of this function to the heading control, with the control variable made to be the negative of the first, enables the vehicle to perform a transfer smoothly and without overshoot from one parallel path to another. With the vehicle moving in reverse the application of this technique permits the automatic parking of a wheeled vehicle. The use of this function would also enable other 'complex' manoeuvres to be programmed off-line and the results of the mobile robot displayed graphically prior to executing the task for real.

The desirable characteristics of a modulating function are that it should have a defined area and be smooth over the range of times it is active. Ideally it should start and finish at zero value. After some experimentation with various candidate functions the one that had some attractions was the Gaussian.

The change in steer angle is now assumed to be governed by a control system that can change the steer angle according to

$$\varphi(t) = A.\exp[- (t - m)^2/(2.s^2)] \qquad 6.6$$

where A is the maximum angle of the steered wheel, m is the time that the

steered wheel is to be at at a maximum, s is the standard deviation of the distribution, and t is time. The result of applying this control schedule in simulation to the deduced reckoning equations of chapter 2.0 is illustrated (see figure 6.11) for a particular value of A, m, and t shown in figure 6.10.

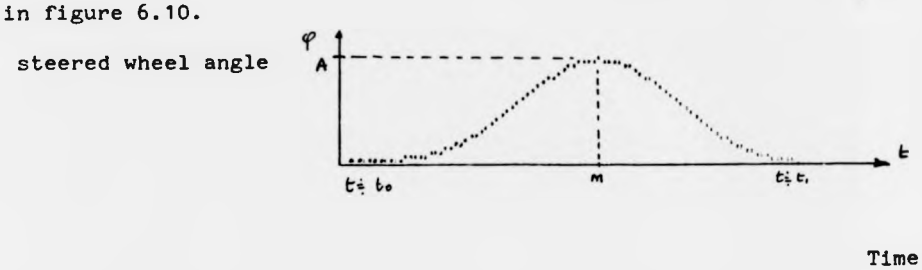

Figure 6.10 Steered wheel angle schedule based on a Gaussian distribution. as defined by (6.6).

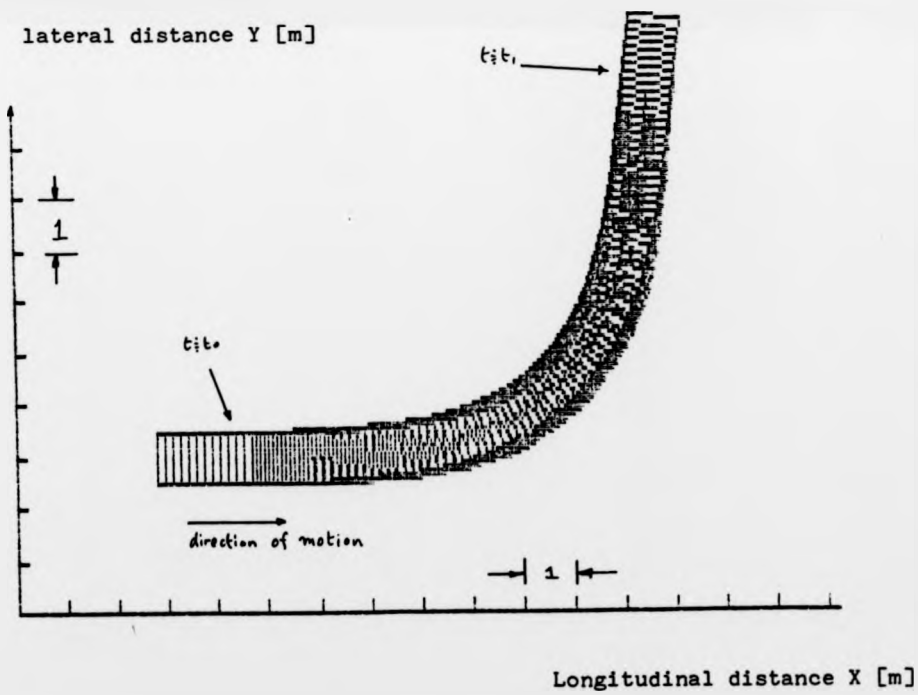

Figure 6.11 Example from a simulation to determine the position and orientation of the robot after the application of a Gaussian pulse to the steered wheel.

A simulation to explicate the relation between vehicle speed v_1, A , and the resulting heading and position of the vehicle is shown below. In the simulation the standard deviation was kept constant, and the amplitude A , varied. The general form of the results is given below in Figure 6.12.

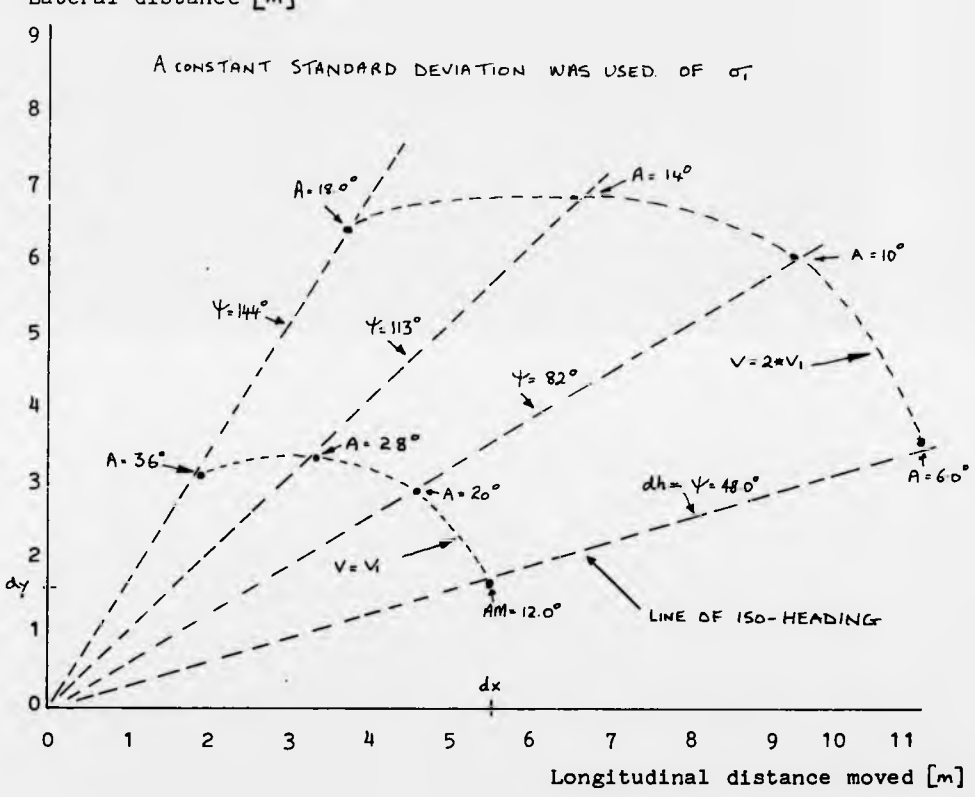

Figure 6.12 The relation between position and heading of the tricycle vehicle after passing Gaussian pulses of various amplitudes through the kinematic equations, with the vehicle moving at different speeds.

Given a desired position and heading for the robot vehicle, and a control system capable of altering the steered wheel angle according to this schedule, then this diagram can be used to calculate the necessary

maximum amplitude for the steered wheel angle and the speed of the vehicle as it moves, to be able to achieve that demand. For example, to move dx and laterally dy, and finish with the steered wheel pointing dead ahead, and with a change in body heading of dh it is necessary for the robot to change its steer angle to A_m with a standard deviation of σ_1 and move with a velocity v_1. The concatenation of two such pulses modulating the steered wheel angle enables the 'dog leg' manoeuvre to be accomplished, (see figure 6.13). The concatenation of this manoeuvre enable the vehicle to return to its original track, (see figure 6.15).

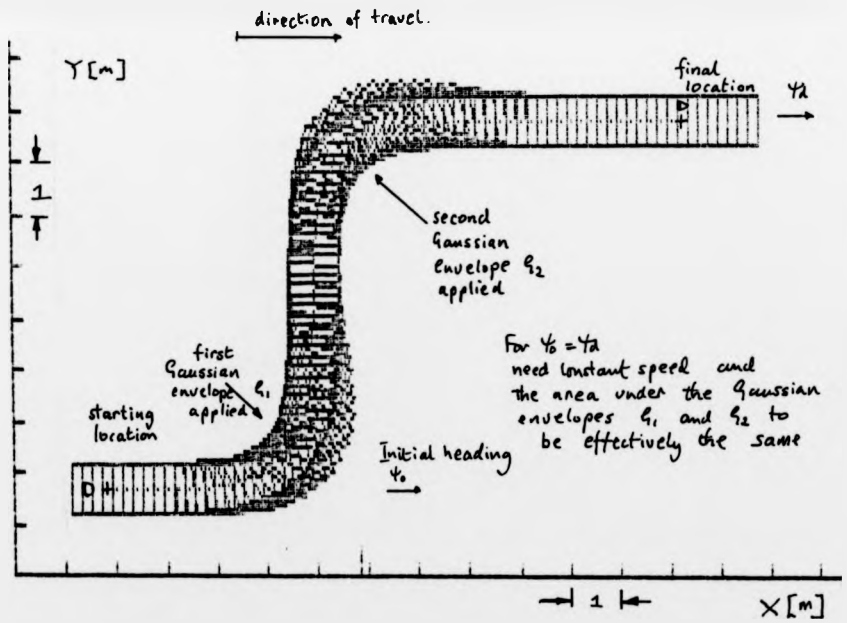

Figure 6.13 Forward 'dog-leg' manoeuvre, the concatenation of two Gaussian pulses of equal area but of opposite sign through the kinematic equations,

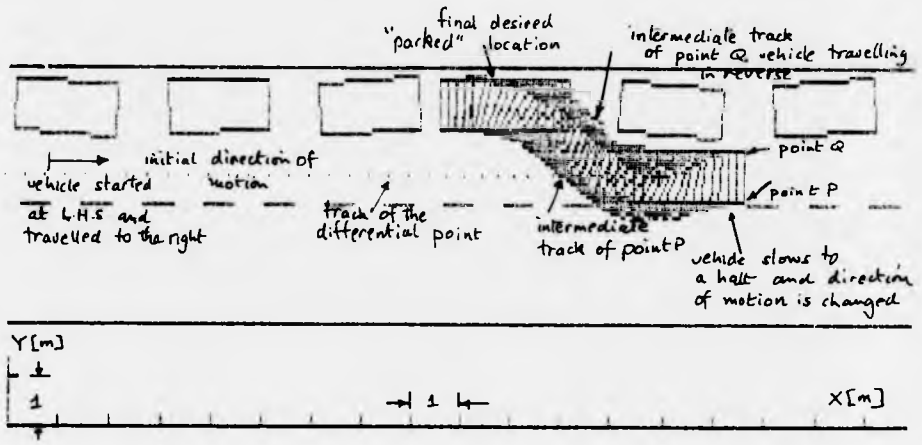

Figure 6.14 The movement of the vehicle in the reverse direction permits 'critically damped' parking manoeuvres to be accomplished.

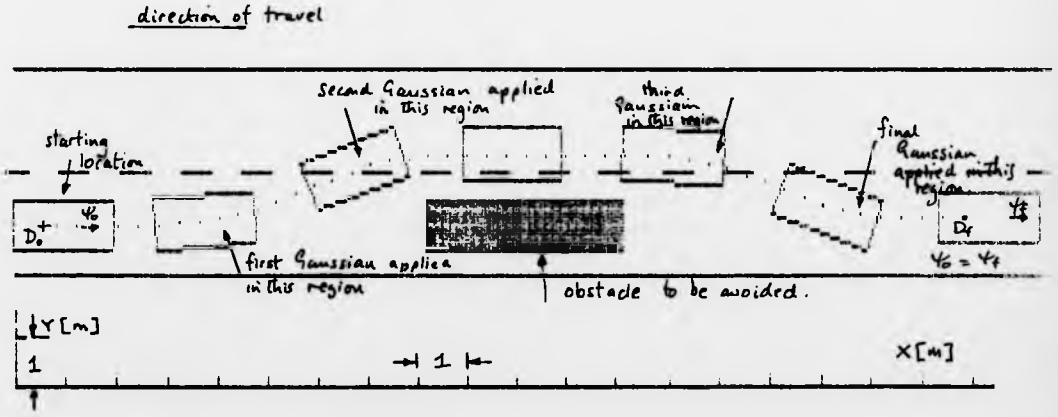

Figure 6.15 The 'obstacle avoidance'/ overtaking manoeuvre accomplished with the concatenation of two 'dog-leg' manoeuvres, with time order of the initial 'dog-leg' reversed.

The problem of moving an object through a 'field' with polyhedral objects was considered by [Lozano-Perez 1978]. This work extended the the navigation system of SHAKEY and is described by [Nilsson 1970]. The cost of computing a continuously changing orientation was considered computationally too expensive. This work in contrast has examined that aspect of continuously modifying the steered wheel angle. The simulation results suggest that this method would use less space and time to manoeuvre. A reduction of the reorientation time to move from one path onto another would be a desirable economic feature.

6.4 Conclusions

The reorientation of the tricycle vehicle to take it from one path onto another path has been demonstrated experimentally. The guidance used to achieve this was based on the range information to initiate the change in task, and the odometer to determine when the required change in heading had been achieved.

It has been shown how the received range pattern can be used to identify in principle, four 'types' of intersection.

A change in steer angle versus time whose envelope can be described with a Gaussian function has been shown in simulation to be able to produce desirable kinematic behaviour, with a vehicle that has to move in order to turn. Experimental work needs to be performed to confirm its practical usefulness.

The damping of the steering control system was observed to decrease as the vehicle speed increased. To obtain an improved model of this response more work is needed to establish the effect of rolling speed on the reduction of the frictional forces.

7.0 LONGITUDINAL GUIDANCE from the ODOMETER

7.1 Introduction

The aim was to implement a control scheme to control the robot's longitudinal position; to move the vehicle forwards or backwards with zero curvature, for a fixed distance, and with feedback from the odometer.

7.2 Experimental

Figure 7.1 is a block diagram of the experimental arrangement that was proposed as a means of achieving longitudinal control of the vehicle's position.

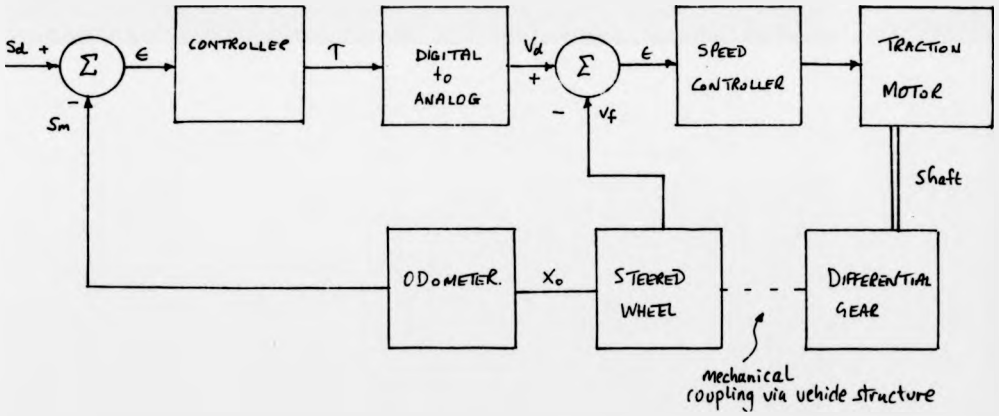

Figure 7.1 Block diagram of the scheme used to investigate the closed loop positioning of the robot, with feedback from odometer.

The demanded run distance was S_d. The measured travel distance was S_m The positional error was (S_d - S_m). n was the minimum distance resolution of the odometer. The input to the controller was the error, and its output was a number corresponding to the desired time that the motor should be energised. The width of the pulse was altered according to the

formula,

$$T = \text{sat}[\ G.(S_d - S_m) + \text{an offset}\ ] \qquad 7.1$$

with the gain G, being the experimental variable. The values of G input were 0.1, 0.2, 0.3, 0.4, and 0.5. The pulse height was held constant at a Vd = 4. The earliest experiments performed and that provide a basis for this section are described in appendix A.2.0.

The following parameters were provided as input S_d, the demanded travel distance, G , the slope of the error detector, sat , the saturation value of this detector, O , the offset value of the error detector, V the digital demand to the speed controller, T , the initial duration of the pulse, Ef, the acceptable error in the final position, and D the dwell period.

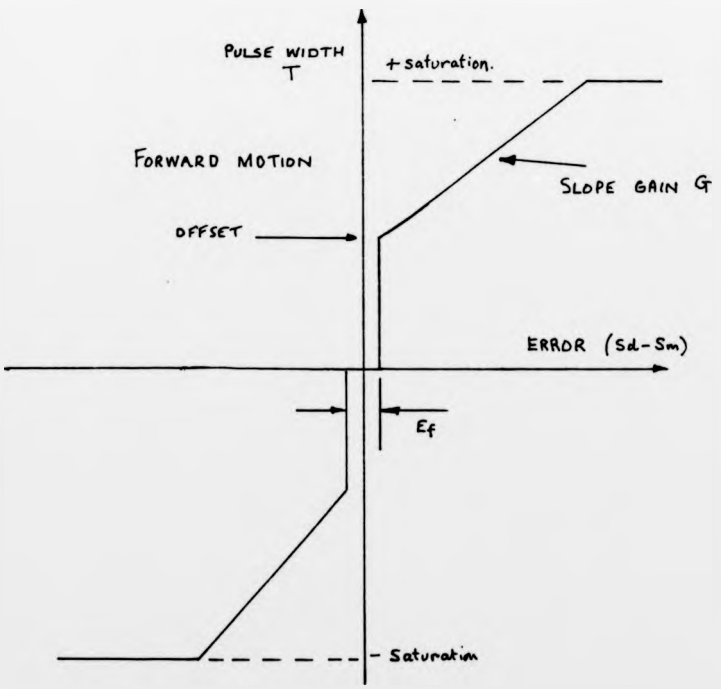

Figure 7.2 Controller characteristics based on open loop experiments. The detailed results from open loop pulse tests are given in Appendix A.2

7.3 Results

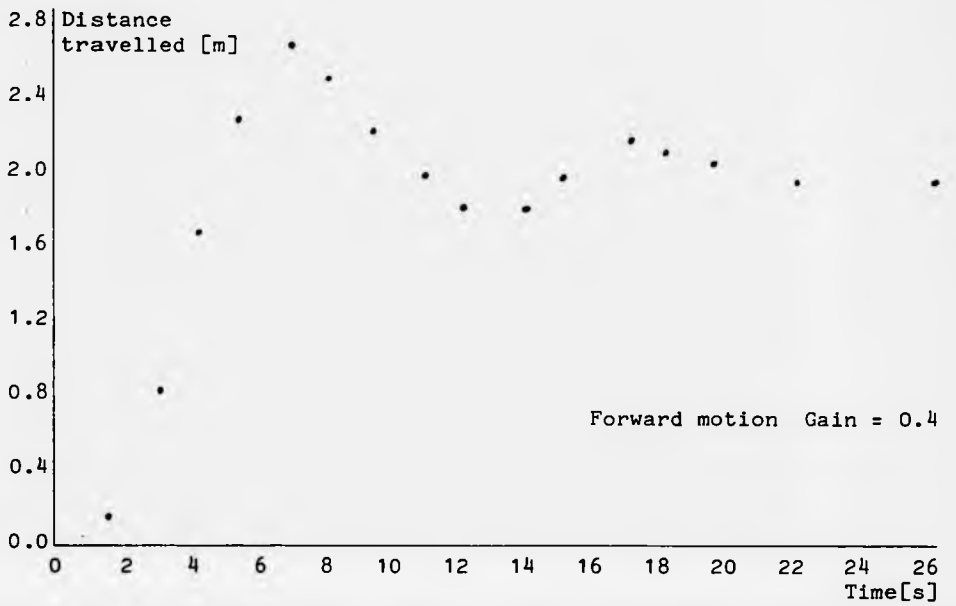

Figure 7.3 A representative result of the oscillatory motion of the vehicle after it had been commanded to move forward a fixed distance with feedback about its longitudinal position obtained from the odometer.

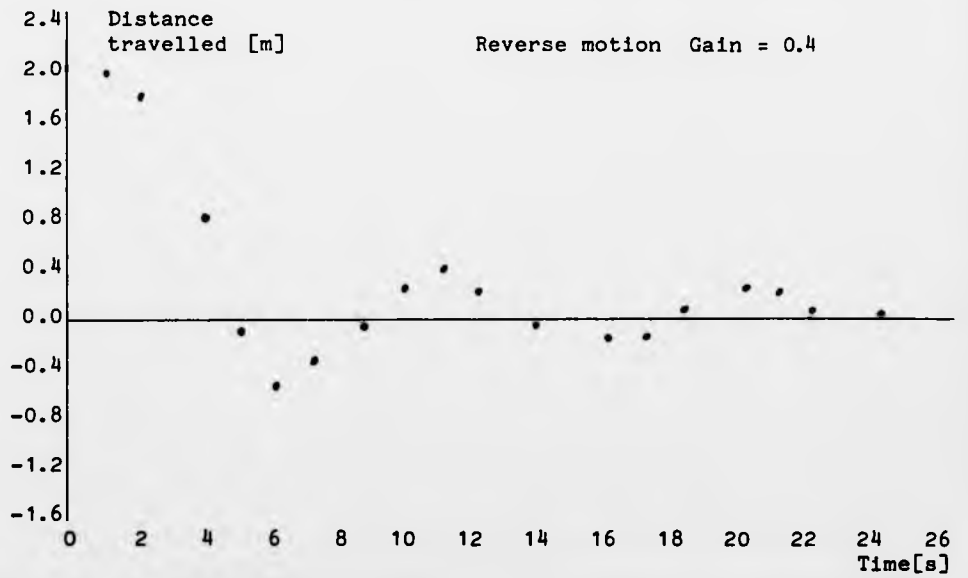

Figure 7.4 A representative result of the oscillatory motion of the vehicle after it had been commanded to move backward a fixed distance with feedback about its longitudinal position obtained from the odometer.

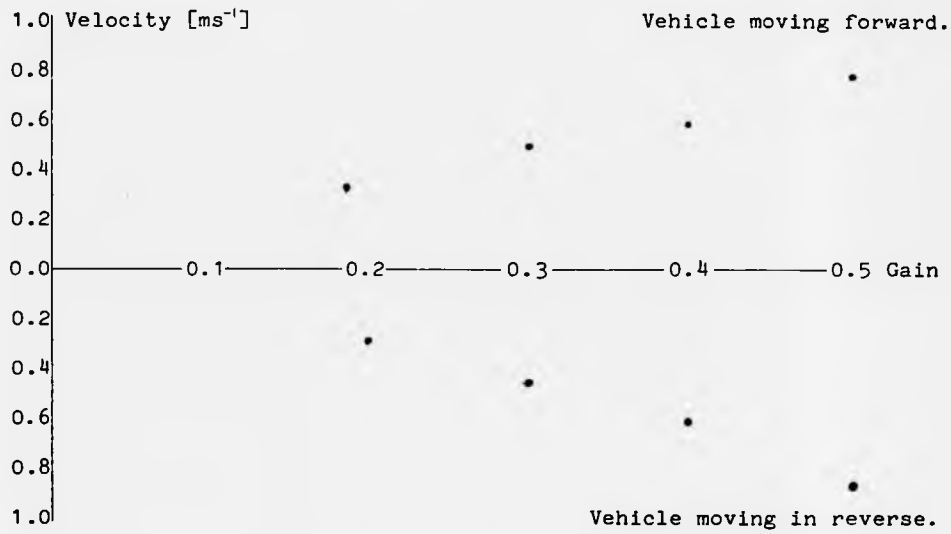

Figure 7.5 Steady state velocity of vehicle for both forward and reverse directions versus gain.

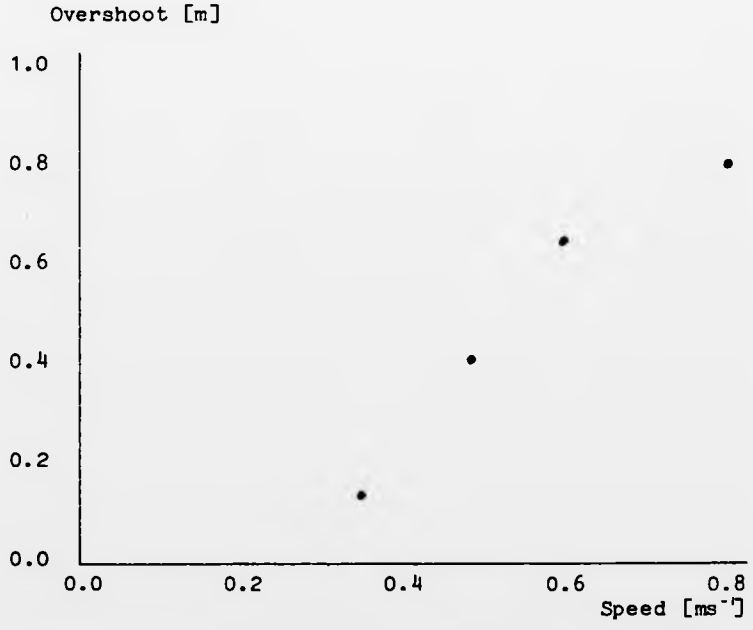

Figure 7.6 Variation in overshoot of the vehicle past its commanded distance versus the speed of approach.

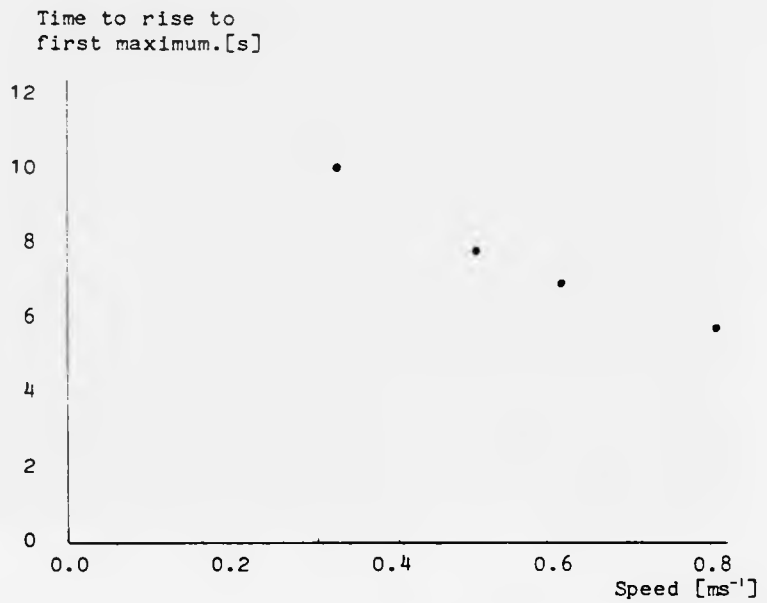

Figure 7.7 Time to rise to first maximum versus steady state speed on approach to desired position.

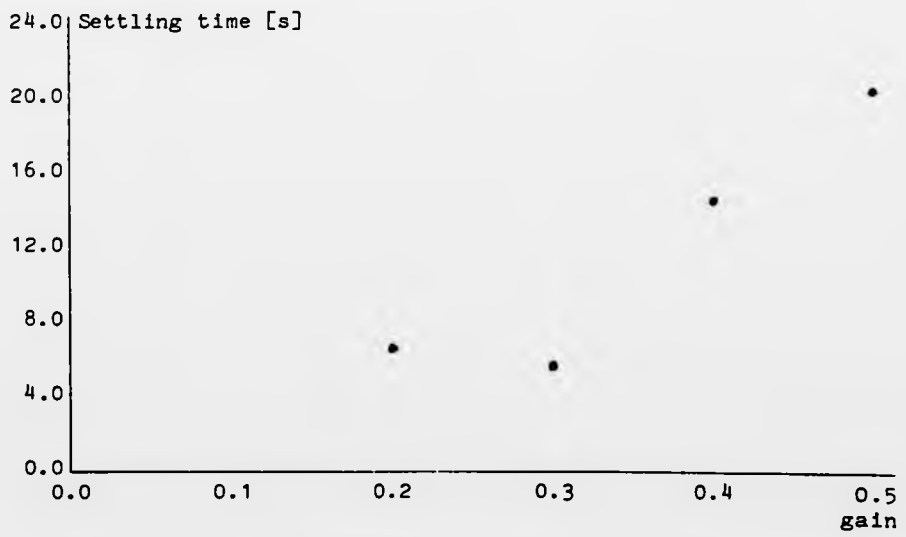

Figure 7.8 The time to settle given the vehicle has once reached the goal position.

7.3.1 Discussion

The controller produced pulses to the transit motor whose duration varied in proportion to the positional error between the measured and demanded travel distance. Above a certain positional error the pulse duration was held constant and independent of the positional error. At zero positional error there was an offset.

The form of the controller was based on the relation obtained earlier, and experimentally, (see Appendix A.2.0) between the duration of the applied motor pulse, and the resulting total distance moved forward by the vehicle. This relation was linearised, and the inverse used to relate the positional error to the pulse duration . The gain G, was the slope of the line joining the offset to the maximum pulse duration. The offset pulse width at zero error was set just below the minimum necessary to produce motion with the vehicle halted.

Figure 7.3 displays what happened when the vehicle was commanded to move forward using this controller. It shows how the distance moved varied with time. Figure 7.4 shows a similar response but with the vehicle commanded to move backward. Although the slope and offset parameters of the controller for both directions appear to be the same the response for the same value of gain was different. The duration of the pulse, with the vehicle moving backwards, needed to be increased by a third to achieve about the same approach speed. This observation remains to be explained. The initial transient is related to the inertia and load of the traction motor, as given in Appendix A.2. equation (a.2.2) .

Figure 7.3 has a linear portion which represents the vehicle moving toward the goal position at a constant speed. The speed was found to be proportional to the gain. The time to reach the goal is about s/v seconds, for a constant speed of approach of v ms^{-1}, and a distance s.

Some oscillation of the vehicle around the demanded position occured before being positioned correctly. This is illustrated in Figure

7.8 For low values of gain this was a constant. Above an approach speed of about 0.4 ms^{-1}, the time to settle started to increase linearly. The samples from the odometer were available according to (7.2). To move the vehicle forward at controllable low speeds it was found necessary to pulse width modulate the traction motor. As a result the sampled odometer output was not used as soon as it became available. The rate at which odometry samples become available is given by the formula

$$t = 2.\pi.r\ /n.v \qquad 7.2$$

for a wheel of radius r , digitised into n segments, moving with a linear velocity of v. For the experimental vehicle moving at 0.5 ms^{-1}, this implies sampling every 0.040 [s]. To quantify this the motor could have been energised continuously and the odometer sampling rate varied to determine if the settling time and overshoot could be improved with the higher values of gain. Further work is also required to determine the limits of stability of this form of control. For example, at short distances with fast approach speeds.

For speeds from 0.05 to 0.25 ms^{-1}, the overshoot remained constant at about 0.3 m. From 0.25 ms^{-1}, the overshoot is proportional to the approach speed. By 0.8 ms^{-1}, the overshoot was 0.8m. This is shown in figure 7.6. In all experimental cases there was overshoot. Additional work would be required to produce a response with no overshoot. The time taken for the vehicle to reduce its speed to zero with gains of 0.3, 0.4, and 0.5 was about 1 second and independent of the approach speed. The distance travelled before the speed became zero was quadratic.

Although control over the vehicle's position has been attained this control scheme was based on the distance run to pulse duration relation obtained with the vehicle starting with zero speed. Since some of the energy associated with the pulse would have been absorbed in overcoming the static friction the error to pulse duration that is actually needed when the vehicle is moving may be expected to be less.

Associated with each approach speed is a time taken to come to a halt that may be associated with frictional forces arising from sources other than the active braking forces. An alternative control strategy would have been to switch the motor off at a certain distance away from the goal and allow it to coast to halt. For each speed there is an associated time to halt, T , governed by the formula T = f(v). This relation is embodied in the results shown in Appendix A.2 Fig A.2.6. The integration of f(v) between the time taken to halt at that speed and to zero gives the distance away from the goal at which the motor should be switched off. As the vehicle's mechanical components age, or the tyre surface frictional forces change, this relation would change. If a vehicle was required to work to fine positional resolutions over long periods of time, either a controlled deceleration characteristic should be built in or the 'tool' the robot is carrying should be able to accommodate and make up for the imprecision in the positioning of the mobile robot.

With controlled braking the time taken to halt will be less than by simply allowing the vehicle to coast to a standstill. Further work would be required to obtain an estimate of the active braking deceleration time constants, and to determine the benefit of such an improvement.

For a particular motor there will be a maximum torque that it can develop. This limits the maximum speed of the vehicle. Although the demanded run distance was only 2 metres, this was sufficient for the motor to drive the vehicle up to a steady state speed prior to decelerating. In practise a mobile robot would be required to move over larger distances. This positioning strategy could be used when the robot was within a few metres of the goal.

The distance as measured by the odometer was compared with the real distance. In all cases the vehicle had moved the required distance, to within the positional resolution demanded. It should be noted that at this stage of the work the detailed dead reckoning calibrations had not

been performed, and a quantitative measure of the dead reckoning errors over larger distances were not available.

As the batteries discharge the power that can be delivered to the motor for a given error signal falls. This will change the distance moved per unit error. There would be a increase in the time taken to achieve the goal position. A mobile robot operating only on its own power resources should be designed so that for a given working or experimental cycle sufficient power is available.

7.4 Conclusions

A simple control strategy can been used to move a vehicle of significant mass, forwards from a stationary position, for a fixed distance with positional feedback from an odometer.

The vehicle could be positioned to within the resolution of the odometer, over the distances moved as determined by an external observer.

The position of the vehicle was controlled by speed demands to a series d.c. motor proportional to the positional error from the goal. The parameters of this controller can be obtained from simple open loop pulse tests on the motor.

The control was stable over the range of speeds used.

Appendix A.1.0 The experimental vehicle

A.1.1 General description

The experiments were performed with an electrically powered 417kg. tricycle wheeled industrial burden carrier, capable of carrying a load of 680 kg, [Bradshaw 1981]. The tyres were tread pneumatic. The vehicle was converted so that it could be driven either manually or under computer control. The power for all the onboard systems was obtained from six 190 a.h. 6 V traction batteries.

Figure A.1.1 The vehicle in its original form.

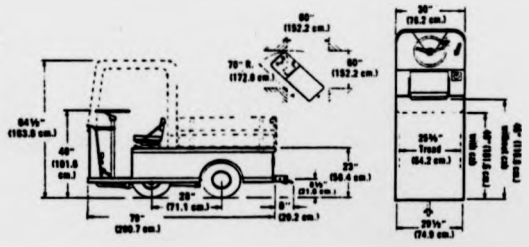

Figure A.1.2 Side and plan view of vehicle

Appendix A.1.0 The experimental vehicle

A.1.1 General description

The experiments were performed with an electrically powered 417kg. tricycle wheeled industrial burden carrier, capable of carrying a load of 680 kg, [Bradshaw 1981]. The tyres were tread pneumatic. The vehicle was converted so that it could be driven either manually or under computer control. The power for all the onboard systems was obtained from six 190 a.h. 6 V traction batteries.

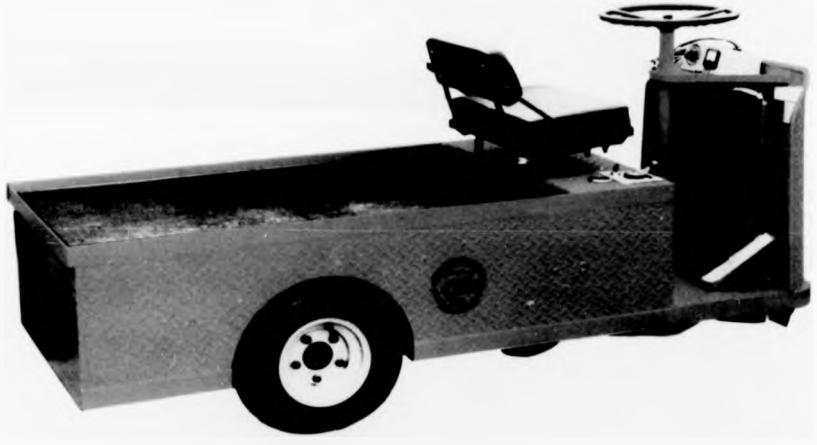

Figure A.1.1 The vehicle in its original form.

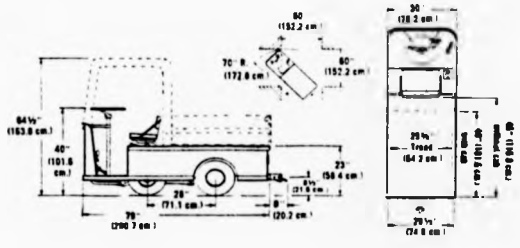

Figure A.1.2 Side and plan view of vehicle

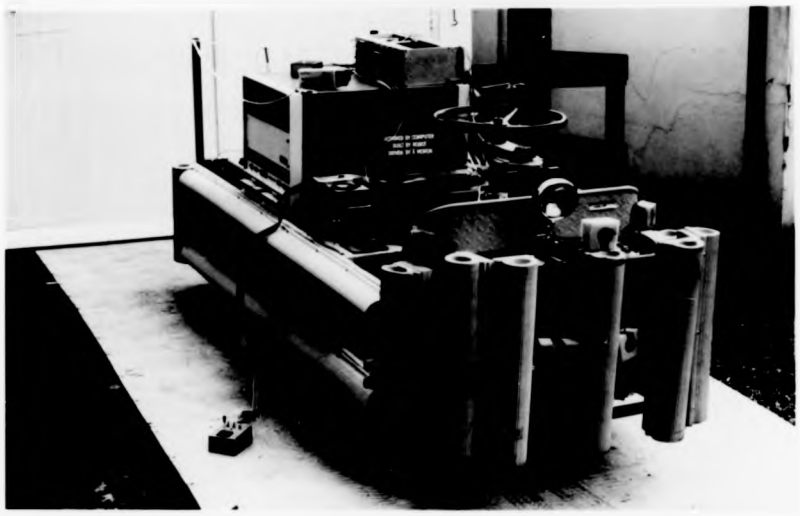

Figure A.1.3 The modified vehicle.

The grey sections are the protective rubber fenders. At the front can be seen three of the sonar transducers mounted in their beam forming inserts. On the starboard side can be seen the flank and lateral sonar. Beneath the steering wheel, and attached by a sprocket and chain is the steering motor. The drivers seat is in front of the development computer 'cube'. The interface electronics can be seen standing on top of the computer. Also shown is a bank of general purpose switches and the joystick controller.

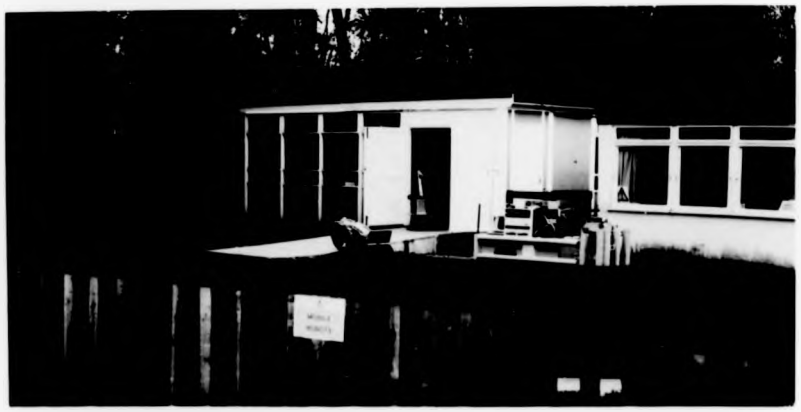

Figure A.1.4 The mobile robot shown in relation to an environment.

Figure A.1.3 The modified vehicle.

The grey sections are the protective rubber fenders. At the front can be seen three of the sonar transducers mounted in their beam forming inserts. On the starboard side can be seen the flank and lateral sonar. Beneath the steering wheel, and attached by a sprocket and chain is the steering motor. The drivers seat is in front of the development computer 'cube'. The interface electronics can be seen standing on top of the computer. Also shown is a bank of general purpose switches and the joystick controller.

Figure A.1.4 The mobile robot shown in relation to an environment.

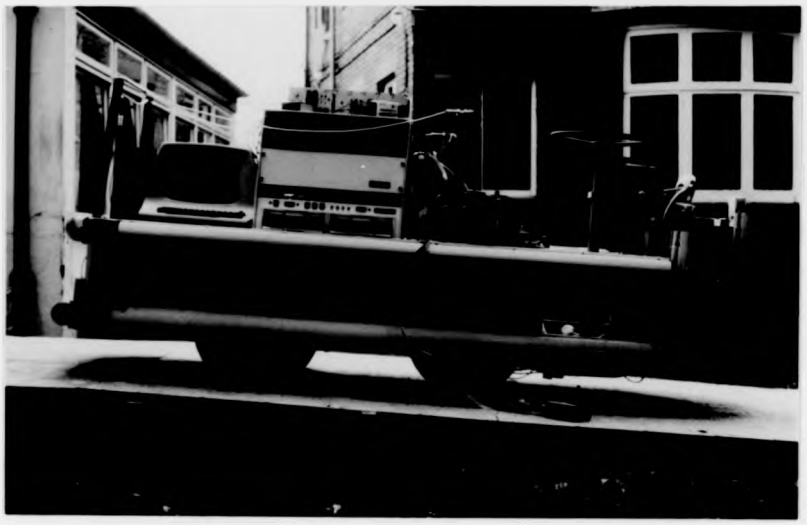

Figure A.1.5 A side view.

This shows the short wheel base, of 0.72m. At the rear can be seen the terminal. The starboard flank and lateral sonar can now be seen. The steering control system electronics was housed behind the front plate. Behind the facing yellow plate and beneath the computer were the batteries, traction motor, differential, and thyristor motor controller. The robot comprised the following main systems; transit, steering, sonar ranging, opto-magnetic compass, status and safety, and the computer.

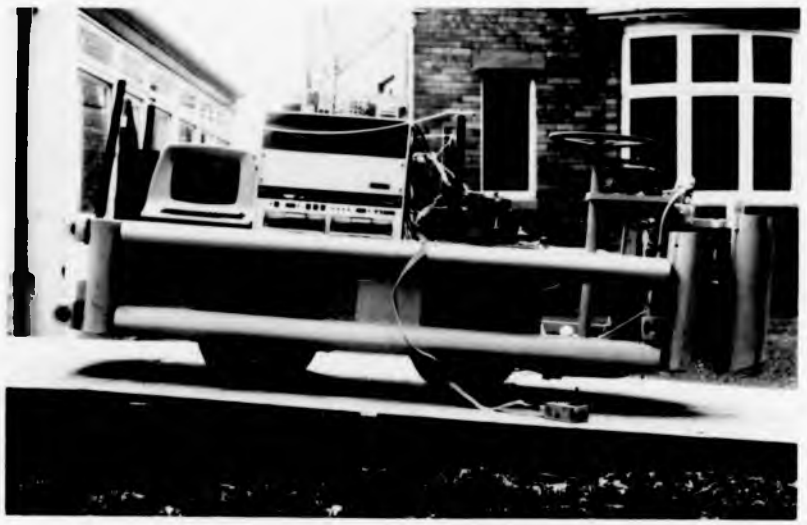

Figure A.1.5 A side view.

This shows the short wheel base, of 0.72m. At the rear can be seen the terminal. The starboard flank and lateral sonar can now be seen. The steering control system electronics was housed behind the front plate. Behind the facing yellow plate and beneath the computer were the batteries, traction motor, differential, and thyristor motor controller. The robot comprised the following main systems; transit, steering, sonar ranging, opto-magnetic compass, status and safety, and the computer.

A 1.2 The vehicle systems

A 1.2.1 Transit

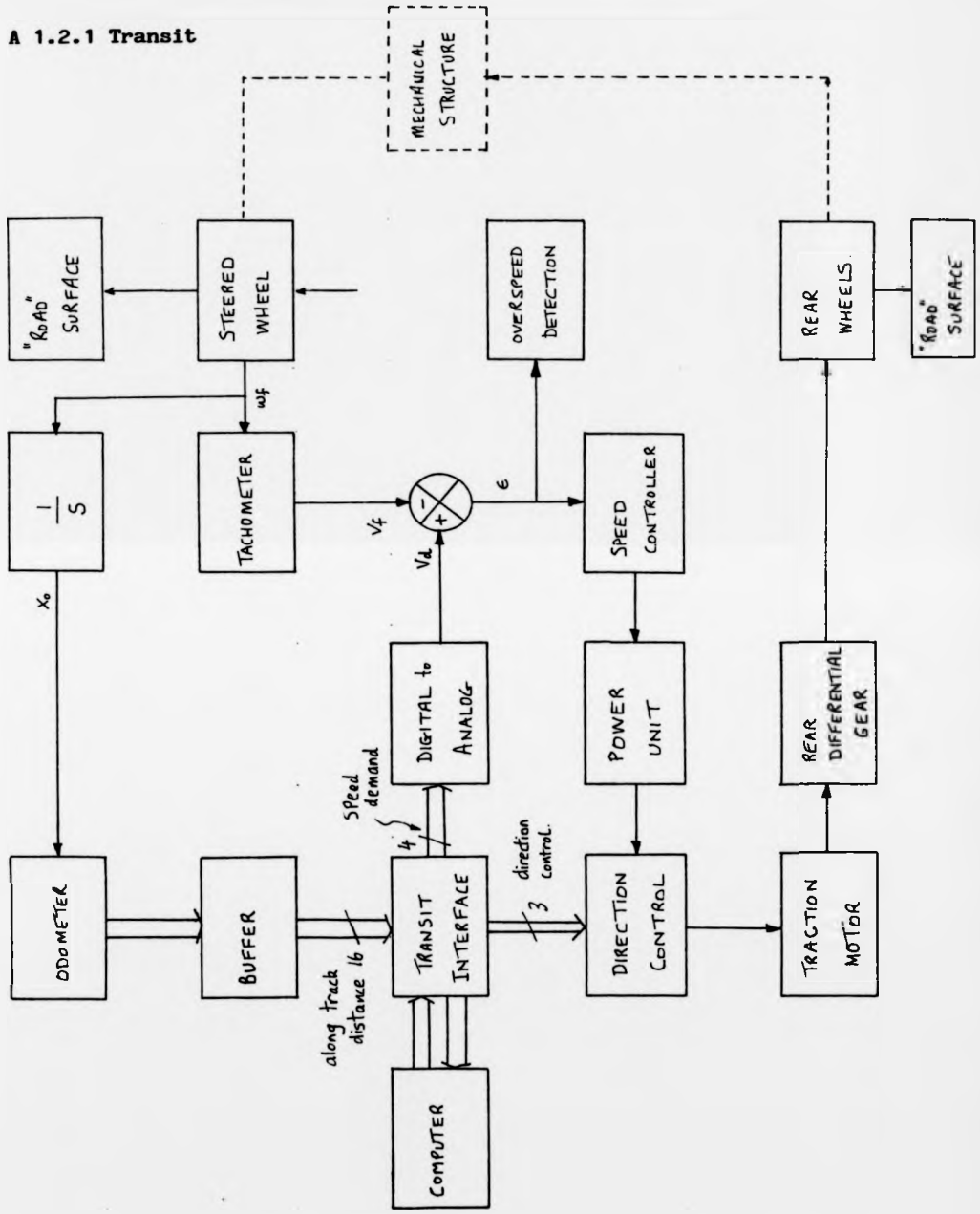

Figure A.1.6 The components of the transit control system.

The computer was able, via this interface, to control and receive data on the following vehicle functions:

A. Control to the vehicle.

1. The release and application of a parking brake.
2. The direction of rotation of the traction motor, and hence the direction of motion of the vehicle.
3. The amount of electromagnetic braking effort.
4. The speed of rotation of the traction motor, and thus the speed of the vehicle.
5. Clearing the odometry counter.

B. Data from the vehicle.

1. The latest value in the odometry register.

The following is a description of the traction motor and its method of control. The main transit drive was from a 2 h.p. 36 volt series wound d.c electric traction motor. The output of this motor was connected to the rear wheels via a differential mechanism. The series speed control resistor was replaced by a device that supplied the motor with pulses of source voltage whose average value was controlled by the ratio of on to off time of the pulses. A thyristor was used to connect and disconnect the motor from the source, that is, to chop the source voltage. The thyristor required a forced commutation circuit to reduce its current to zero and hold it long enough for the thyristor to revert to its blocking state at the end of each pulse. A capacitor and an auxiliary thyristor are needed to achieve this. This is the power circuit. The logic circuitry to control this was contained in the speed controller. The direction of current and the main switching were controlled by relays. This was done with commercially available equipment.

The odometer system which was attached to the steered wheel was a castellated concentric ring. As the wheel rotated the castellations passed through a photo-diode pair. The phase relation of the generated pulses was

used to infer the direction of rotation of the wheel. An up or down pulse was used to appropriately increment an up down counter. The output of the counter was buffered. The computer could clear, enable, and read this buffer.

The interface was designed so that if it was not refreshed by the controlling software, with the appropriate bit pattern, the vehicle was placed in the parked state. This was done at the hardware level, and refresh had to be carried out at least once every 1200ms. As a further safety feature the interface had to be correctly enabled by the computer to perform these functions. It would not pass the control signals unless it had been correctly addressed. The speed of the vehicle's steered wheel was sensed by a tachometer and fed-back to the speed controller to ensure demanded speed equalled achieved speed. This was also performed at the hardware level. The maximum speed of the vehicle was constrained to 1.5 ms^{-1}. If the vehicle speed exceeded this value the vehicle was returned to the manual mode. Return to manual mode was independent of the computer, and also performed at the hardware level.

A 1.2.2 Steering

A block diagram is shown in Fig. A.1.6

The computer was able, via the interface, to control and receive data on the following vehicle functions:

A. Control to the steering system.

1. The angle of the steered wheel with respect to the longitudinal body axis.
2. An enable - disenable signal to the motor.

B. Data from the steering system.

1. The steering wheel angle.

The steered wheel rotated vertically within the front fork assembly. The front fork rotated horizontally with respect to the body of the vehicle through an angle of ± 60 degrees. The system comprised the motor, and its associated controller, a sprocket and chain reduction gearing to the front fork, feedback of the angular position of the fork, and hence the wheel, and an interface unit to the computer. A printed circuit permanent magnet d.c. motor. was connected across the centre of an H-bridge. The speed of the motor shaft was controlled by pulse width modulation of the signals to the bridge logic. The width of these pulses was controlled by the digital difference between the demanded steer angle from the computer and the digitised feedback from the shaft potentiometer. The pulse width to the motor remained at a constant value when the error exceeded a certain magnitude, and this width reduced proportionally, as the steered wheel approached its demanded value.

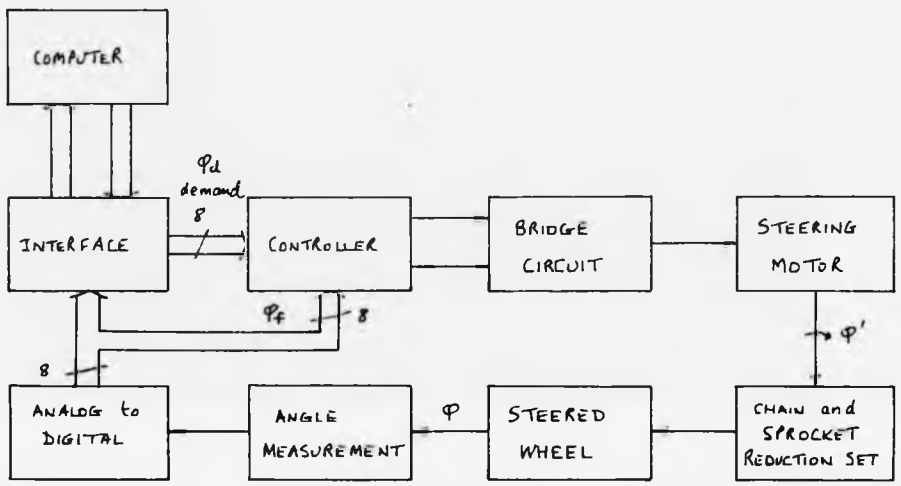

Figure A.1.7 Block diagram of steering sub-system.

A 1.2.3 The sonar ranger

This comprised an acoustical transducer, and an ultra-sonic circuit board. The transducer was designed to act both as transmitter and receiver. It emitted a 1ms. 'chirp' of pulses. The four frequencies used were 50, 53, 57, and 60 kHz. This method of transmission was designed to reduce the chance of a pulse attenuating itself owing to phase cancellation which can occur near to a reflecting surface. After the transmission of the 'chirp' the transducer acted as a receiver. In this mode the received sound energy was transduced, amplified in its analog form, and then detected digitally. The elapsed time between transmission of the pulse and reception of the echo, with respect to the speed of sound, being used as the basis of the range measurement. During the flight time of the pulse, the amplifier gain was increased, and the bandwidth decreased to overcome the range dependent attenuation of the pulse amplitude, [Polaroid Corporation 1980].

The sensor characteristics of interest are the range, the range resolution and the beamwidth. The measured range R is

$$R = ct/2$$

for a speed of sound c in ms^{-1}, and time t in seconds. Range measurements could be made from 0.27 [m] - 10.66 [m]. The sound energy attenuation is related to the nature of the gas mixture, and to the transmit frequency. The attenuation increases with frequency. The lower range bound is related to the speed of sound divided by the time for the 1ms 'chirp' to have completed its passage away from the transmitter. Clearly, the transducer cannot become a receiver until the pulse has left the transducer. The lowest frequency, within the 1 ms chirp of 50 kHz corresponds to a wavelength of 0.007 [m]. As a first approximation the ranging accuracy is related to this wavelength. The effective beamwidth θ_s , of a rectangular aperture is related to the formula,

$$\theta_s = \sin^{-1}(L / A)$$

for a wavelength, L , and aperture of width, A , both in metres. The transducer aperture was circular. Assuming the same theory is valid then with an aperture width of 0.0384 metres operating at a frequency of 55 kHz this simple theory predicts that the first zero of the beam will be at 8.9 degrees. The effective beamwidth with the environment used was $\pm$20 degrees. The amount of energy returned to the sensor can vary from material to material. The acoustic 'smoothness' determines the angle that the normal to the transducer can be orientated away from the perpendicular to the object before the returned energy falls below the minimum detectable by a transducer. It is this specular reflection that alters the 'effective beamwidth' of the range sensor. The effective beamwidth is graphed for two materials in Fig. A.1.8 [Clemence 1983]. The placement and orientation of the normal from the range sensors as distributed around the robot is shown in Fig. A.1.9.

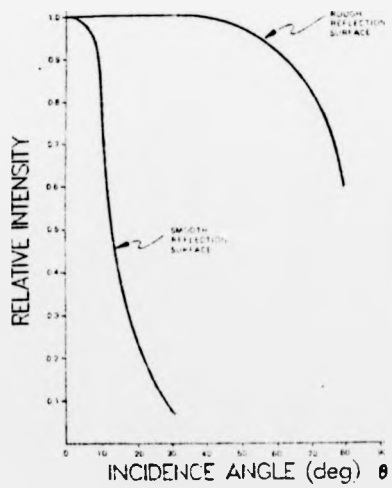

Figure A.1.8 Relative intensity of received signal versus variations in the angle between the normal from the transducer and the normal from the object.

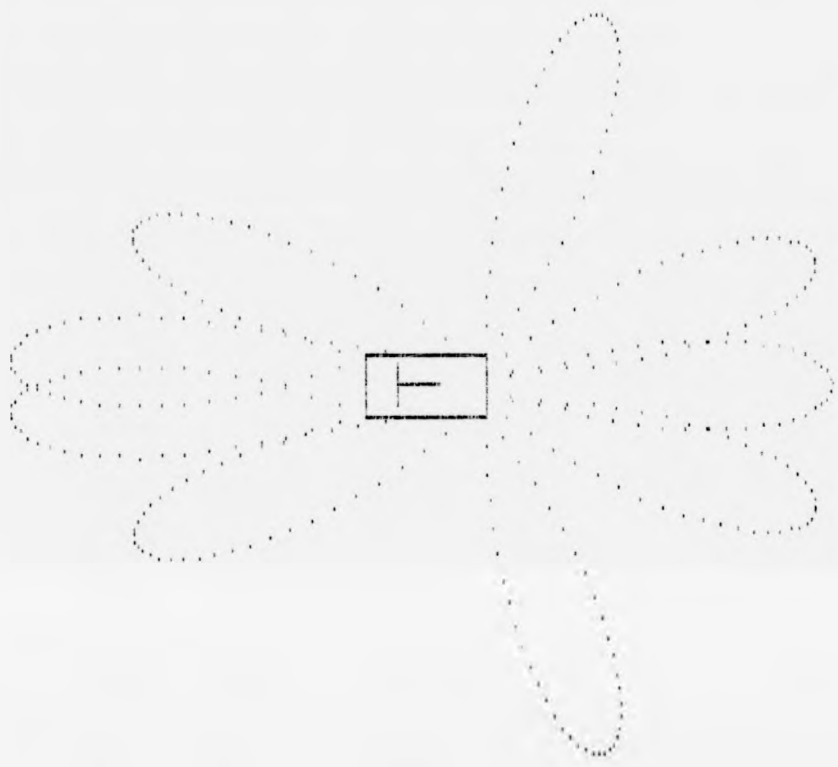

Figure A.1.9 Sonar-ranging coverage with the nine sonar heads.

The interface allowed the selection of individual transducers, or a programmable sequence of transducers to 'range'. The programmable sequence once initiated would 'cycle and range' without further intervention. Before the pulse was transmitted the correct interface protocol needed to be carried out to ensure the correct clearing and setting of bits. The 3 bit address of an individual sonar ranger needed to be strobed in, and then the ranging process could start. When a returned pulse was received the interface raised a flag. This indicated the fact to the main computer. The reading of the range could then be performed. The sonar range was held to 10 bits

A 1.2.4 Opto-magnetic compass

The compass provided information on the body heading of the vehicle relative to magnetic North. As the compass needle rotated it passed between a light emitting diode, and a photo-diode pair, set mechanically opposite each other. As a result the current flowing was altered. The cutput from the photo-diode was sampled and digitised. The analog to digital conversion was initiated by a call from the software to sample a particular pair. A conversion done signal was available. There were seventeen pairs. The analog signal corresponding to the bearing may be further processed using the compass calibration to obtain an interpolated value of the vehicle bearing, although this research did not do so.

A 1.2.5 The computer

Hardware

Processor:	KD 11 HD LSI 11/2
Memory:	32 K words MOS.
Interfaces:	4 serial lines. DLV11J.
	8 X 16 bit parallel ports. DRV11
Floppy discs:	2 AED 6200LP
Input & Output:	CRT terminal [ADM dumb Terminal]
Auxiliary I/O:	Two degree of fredom joystick with three push buttons.
Microterminal	TM77

General purpose set of switches to a parallel port.

Software

Operating System.	RT-11	A single user operating system for the PDP-11 series of computers.
Languague.	RTL-2	A systems programming language, with support for real arithmetic. Assembly language statements may be included within the main text of the langauge.

The processing hardware had already been purchased when the research began. The RTL-2 language was developed by Imperial Chemical Industries to meet the need to control their industrial processes. Other languages were not readily available for the hardware.

Appendix A.2.0 'Calibration' and assessment of the traction motor

A.2.1 Introduction

In order to simply move the vehicle forwards and backwards in a controlled manner an assessment of how the vehicle responded to commands from the transit motor was made.

A.2.2 Theory

The longitudinal dynamics of a vehicle may be modelled as

$$M.A = F - f(v) \qquad \text{a.2.1}$$

for a vehicle of constant mass M, with an opposing frictional force f(v), a tractive force F , at the rear and an acceleration or deceleration of A. The linear form is

$$M.\frac{d^2x}{dt^2} = K.e - T.\frac{dx}{dt} \qquad \text{a.2.2}$$

with a linear coefficient of friction T , gain K , and an error between demanded and actual speed of e.

A.2.3 Initial testing

To gain a preliminary understanding of the vehicle's response a pulse of specified duration T , and amplitude V , was applied to the traction motor and its control system. Figure A.2.1 is a block diagram of the experimental arrangement. The experiment started with the vehicle stationary. The odometer was used to measure the distance moved. The vehicle was placed in the automatic mode, with the brake fully released. The traction motor was energised for various values of V.T . Continuous readings were taken from the odometer until the vehicle came to rest. The range of analog voltages applied to the traction motor are given in Table A.2.1 overleaf

Digital demand	Vd	2	3	4	6	8	10	12
Analog voltage	V	2.35	3.12	4.00	4.94	5.45	6.01	6.51

Table A.2.1 Relation between digital demand Vd, and analog voltage V, applied to speed controller. Vd decimal value of four bit pattern input to digital to analog converter.

Each pulse was applied for a fixed period T . T took the values 0.2, 0.4, 0.6, 0.8, and 1.0 second. The detailed results for one of the experiments are given in Figs. A.2.2 and A.2.3 for V = 4.00 and for all values of T .

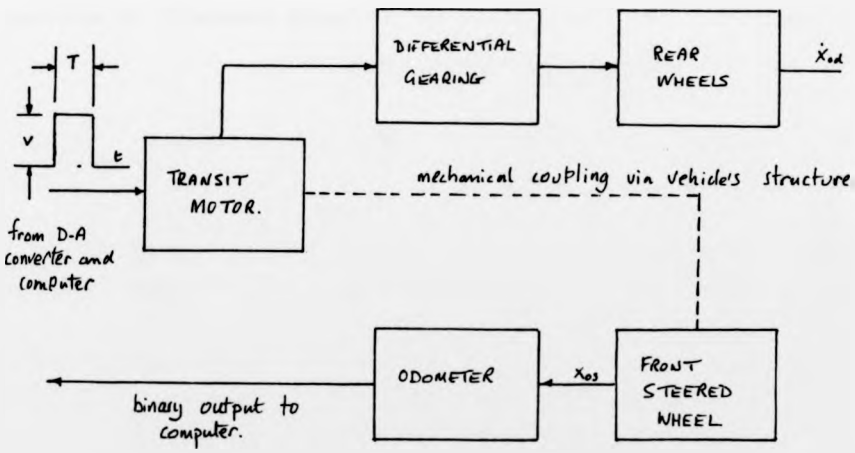

Figure A.2.1 Block diagram of experimental arrangement to determine the distance moved by the vehicle in response to pulses of specified duration, and amplitude.

A.2.4 Results

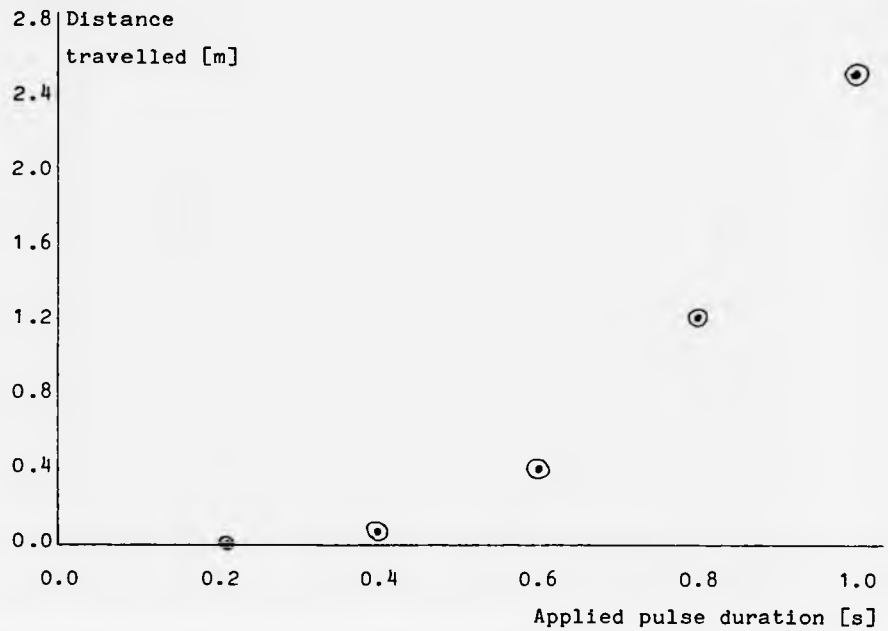

Figure A.2.2 Representative experimental result for Vd = 4. of the increase in distance moved by the vehicle for increases pulse duration.

Duration of applied pulse									
0.2s		0.4s		0.6s		0.8s		1.0s	
V.T	S	V.T	S	V.T	S	V.T	S	V.T	S
0.47	-	0.94	0.08	1.41	0.28	1.88	0.68	2.35	1.32
0.62	-	1.25	0.08	1.87	0.36	2.50	0.92	3.12	2.20
0.80	-	1.60	0.08	2.40	0.44	3.21	1.16	4.00	2.52
0.99	0.04	1.98	0.08	2.96	0.52	3.95	1.28	4.94	-
1.09	0.04	2.18	0.08	3.27	0.48	4.36	1.24	-	-
1.20	0.04	2.40	0.08	3.61	0.56	4.81	1.20	-	-
1.30	0.04	2.60	0.08	3.91	0.52	5.21	1.20	-	-

Table A.2.2 Values of distance travelled versus the product of applied voltage and pulse duration. T in seconds, V in volts, and S the distance in metres. The product V.T , has the dimensions of Nm A^{-1}.

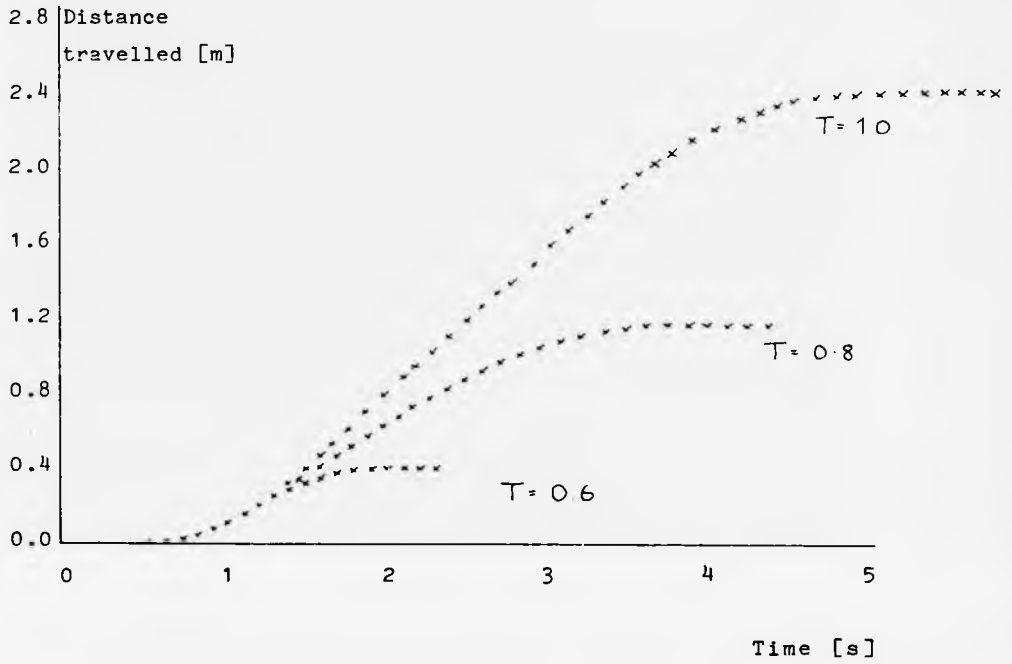

Figure A.2.3 Representative experimental result of the initial transient, the constant speed, and the deceleration phase of the vehicle. The deceleration is caused by frictional forces other than active braking.

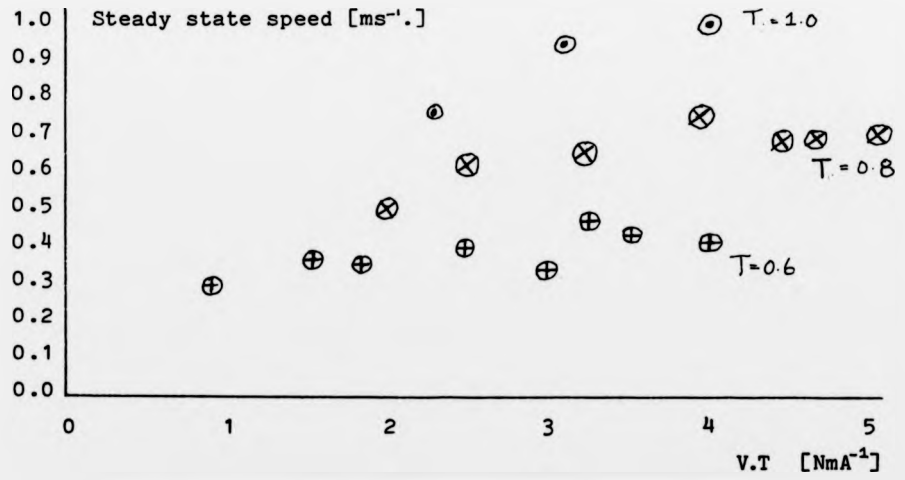

Figure A.2.4 Displays the relation between steady state speed of vehicle for variations in V.T.

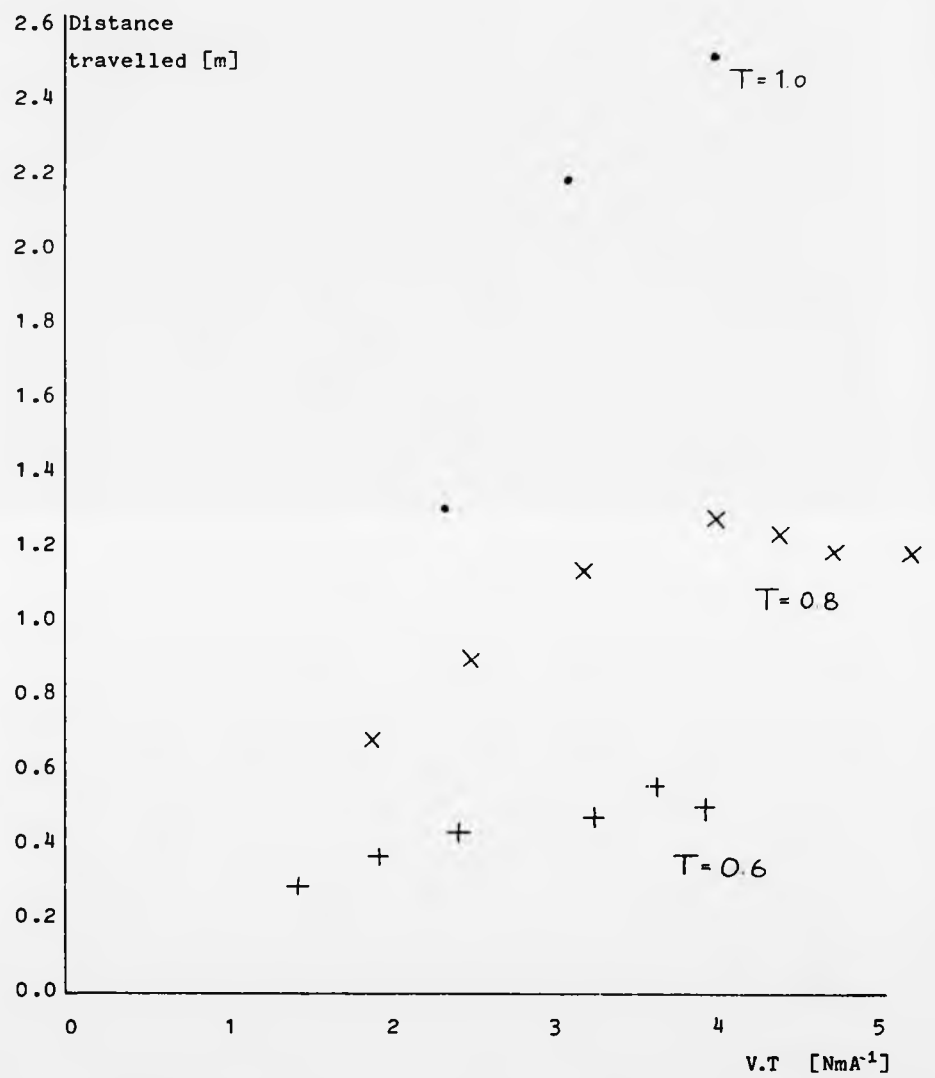

Figure A.2.5 Shows the linear increase in distance travelled S, along lines of iso-pulse width. Linear increases in pulse duration caused a doubling of the distance travelled. Above a certain applied voltage the distance moved remained constant.

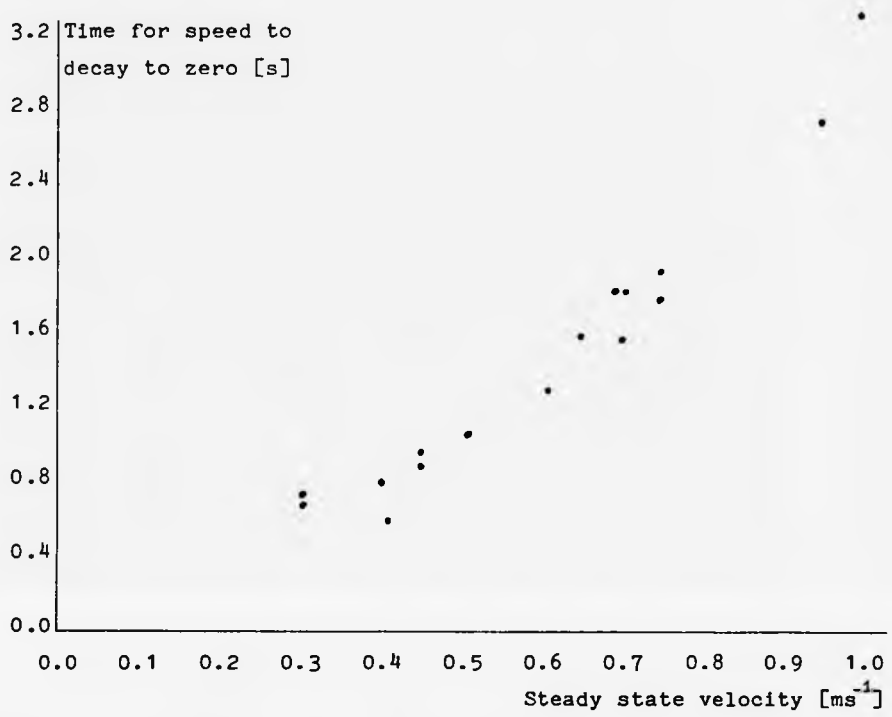

Figure A.2.6 Displays relation between time taken for vehicle speed to fall from its steady state value to zero, based on experimental results.

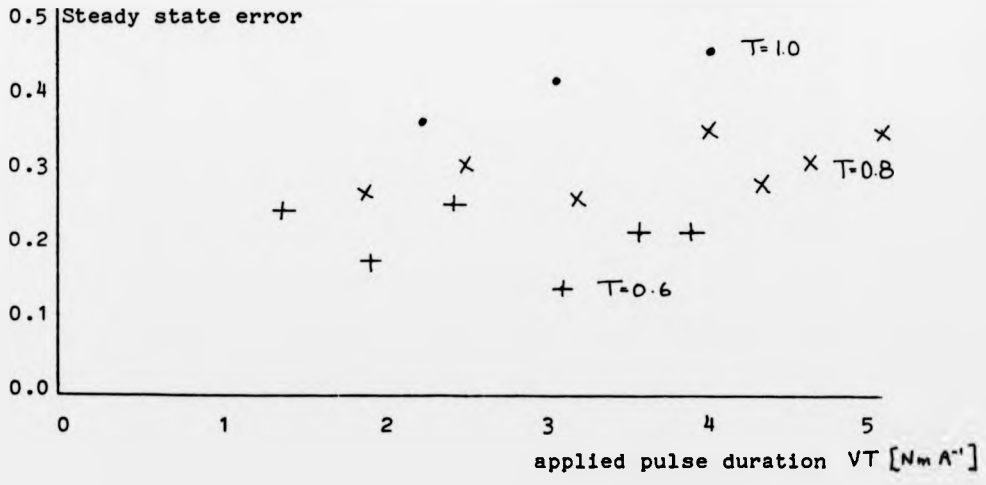

Figure A.2.7 The steady state error associated with the increase in applied pulse duration.

A.2.5 Discussion

The representative distance time curve displayed in figure A.2.2 has the expected three phases of motion.

The experimental result embodied in figure A.2.5 shows that for a fixed amplitude V, and a linear increases in pulse duration T , the vehicle could be moved forward a repeatable distance S. There are two regions. A linear segment in which a linear increase in pulse amplitude along a line of iso-pulse width causes the distance travelled increase linearly. There is a constant region in which further increases in pulse amplitude have no additional effect on the distance travelled.

The general motor torque formula is $T = i.\phi$ for a torque T, current i, and flux ϕ . In a series motor, ϕ is approximately proportional to i. The formuala

$$T = g.i^2 \qquad \text{a.2.3}$$

is then the relevant one for the torque T , g , being a constant. Above full load magnetic saturation becomes more marked, and the torque does not increase so rapidly, [Hughes 1966]. The constant distance travelled irrespective of further increases in pulse amplitude along lines of iso-pulse width arises from this magnetic saturation.

Figure A.2.6 shows that increases in the time taken for the vehicle to come to a halt are correlated with increases in the steady state speed, as would be expected.

Figure A.2.7 shows the relation between the velocity lag and V.T. There is a linear relation between ϵ_{ss} and T .

Factors that are expected to have influenced these results, but whose effects were not directly investigated in these experiments are: the load carried by the vehicle, the available power from the battery, the static frictional forces, the dynamic frictional forces, the electrical properties of the motor used, the initial velocity of the vehicle.

A.2.6 Conclusions

A simple experimental procedure can be used to yield a qualitative insight into the longitudinal dynamics of a vehicle moving at speeds of about 1 ms , or less, and that the longitudinal motion could be modelled as a linear first order system.

The dynamic response has the expected acceleration, constant speed, and deceleration phase.

A number of factors have been identified as likely to cause variations in these relationship. Further research would be required to quantify these effects.

A.2.6 Conclusions

A simple experimental procedure can be used to yield a qualitative insight into the longitudinal dynamics of a vehicle moving at speeds of about 1 ms , or less, and that the longitudinal motion could be modelled as a linear first order system.

The dynamic response has the expected acceleration, constant speed, and deceleration phase.

A number of factors have been identified as likely to cause variations in these relationship. Further research would be required to quantify these effects.

Appendix A.3.0 Calibration of the steering control system

A.3.1 Introduction

The purpose of these tests was to obtain the time domain response of the steering control system. Appendix A.1 gives further details of the hardware. Step response tests were performed with the vehicle stationary. Under this condition the magnitude of frictional torques arising from the ground-tyre interface were expected to provide the largest damping. The steer angle was set to the central position and the values of steer angle resulting from a step demand to the system were recorded.

A.3.2 Results

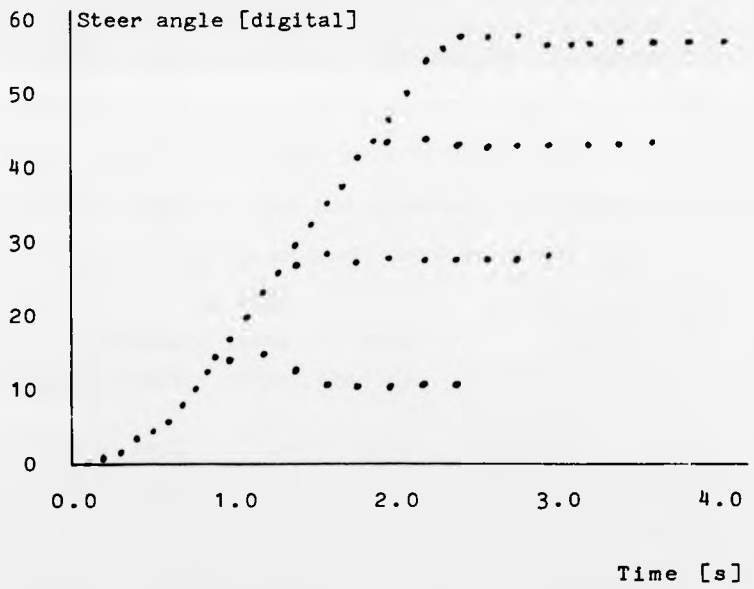

Figure A.3.1 The port side time domain response of the steering control system to achieve the demanded step input from the central or zero position. The digital values used as step inputs were 15,30,45,and 60. The relation between digital units and degrees was obtained from the constant curvature runs, with the steer angle held at these digital values.

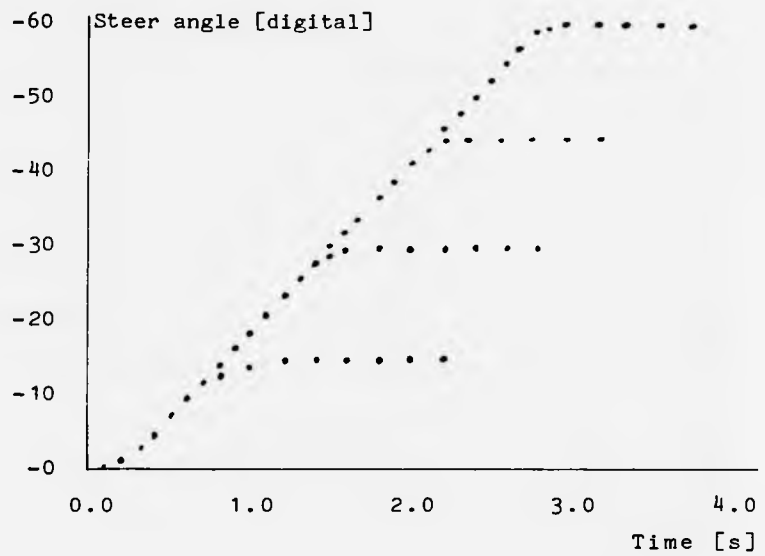

Figure A.3.2 The starboard side time domain response of the steering control system to achieve the demanded step input from the central or zero position. The digital values used as step inputs were 15,30,45,and 60. The relation between digital units and degrees was obtained from the constant curvature runs, with the steer angle held at these digital values.

Demand digital	Demand [deg]	Steady state error	Slew rate [rad s]	Time to achieve digital demand	
60	38.4	-2	0.27	2.62 ±0.03	
45	28.8	-2	0.25	2.11 ±0.07	Port
30	19.2	-2	0.22	1.61 ±0.17	side
15	9.6	-4	0.15	1.17 ±0.05	
-15	9.6	0	0.15	1.53 ±0.29	star-
-30	19.6	0	0.20	1.71 ±0.07	board
-45	28.2	0	0.23	2.34 ±0.15	side
-60	38.4	0	0.23	3.13 ±0.40	

Table A.3.1 The demanded steer angle and the steady state angle, the slew rate or rate of change of steer angle with time, and the time to achieve the demanded digital input, for the digital step demands as shown .

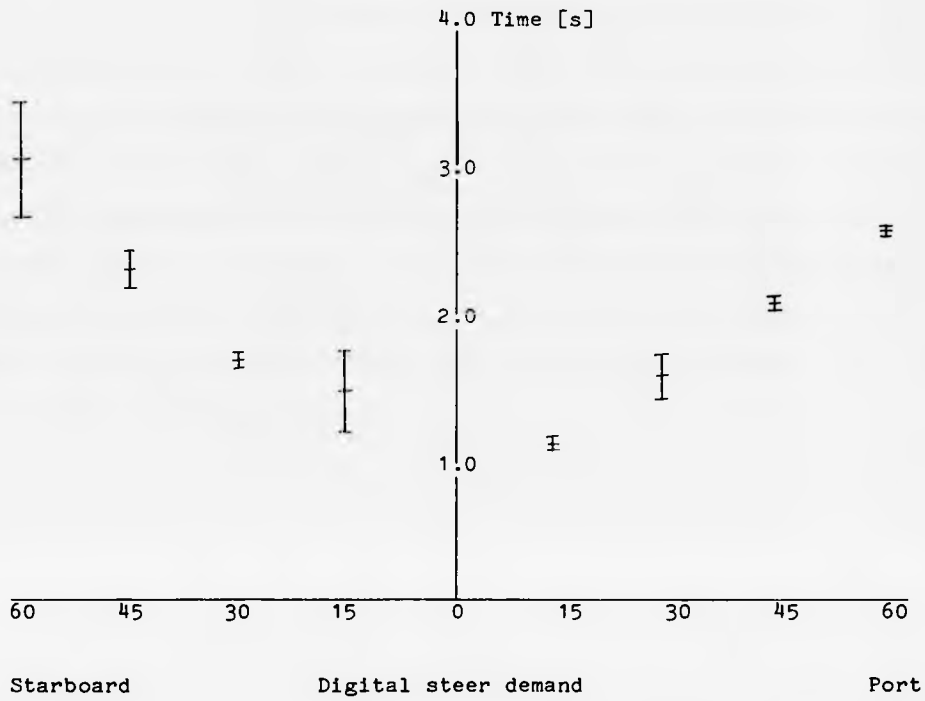

Figure A.3.3 The variation in the time taken for the steering control system to achieve its demanded input.

A.3.3 Discussion

The overall response takes the form of a constant change in steer angle until the steady state value is reached. The difference in slew rates are attributed to component differences in the H-bridge controller. A least squares fit of the rate of change of mean time to achieve the steady state versus demanded steer angle as shown in Figure A.3.3 yields a port slope of 0.042, and starboard slope of 0.031. The response for changes in the steer angle of less than 5 degrees is an exponential rise to the mean rate of 0.21 rad s^{-1} with a time constant of 0.2 [s]. These differences in the rate at which the steered wheel turns means there can be differences in the final location when the steered wheel reaches its steady state value.

The final angular position on the port side is in error. The steady state value of the steer angle for digital demands 30,45,and 60 corresponds to an error in degrees of 1.28, and for digital demand 15 to an error 2.56 degrees. This angular error will cause the curvature of the path the vehicle moves along to be different from that desired. With more accurate measurement in the control system, these errors could be further reduced. However, the effect of the elasticity of the tyre, its pressure, the surface moved over, the area of contact with that surface, and the speed at which the wheel moves, are all additional factors from which the 'noise' could arise from

A.3.4 Conclusion

The measurement of the heading control variable, the steered wheel angle, has a finite resolution. Additionally, variations and differences in other parameters involved in controlling the steered wheel angle result in a 'scatter' in the steered wheel response. To reduce the effect of this scatter, on the physical displacement in vehicle position and heading, additional information is needed. This information can be gained from the environmental sensors.

Appendix A.4.0 The Kinetics of motion of a tricycle vehicle

A.4.1 The steady state motion

The motion of the vehicle has a translatory and a rotational part. For a linear system these motions will consist of a steady state and transient portion. The geometry of the wheels and their arrangement for a tricycle vehicle is repeated below

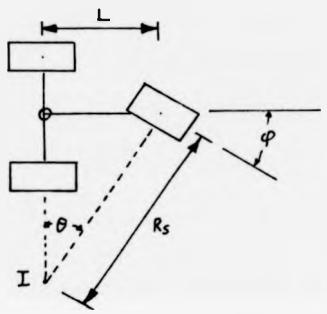

Figure A.4.1 Steering wheel geometry.

where L = The length of the wheelbase,

R_S = The distance from the instantaneous centre to the steered wheel

I = The instantaneous centre of turning

From geometry

$$\sin(\Theta) = L/R_S \qquad \text{a.4.1}$$

with $$\sin(\theta) = \sin(\varphi) \qquad \text{a.4.2}$$

If a pneumatic tyre is acted upon by a side force while it is rolling it will develop a slip angle,

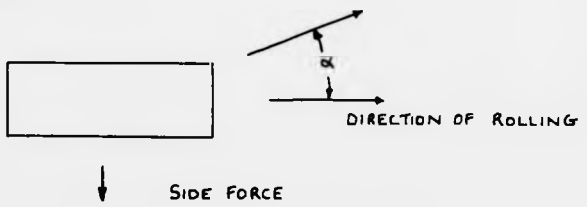

Figure A.4.2 Slip angle α , for a rolling wheel under a side force.

Such a side force could arise from centrifugal action when cornering. The reaction to this force by the surface is equal and opposite and it is this force which actually causes the vehicle to turn and is called the cornering force. Each tyre developes its appropriate slip angle for an applied force. The directions of the slip angles adjust and now give rotation about a point I the actual instantaneous centre. In the analysis it will be assumed that the rear slip angles developed are the same, and can be lumped together as one. The relationship between the slip angles and the radius of turn are shown below.

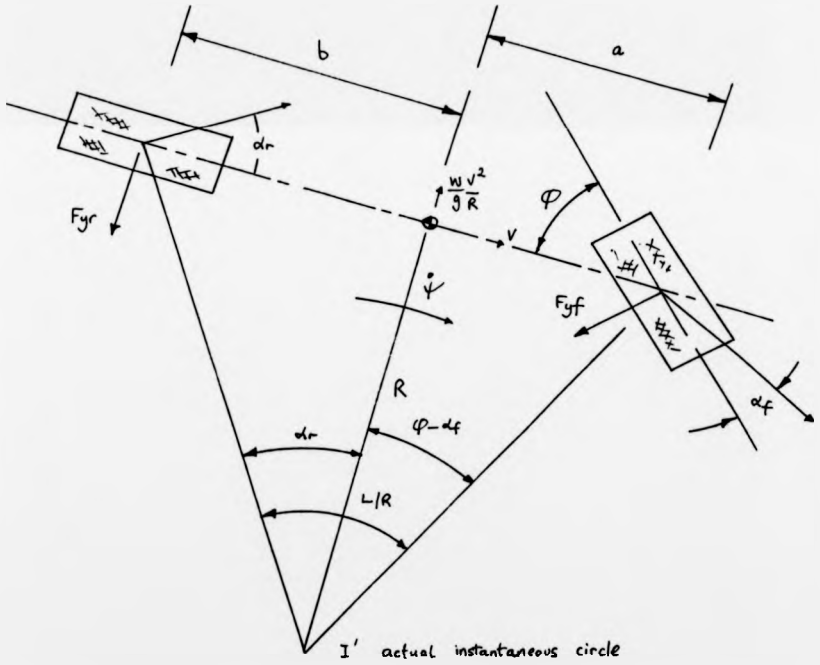

Figure A.4.3 The actual instantaneous centre.

With the notation r = rear and f = front and (a + b) = L, and for small steer angles, then the ratio of the wheelbase to the turning radius is equal to the steer angle minus the sum of the two slip angles

$$L/R = \varphi - \{\alpha_r + \alpha_f\} \qquad a.4.3$$

The force F_{yf}, normal to the direction of rolling of the front tyre is

$$F_{yf} = \frac{b.m.\ddot{x}}{L} \qquad a.4.4$$

for a mass m, and acceleration $\ddot{x}$.

For a steady turn

$$F_{yf} = \frac{b.W.V^2}{L.g.R} \qquad a.4.5$$

with a constant forward speed V and acceleration g, and weight W.

Similarly the force F_{yr}, normal to the direction of rolling of the rear tyre is

$$F_{yr} = \frac{a.m.\ddot{x}}{L} \qquad a.4.6$$

or

$$F_{yr} = \frac{a.W.V^2}{L.g.R} \qquad a.4.7$$

The load on the front and rear tyres is

$$W_f = \frac{W.b}{2.L} \qquad a.4.8$$

$$W_r = \frac{W.a}{2.L} \qquad a.4.9$$

so

$$F_{yf} = \frac{2.W_f.V^2}{g.R} \qquad a.4.10$$

and $$F_{yr} = \frac{2.W_r.V}{g.R} \qquad a.4.11$$

and if the slip angles are defined to be

$$\alpha_f = \frac{F_{yf}}{C_{\alpha f}} = \frac{2.W_f.V^2}{C_{\alpha f}.g.R} \qquad a.4.12$$

and

$$\alpha_r = \frac{F_{yr}}{2.C_{\alpha r}} = \frac{W_r.V^2}{C_{\alpha r}.g.R} \qquad a.4.13$$

so that the steer angle is

$$\varphi = \frac{L}{R} + \left\{\frac{2.W_f}{C_{\alpha f}} - \frac{W_r}{C_{\alpha r}}\right\}\frac{.V^2}{g.R} \qquad a.4.14$$

These equations may be interpreted that if the cornering coefficient for the front tyre is double that of the rear tyre then, when the slip angles are equal then the applied force produces a resultant motion in a new straight line path. This motion is without any yaw

velocity and is normally called neutral steer. If a side force causes the front slip angle to have a larger mean steady state value than that of the rear wheels, then the path of the vehicle is away from the applied force. The vehicle has a yaw velocity about the centre of gravity plus a linear velocity, with the vehicle as a whole rotating about the instantaneous centre. This condition is termed understeer. If the applied force produces a steady state mean slip angle such that the rear slip angle is greater than the front then the path of the vehicle is towards the applied force. The vehicle yaw velocity is opposite to that in understeer, and the condition is called oversteer.

A.4.2 The transient phase

In contrast to the steady state handling behaviour the inertia properties need to be taken into account. The robot will be in a transient state between the application of a steering input, and the attainment of steady state motion.

The equations are formulated by expressing the absolute acceleration with respect to the frame of reference attached to the vehicle chassis, as a result the mass momemts of inertia of the vehicle can be regarded constant.

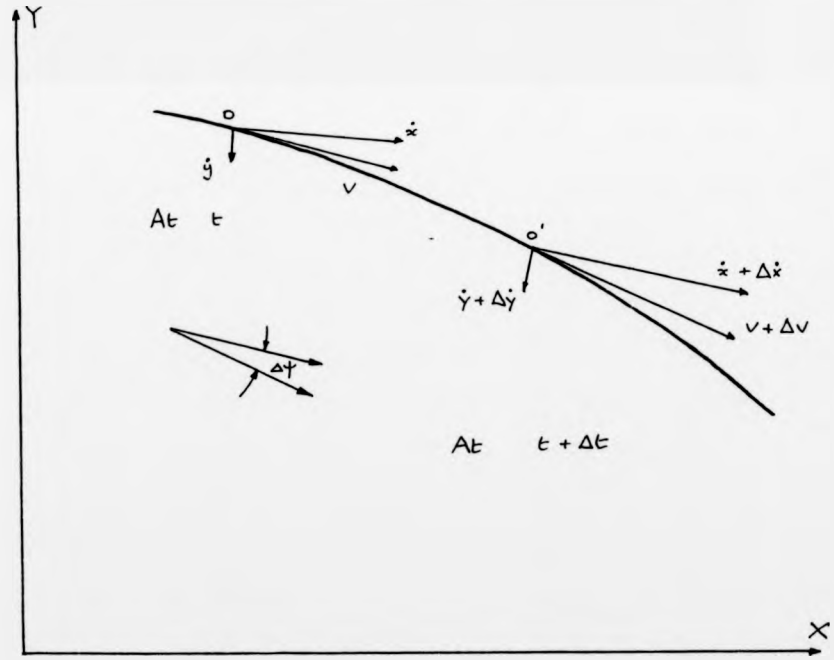

Figure A.4.4 Motion of a vehicle along a path with axes fixed to the vehicle chassis.

The longitudinal and lateral axes are, ox, and, oy, V_x and V_y are the components of the velocity $\underline{V}$ of the centre of gravity, along the axes ox, and oy respectively, at time, t. The vehicle may change in both translation and rotation during a turn at a time, $t + \Delta t$, the direction and the magnitude of the velocity of the C of G as well as the orientation of the ox, and oy axes of the vehicle can change (see figure A.4.4).

The change in velocity component parallel to the ox axis is

$$[\ V_x + V_y\ ].\cos(\Delta\Psi) - V_x - [V_y + \Delta V_y\ ].\sin(\Delta\Psi) \qquad \text{a.4.15}$$

for $\Delta\Psi$, small and neglecting second order terms this becomes

$$\Delta V_x - V_y.\Delta\Psi \qquad \text{a.4.16}$$

The component along the longitudinal axis of the absolute acceleration of the C of G of the vehicle is obtained by dividing by Δt, and in the limit,

$$\ddot{x} = \dot{V}_x - V_y.\dot{\Psi} \qquad \text{a.4.17}$$

The component $\dot{V}_x$, is the result of the changing magnitude of the velocity component V_x , and is directed along the ox axis, and the component $V_y.\dot{\Psi}$, is due to the rotation of the vehicle component V_y .

The change in velocity component parallel to the oy axis is

$$[\ V_y + \Delta V_y\ ].\cos(\Delta\Psi) - V_y - [V_x + \Delta V_x\ ].\sin(\Delta\Psi) \qquad \text{a.4.18}$$

or

$$\Delta V_y + V_x\ .\Delta\Psi$$

and dividing by Δt, gives in the limit the absolute acceleration of the C of G along the lateral axis as

$$\ddot{y} = \dot{V}_y + V_x\ .\dot{\Psi} \qquad \text{a.4.19}$$

If now the vehicle is represented as in Figure A.4.5 then the application of $F = m.a$, where , a , is the acceleration and $T = I\ddot{\Psi}$, yields the equations of plane motion for the vehicle.

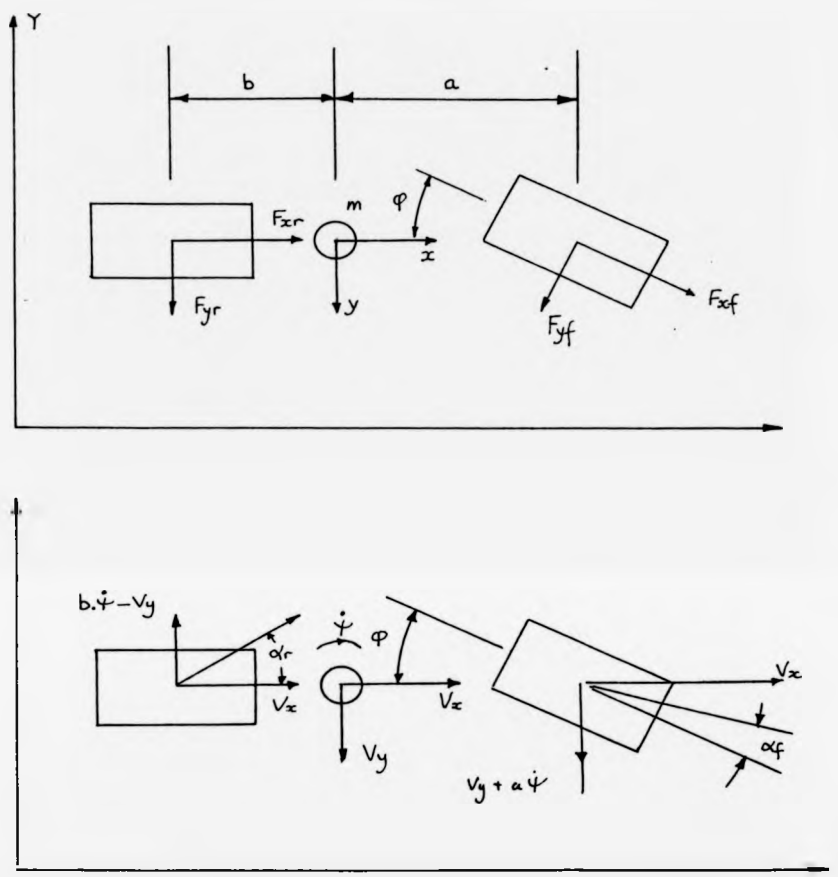

Figure A.4.5 The forces and velocity components of the vehicle.

where

F_{yf} , F_{yr} = The lateral forces acting on the rear and front tyres.

F_{xf} , F_{xr} = The braking and accelerating forces at the front and rear

a , b = The distance from the centre of the wheel axles to the C of G from the front and rear.

$\dot{\psi}$ = The yaw velocity

φ = The steer angle

m = The mass of the vehicle.

I = The mass moment of inertia of the vehicle about the vertical z axis.

$C_{\alpha f}$, $C_{\alpha r}$ = The cornering stiffness of the front and rear pneumatic tyres and are the slope of the cornering forces versus slip angle.

With this notation the three equations are

$$m[\dot{V}_x - V_y.\dot{\psi}] = F_{xf}.\cos(\varphi) + F_{xr} - F_{yf}.\sin(\varphi) \quad \text{a.4.20}$$

$$m[\dot{V}_y + V_x.\dot{\psi}] = F_{yf}.\cos(\varphi) + F_{yr} + F_{xf}.\sin(\varphi) \quad \text{a.4.21}$$

$$I\ddot{\psi} = a.F_{yf}\cos(\varphi) - b.F_{yr} + a.F_{xf}\sin(\varphi) \quad \text{a.4.22}$$

If the vehicle is symmetric about the longitudinal plane, and the roll motion can be neglected. The slip angle α_r , and α_f , can be defined in terms of the vehicle motion variables $\dot{\psi}$, and V_y , with the assumption that the slip angles are small

$$\alpha_f = \varphi - \left(\frac{V_y + a.\dot{\psi}}{V_x}\right) \quad \text{a.4.23}$$

$$\alpha_r = \frac{b.\dot{\psi} - V_y}{V_x} \quad \text{a.4.24}$$

now $$F_{yf} = C_{\alpha f}.\alpha_f \quad \text{a.4.25}$$

and $$F_{yr} = 2.C_{\alpha r}.\alpha_r \quad \text{a.4.26}$$

so $$F_{yf} = C_{\alpha f}.\left[\frac{\varphi V_x - a.\dot{\psi} - V_y}{V_x}\right] \quad \text{a.4.27}$$

and

$$F_{yr} = 2.C_{\alpha r}.\left[\frac{b.\dot{\psi} - V_y}{V_x}\right] \quad \text{a.4.28}$$

Since the vehicle is a rear drive vehicle $F_{xf} = 0$, and the accelerating and decelerating force F_{Xr} , at the rear would need to be determined substituting and rearranging,

$$\ddot{x} = \frac{F_{xr}}{m} + \frac{C_{\alpha f}\sin(\varphi)\dot{y}}{m.V_x} + \left[\dot{y} + \frac{aC_{\alpha f}\sin(\varphi)}{m.V_x}\right].\dot{\psi} - \varphi\frac{C_{\alpha f}.\sin(\varphi)}{m} \quad \text{a.4.29}$$

$$\ddot{y} = -\left[\frac{2.C_{\alpha r} + C_{\alpha f}\cos(\varphi)}{m.V_x}\right]\dot{y} + \left[\frac{2bC_{\alpha r} - aC_{\alpha f}\cos(\varphi)}{m.V_x} - V_x\right].\dot{\psi} + \frac{C_{\alpha f}\varphi\cos(\varphi)}{m} \quad \text{a.4.30}$$

$$\ddot{\psi} = \left[\frac{2bC_{\alpha r} - aC_{\alpha f}\cos(\varphi)}{I\,V}\right]\dot{y} - \left[\frac{a^2 C_{\alpha f}\cos(\varphi) + 2b^2 C_{\alpha r}}{I\,V}\right].\dot{\psi} + \frac{a\,\varphi\,C_{\alpha f}\cos(\varphi)}{I} \quad \text{a.4.31}$$

Considering only the yaw and lateral dynamics, and with $\cos(\varphi) \doteq 1$, and

$\sin(\varphi) \doteq \varphi$, then with the state defined

$$\underline{x} = [\, y \,,\, \dot{y} \,,\, \dot{\psi} \,,\, \psi \,]^T$$

then

$$\dot{\underline{x}} = F.\underline{x} + G.\underline{u} \qquad \text{a.4.32}$$

where

$$F = \begin{bmatrix} 0 & 1 & 0 & V_x \\ 0 & A_1 & B_1 & 0 \\ 0 & A_2 & B_2 & 0 \\ 0 & 0 & 1 & 0 \end{bmatrix}$$

and

$$G = [0 \quad C_1 \quad C_2 \quad 0]^T$$

and

$$A_1 = -\frac{(2.C_{\alpha r} + C_{\alpha f})}{m.V_x}$$

$$B_1 = \frac{(2.b.C_{\alpha r} - a.C_{\alpha f})}{m.V_x} - V_x$$

$$C_1 = \frac{C_{\alpha f}}{m}$$

$$A_2 = \frac{(2.b.C_{\alpha r} - a.C_{\alpha f})}{I.V_x}$$

$$B_2 = -\frac{(a^2.C_{\alpha f} + 2.b^2 C_{\alpha r})}{I.V}$$

$$C_2 = \frac{a.C_{\alpha f}}{I}$$

REFERENCES

Affinito, F. J., Wang, S. S. & Yee, Y. S. 1976 "Computer controlled robot with an ultrasonic sensor". IBM Tech. Disclosure Bull. Vol. 18 No. 8. Jan.

Anderson, R. L. & Bajcsy, R. K. 1982 "SCIMR - A test bed for real time processing of sensory data". Computer and information Sciences Dept. University of Pennsylvania, Philadelphia, PA

Bauzil, G., Broit, M. & Rives, P. 1981 "A navigation sub-system using ultra-sonic sensors for the mobile robot Hilare". Proc. 1st Int. Conf. on robot vision and sensory controls. Apr., 47-58

Bradshaw 1981 "Model C Carrier and Tractor.". Model CO-014-32, New Lane, Stibbington, Peterborough, England

Bullock, B., Kiersey, D., Mitchell, J., Nussmeier, T. & Tseng, D. 1983 "Autonomous vehicle control: An overview of the Hughes project". Proc. of Trends and Applications 1983. Automating Intelligent Behaviour. 25-26th May, Pub. IEEE, New York.

Cahn, D. F. & Philips, S. R. 1975 "Robnav: A range based robot navigation system and obstacle avoidance algorithm". IEEE Trans. on Systems Man & Cybernetics: Sep. 544-551

Caudill, R. J. 1980 "Model reference longitudinal control for automated vehicle systems". J. of Dynamic Systems, Measurement and Control": Vol. 102, June, 77-84

Clemence, G. T. & Hurlburt, G. W. 1983 "The application of acoustic ranging to the automatic control of a ground vehicle". IEEE Trans. on Vehicular Technology Vol. VT-35 No. 3

Cormier, W. H. & Fenton, R. E. 1980 "On the steering of automated vehicles a velocity-adaptive controller". IEEE Trans. on Vehicular Technology, VT-29, No. 4, Nov.

Doran, J. 1970 "Planning and robots" Machine Intelligence No 5: Meltzer, B. & Michie, D., Eds. N.Y. Elsevier 519-532

Ellis, J. R 1963 "The dynamics of vehicles during braking". Symposium on Control of Vehicles: Institute of Mechanical Engineers, Paper 4.

Fenton, R. E., Melcock, G. C., & Olson, K. W. 1976 "On the steering of automated vehicles:- Theory and experiment" IEEE Trans. on Automatic control: AC-21, 3, 306-315

Hooke, A. A., Larman, B. T. & Whitney, W. M. 1973 "The impact of robots on planetary mission operations": Proc of Int. Telemetering Conf. 15-17th, Oct., Hawii. 568-579

Hughes, E. 1972 "Electrical Technology". The Chaucer Press.

Larcombe, M. H. E. 1978 "University of Warwick Mobile Robot Project". Colloquium on Robotics 30-31 Mar. Nat. Eng. Lab. East Kilbride. Glasgow.

Larcombe, M. H. E. 1981 "Terrain comparison guidance". Proc. 1st Int. Conf. on Automated Guided Vehicle Systems: Stratford-upon-Avon, 2-4 June, 122-128

Larcombe, M. H. E. & Halsall, J. R. 1984 "Robotics in Nuclear Engineering". Commission of the European Communities Contract No. ECI-978-b-7223-83-UK: Study on possible advances in remotely controlled operations in hostile environments, and particularly under severe radiation fields. Pub. Graham & Trotman, London.

Lezniak, T. W. & McMillen R. A., 1977 "A dead reckoning/map correlation system for Automatic Vehicle tracking". IEEE Trans. on Vehicular Technology, Vol VT-26 No. 1 Feb.

Lozano-Perez, T. 1978 "An algorithm for planning collision free paths amongst polyhedral obstacles". I.B.M. Thomas J. Watson Res. Centre: P.O Box 218 Yorktown Heights, N.Y. 10598

Mavaddat, F. 1983 "WATSON/I: WATerloo's SONically guided robot". J. of Microcomputer Applications 6, 37-45

Marce, L. Jullierre, M. & Place, H. "An autonomous computer controlled vehicle". Proc. 1st Int. Conf. on Automated Guided Vehicle

Systems: Stratford-upon-Avon, 2-4 June, 113-122

McGhee, R. B. & Iswandhi, G. I. 1979 "Adaptive locomotion of a multi-legged robot over rough terrain". IEEE Trans. on Systems, Man, and Cybernetics, Vol. SMC-9, No. 4, Apr.

Miller, J. A. 1977 "Autonomous guidance and control of a roving robot". Proc 5th Int. Joint Conf. on Artificial Intelligence: Cambridge, MA. 759-760

Moravec, H. P. 1980 "Obstacle avoidance and navigation in the real world by a seeing robot rover": Ph.D Thesis Univ. of Stanford, Calif.

Munson, J. H. 1973 "Robot planning, execution, and monitoring in an uncertain environment". Proc. 3rd Int. Joint Conf. on Artificial Intelligence: 338-349

Myer, J. 1971 " VEPOL A vehicular planimetric dead reckoning computer". IEEE Trans. on Vehicular Technology: VT-26 2, 161-172

Nillson, N. J. 1969 " A mobile automaton: An apllication of artificial intelligence techniques". Proc. 1st Int. Joint Conf. on Artificial Intelligence": 509--520

Polaroid Corporation 1980 "Ultrasonic ranging system". 1 Upland Road, Norwood, Massachusetts 02062

Russell, G. T. 1981 "The automatic guidance and control of an unmanned submersible". In Proc. of 1st Science and Engineering Council Vacation School in Robot Technology. Pub. I.E.E. London, (Ed.), Pugh, A.

Segal, L. 1956-1957 " Theoretical prediction and experimental substantiation of the reponse of the automobile to steering control". Proc. of the Automotive Division: Institution of Mechanical Engineers. 310-330

Shladover, S. E,. Wormley, D. E., Richardson, H. H. & Fish, R. 1978 "Steering controller design for automated guidway transit vehicles". J. Dynamic Sys. Measurement and Control: Vol 100, 1-7

Smisek, R. A. 1979 "Automated control of guideway transit vehicles" Proc 29th IEEE Veh. Tech. Conf. Mar 27-30 57-64

Thompson, A. M. 1977 "The navigation system of the J.P.L. robot". J.P.L. Publ. 77-20 July

Tsumura, T. & Fujiwara, N., 1978 "An experimental system for processing movement information of vehicle". Proc. 28th IEEE Vehicular Technology Conf. 163-168